

SYNTHESIS AND EVALUATION OF HEPATOPROTECTIVE EFFECTS OF A
TETRAHYDROCURCUMIN-DIGLUTARIC ACID PRODRUG



A Thesis Submitted in Partial Fulfillment of the Requirements
for the Degree of Master of Science in Pharmaceutical Sciences and Technology

Common Course

FACULTY OF PHARMACEUTICAL SCIENCES

Chulalongkorn University

Academic Year 2021

Copyright of Chulalongkorn University

การสังเคราะห์ และการประเมินฤทธิ์ปกป้องตับของเตตระไฮโดรเคอร์คิวมิน-ไดกลูตาริกแอซิดโพดรัก



วิทยานิพนธ์นี้เป็นส่วนหนึ่งของการศึกษาตามหลักสูตรปริญญาวิทยาศาสตรมหาบัณฑิต

สาขาวิชาเภสัชศาสตร์และเทคโนโลยี ไม่สังกัดภาควิชา/เทียบเท่า

คณะเภสัชศาสตร์ จุฬาลงกรณ์มหาวิทยาลัย

ปีการศึกษา 2564

ลิขสิทธิ์ของจุฬาลงกรณ์มหาวิทยาลัย

Thesis Title	SYNTHESIS AND EVALUATION OF HEPATOPROTECTIVE EFFECTS OF A TETRAHYDROCURCUMIN-DIGLUTARIC ACID PRODRUG
By	Mr. Nattapong Jongjitphisut
Field of Study	Pharmaceutical Sciences and Technology
Thesis Advisor	Associate Professor Pornchai Rojsitthisak, Ph.D.

Accepted by the FACULTY OF PHARMACEUTICAL SCIENCES, Chulalongkorn University in Partial Fulfillment of the Requirement for the Master of Science

..... Dean of the FACULTY OF
PHARMACEUTICAL SCIENCES
(Professor PORNANONG ARAMWIT, Ph.D.)

THESIS COMMITTEE

..... Chairman
(Associate Professor VORASIT VONGSUTILERS, Ph.D.)
..... Thesis Advisor
(Associate Professor Pornchai Rojsitthisak, Ph.D.)
..... Examiner
(Associate Professor SUPAKARN CHAMNI, Ph.D.)
..... External Examiner
(Professor Apichart Suksamrarn, Ph.D.)

นันทพงษ์ จงจิตพิศุทธิ์ : การสังเคราะห์ และการประเมินฤทธิ์ปกป้องตับของเตตระไฮโดรเคอร์คิวมิน-ไดกลูตาริกแอซิดโพรดรั๊ก. (SYNTHESIS AND EVALUATION OF HEPATOPROTECTIVE EFFECTS OF A TETRAHYDROCURCUMIN-DIGLUTARIC ACID PRODRUG) อ.ที่ปรึกษาหลัก : รศ. ภก. ดร.พรชัย โรจน์สีหิตศักดิ์

โรคตับจากแอลกอฮอล์ (ALD) เป็นโรคสำคัญที่กระทบต่อสุขภาพของประชากรทั่วโลก สารจากธรรมชาติหลายชนิดรวมทั้งเคอร์คิวมินถูกนำมาศึกษาเพื่อจะนำมาใช้เป็นยารักษาโรคดังกล่าว จากข้อมูลการศึกษาที่ผ่านมาพบว่า เตตระไฮโดรเคอร์คิวมิน (THC) ซึ่งเป็นอนุพันธ์ของเคอร์คิวมินมีฤทธิ์ต้านอนุมูลอิสระที่ดี และสามารถช่วยป้องกันโรคที่เกิดจากภาวะเครียดออกซิเดชันได้ จึงมีแนวคิดในการนำ THC มาใช้พัฒนาเป็นยารักษาโรค ALD อย่างไรก็ตาม THC มีข้อจำกัดในการใช้เป็นยา เนื่องจาก THC มีคุณสมบัติการละลายน้ำที่ต่ำ ดังนั้นในการศึกษาค้นคว้านี้ได้ทำการสังเคราะห์เตตระไฮโดรเคอร์คิวมิน-ไดกลูตาริกแอซิด (TDG) ที่เป็นโพรดรั๊กของ THC และพบว่า TDG มีค่าการละลายเพิ่มขึ้นประมาณ 20 เท่าเมื่อเทียบกับ THC ในสารละลายพีเอช 6.8 และมีค่าสัมประสิทธิ์การกระจายตัว (LogP) เท่ากับ 3.03 จากการศึกษาความคงตัวพบว่า TDG คงตัวในสถานะที่เป็นกรด และลดลงในสถานะที่เป็นด่าง นอกจากนี้ TDG จะเกิดการเปลี่ยนแปลงทางเคมีและสลายตัวในพลาสมาภายในระยะเวลา 4 ชั่วโมง โดยมีค่าคงที่อัตรา 0.758 h^{-1} และมีค่าครึ่งชีวิตเท่ากับ 0.9 ชั่วโมง ผลการศึกษาฤทธิ์ในหลอดทดลองของ THC และ TDG ในการปกป้องเซลล์ตับที่ถูกเหนี่ยวนำให้เกิดบาดเจ็บโดยใช้เอทานอลในเซลล์มะเร็ง HepG2 พบว่า TDG สามารถป้องกันการบาดเจ็บของเซลล์ตับได้ดีกว่า THC โดยการลดระดับของอนุมูลอิสระออกซิเจน และเพิ่มการทำงานของระบบป้องกันด้วยสารต้านอนุมูลอิสระของร่างกายได้แก่เอนไซม์แคตาเลส เอนไซม์กลูตาไรโอนเปอร์ออกซิเดส และกลูตาไรโอน นอกจากนี้ TDG ยังสามารถยับยั้งการกระตุ้นให้เกิดการตายของเซลล์แบบอะพอพโตซิสจากการใช้เอทานอลได้โดยการควบคุมการทำงานของเอนไซม์แคสเปส-3 และเอนไซม์แคสเปส-9 ผลการศึกษาทั้งหมดนี้แสดงให้เห็นว่า TDG มีแนวโน้มให้ประสิทธิภาพดีกว่าในการปกป้องตับจากพิษของแอลกอฮอล์เมื่อเทียบกับ THC

สาขาวิชา เกษศาสตร์และเทคโนโลยี

ลายมือชื่อนิสิต

ปีการศึกษา 2564

ลายมือชื่อ อ.ที่ปรึกษาหลัก

ACKNOWLEDGEMENTS

I would like to express my deepest gratitude to my thesis advisor, Associate Professor Pornchai Rojsitthisak, for his expert advice, invaluable help, and constant encouragement throughout my graduate study. I would also like to sincerely thank the thesis committees for their valuable comments on this thesis.

My genuine appreciation also goes to Professor Paitoon Rashatasakhon for his helpful suggestions and support for the experimental work, especially synthesis at the Faculty of Science, Chulalongkorn University.

I would like to acknowledge the Pharmaceutical Research Instrument Center of the Faculty of Pharmaceutical Sciences, Chulalongkorn University, and Pharma Nueva Co., Ltd for providing the research facilities and instruments. I also thank the staff and my friends at Chulalongkorn University for staying with me and giving me insightful pieces of advice during challenging times.

This research was supported by the 90th Anniversary Chulalongkorn University Fund (Ratchadaphiseksomphot Endowment Fund, Grant No. GCUGR1125642014M) and the scholarship from Government Pharmaceutical Organization.

Finally, I would like to express my most profound appreciation to my family for their support, encouragement, and inspiration throughout this research. They all kept me working hard, and this thesis would not have been completed without them.

Nattapong Jongjitphisut

TABLE OF CONTENTS

	Page
ABSTRACT (THAI).....	iii
ABSTRACT (ENGLISH).....	iv
ACKNOWLEDGEMENTS.....	v
TABLE OF CONTENTS.....	vi
LIST OF TABLES.....	x
LIST OF FIGURES.....	xi
CHAPTER 1 INTRODUCTION.....	1
CHAPTER 2 LITERATURE REVIEW.....	5
2.1 Alcoholic Liver Disease (ALD).....	5
2.1.1 The incidence of Alcoholic Liver Disease (ALD).....	5
2.1.2 The burden of ALD in Thailand.....	6
2.1.3 Pathophysiology of ALD.....	7
2.1.3.1 Oxidative stress.....	7
2.1.3.1.1 The nuclear factor erythroid 2–related factor 2 (Nrf2) ...	11
2.1.3.2 Apoptosis.....	13
2.1.3.2.1 Extrinsic pathway.....	14
2.1.3.2.2 Intrinsic pathway.....	15
2.1.3.2.3 Ethanol and apoptosis.....	16
2.1.4 The current management of ALD.....	17
2.2 Tetrahydrocurcumin.....	18
2.2.1 The overview of tetrahydrocurcumin.....	18

2.2.2 The pharmacological activity of THC	19
2.2.3 The limitation of THC	26
2.3 Prodrug design approach.....	26
2.3.1 Introduction of the prodrug design approach	26
2.3.2 The enhancement of water solubility by prodrug design approach	27
2.3.2.1 Dicarboxylic acid.....	30
2.4 Cell-based model for ethanol-induced hepatotoxicity	32
CHAPTER 3 RESEARCH METHODOLOGY.....	37
3.1 Chemicals, Cell lines, Media, and Equipment	37
3.2 Synthesis of tetrahydrocurcumin-diglutaric acid conjugate	40
3.3 Physicochemical properties evaluation	41
3.3.1 Preparation of buffer solutions.....	41
3.3.2 Solubility test	41
3.3.3 Partition Coefficient.....	42
3.3.4 Stability study.....	42
3.3.5 Drug release kinetics study.....	44
3.4 Chromatographic UHPLC system for THC and TDG analysis	44
3.4.1 UHPLC instrumentation.....	44
3.4.2 Chromatographic condition.....	45
3.5 Pharmacological activity evaluation	45
3.5.1 Cell Culture.....	45
3.5.2 Cell viability assay	45
3.5.3 Measurement of intracellular ROS.....	46

3.5.4 Investigation of antioxidant enzyme activities and reduced glutathione (GSH) level	46
3.5.5 Evaluation of caspase-3 and -9 activities	47
3.6 Statistical analysis	48
CHAPTER 4 RESULTS	49
4.1 Synthesis and Characterization of tetrahydrocurcumin-diglutaric acid	49
4.2 Physicochemical and biopharmaceutical characterization	52
4.2.1 Solubility	52
4.2.2 Partition coefficient (LogP).....	52
4.2.3 Stability in buffer	52
4.2.4 Kinetic drug Release in plasma.....	53
4.3 Evaluation of the hepatoprotective effects of THC and TDG against alcohol induced-oxidative damage in HepG2 cells.....	53
4.3.1 Determination of cytotoxicity in HepG2 cells.....	53
4.3.2 The protective effect of THC and TDG on alcohol-induced cell death ...	54
4.3.3 Effects of THC and TDG on ROS level.....	55
4.3.4 Effects of THC and TDG on CAT, GPx activities and GSH level.....	56
4.3.5 Effects of THC and TDG on caspase-3 and -9 activity	57
CHAPTER 5 DISCUSSION AND CONCLUSION	59
APPENDIX A	70
APPENDIX B	75
APPENDIX C	78
APPENDIX D	79
APPENDIX E	81

APPENDIX F	82
APPENDIX G.....	84
APPENDIX H.....	85
REFERENCES	86
VITA.....	105



LIST OF TABLES

	Page
Table 1 Lists intracellular enzymatic and non-enzymatic antioxidants.....	11
Table 2 Studies on the protective effect of tetrahydrocurcumin against chemical- induced oxidative stress.....	20
Table 3 The lists of FDA-approved prodrugs during 2008-2020 whose objective is to enhance water solubility.....	29
Table 4 the summarize of research studies that have been used HepG2 cell line as an in vitro model for ethanol-induced hepatotoxicity.....	33
Table 5 The time interval for stability study in pH 1.2, 4.5, 6.8, and 7.4	43
Table 6 Solubility of THC and TDG in various conditions	52
Table 7 Rate constant (k) and half-life ($t_{1/2}$) of TDG at pH 1.2, 4.5, 6.8, and 7.4.....	53
Table 8 the report of analytical method validation parameters for quantification of TDG.....	63
Table 9 The r^2 value of different kinetic models for TDG degradation.....	65

LIST OF FIGURES

	Page
Figure 1 The chemical structure of curcumin and tetrahydrocurcumin	3
Figure 2 The metabolizing pathway of ethanol via oxidized enzymes including catalase, ADH, and CYP2E1	8
Figure 3 The reactive oxygen species are generated from the complex series of enzymes in the electron transport chain in the cristae membrane of mitochondria ...	9
Figure 4 The ethanol metabolism through CYP2E1 enzyme using NADPH and oxygen as a cofactor that generated ROS as a byproduct.....	10
Figure 5 The Nrf2-Keap-1 formation under normal and stress conditions.....	12
Figure 6 The schematic of cellular morphologic changes during the apoptosis death process.....	14
Figure 7 The intrinsic and extrinsic pathway of apoptosis	16
Figure 8 The chemical structure of tetrahydrocurcumin (THC) and its tautomerization	19
Figure 9 Schematic representation of prodrug design concept.....	27
Figure 10 the chemical structure of paclitaxel and docetaxel malyl prodrug sodium salt.....	31
Figure 11 The chemical structure of curcumin-diglutaric acid prodrug	32
Figure 12 Methodology of the study.....	39
Figure 13 Synthesis scheme of tetrahydrocurcumin-diglutaric acid (TDG) conjugate via an ester bond linkage.....	41
Figure 14 The degradation pathway of tetrahydrocurcumin-diglutaric acid (TDG) and the equation formula of consecutive kinetic to estimate the concentration of each compound at each time point.	44

Figure 15 ^1H NMR spectrum of TDG.....	50
Figure 16 ^{13}C NMR spectrum of TDG.....	50
Figure 17 High-resolution mass spectrometry (HRMS) spectrum of TDG.....	51
Figure 18 IR spectrum of TDG	51
Figure 19 Cytotoxicity evaluation using MTT assay in HepG2 cells incubated with various concentrations of (A) THC and TDG and (B) ethanol for 24 h.....	54
Figure 20 Hepatoprotective effects of THC and TDG on HepG2 cells.....	55
Figure 21 Effect of THC and TDG on alcohol-induced ROS generation in HepG2 cells.	56
Figure 22 THC and TDG ameliorate alcohol-induced antioxidant defense depletion (A) CAT activity, (B) GPx activity, and (C) GSH level.....	57
Figure 23 THC and TDG suppress alcohol-induced apoptosis on HepG2 cells.	58
Figure 24 Proposed mechanism reaction of DIPEA, glutaric anhydride, and THC.....	60
Figure 25 The proposed mechanism of TDG for protecting liver cells from alcohol-induced oxidative damage.....	69
Figure 26 The kinetic plots of TDG in buffer solution pH 1.2, n = 3.....	75
Figure 27 The kinetic plots of TDG in buffer solution pH 4.5, n = 3.....	75
Figure 28 The kinetic plots of TDG in buffer solution pH 6.8, n = 3.....	76
Figure 29 The kinetic plots of TDG in buffer solution pH 7.4, n = 3.....	76
Figure 30 The kinetic plots of TDG in human plasma, n = 3	77
Figure 31 UHPLC chromatograms of THC, TMG, and TDG at a concentration of 10 $\mu\text{g}/\text{ml}$	78
Figure 32 The UHPLC chromatogram of 100 $\mu\text{g}/\text{ml}$ of TDG analyzed with 6 replications.....	80
Figure 33 The calibration curve of TDG showed a good relationship between peak response and concentration with R square 0.9999.....	81

Figure 34 COSY spectrum of TDG in CDCl_3	82
Figure 35 HMBC spectrum of TDG in CDCl_3	82
Figure 36 HSQC spectrum of TDG in CDCl_3	83
Figure 37 Effect of THC, TDG, and silymarin on ethanol-induced liver cell death.....	84



CHAPTER 1 INTRODUCTION

Alcoholic liver disease (ALD) is a chronic disease caused by excessive ethanol consumption of over 40 g per day that leads to a broad spectrum of hepatic lesions (cirrhosis), causing chronic liver disease and eventually death in humans (Rehm et al., 2010). According to the previous research, ALD accounts for 588,100 deaths (Shield et al., 2020) or 46.9% of cirrhosis-associated deaths in 2016 (Rehm & Shield, 2019). In addition, ALD also accounts for up to 30% of all hepatocellular carcinoma (HCC) deaths (Seitz et al., 2018). At the primary stage of liver disease, the liver's fats accumulate, causing hepatic steatosis that can be reversed after alcohol abstinence. However, continuous heavy alcohol consumption can develop a more severe liver injury known as steatohepatitis and progress to liver fibrosis, cirrhosis, and HCC (Seitz et al., 2018).

ALD pathogenesis is associated with alcohol oxidative metabolism. Excessive alcohol consumption will be metabolized through the cytochrome P450 2E1 (CYP2E1) enzyme, which plays a major role in alcohol-induced liver injury. This enzyme will metabolize ethanol to acetaldehyde and simultaneously generate reactive oxygen species (ROS) (Osna et al., 2017). However, the overproduction of ROS will promote oxidative stress in the liver cells, which can activate the formation of lipid peroxidation products, including malondialdehyde (MDA) and 4-hydroxynonenal (4-HNE) (Hauck & Bernlohr, 2016). These lipid peroxidation compounds can modify the protein structure and bind to DNA to generate hepatic deterioration and promote cell death (Ayala et al., 2014). Therefore, the accumulation of acetaldehyde, ROS, and lipid peroxidation are attributed to oxidative stress and cellular damage in the occurrence and development of acute alcoholic liver injury.

Despite extensive research on the pathogenesis of ALD, there is no effective drug to treat patients with ALD. However, alcohol abstinence is still the most

effective method to reverse the fatty liver or slow down cirrhosis progression (Osna et al., 2017). Recently, herbal medicines and their phytochemical constituents, including quercetin (Lee et al., 2017), silymarin (Song et al., 2006), and curcumin (Lu et al., 2015), have been evaluated for their hepatoprotective activity against alcohol-induced hepatotoxicity. Their protective effects have involved the amelioration of oxidative stress by the stimulation of the nuclear factor erythroid 2 (NFE2)-related factor 2 (Nrf2) that regulates the expression of several genes associated with the antioxidant defense system of the cells (Iranshahy et al., 2018).

Tetrahydrocurcumin (THC; 1,7-bis (4-hydroxy-3-methoxyphenyl) heptane-3,5-dione) is a primary hydrogenated metabolite of curcumin (Figure 1) (Pan et al., 1999). Unlike curcumin, THC is a colorless compound due to the lack of α , β dienes. However, the key functional groups, phenolic and β -diketone motifs, remain to elicit antioxidant activity (Sugiyama et al., 1996). According to its chemical structure, THC shows similar pharmacological activities to curcumin. For instance, THC showed a hepatoprotective effect against several xenobiotics, which induce oxidative stress and consequently cause liver cell injury (Pari & Amali, 2005; Pari & Murugan, 2004). Interestingly, previous reports suggest that THC has higher antioxidant activity and a better hepatoprotective effect than curcumin (Luo et al., 2019; Okada et al., 2001; Osawa et al., 1995). Therefore, THC can be considered as a potential hepatoprotective agent for alcohol-induced hepatotoxicity. However, THC has a poor water solubility that hinders its pharmacological and pharmacokinetic activities (Setthacheewakul et al., 2011). To overcome this limitation, the prodrug design approach has been extensively applied to modify the chemical structure.

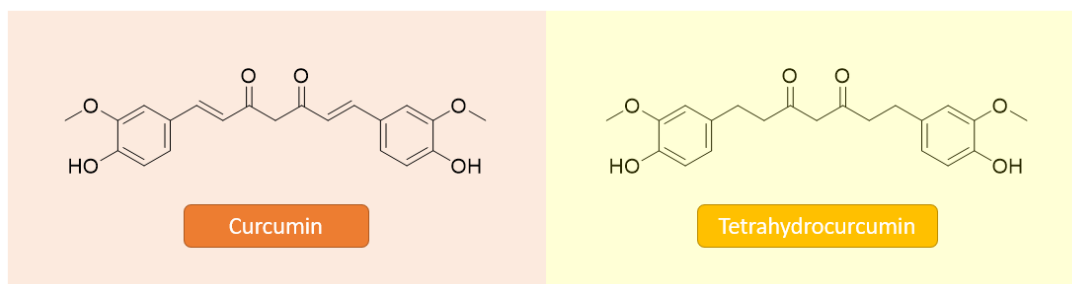


Figure 1 The chemical structure of curcumin and tetrahydrocurcumin

A prodrug is a well-known technique to improve physicochemical properties of the pharmacologically active compound/drug or parent compounds by conjugating with a promoiety or carrier such as amino acids (Vig et al., 2013) or dicarboxylic acids (Muangnoi et al., 2018) through a temporary covalent bond linkage, which can be broken down *in vivo* or systemic circulation to release the parent compound (Huttunen et al., 2011). These conjugated compounds can intensify the water solubility of the parent compound, providing higher drug absorption while subsequently enhancing its pharmacological activity (Sanches & Ferreira, 2019). The examples of commercially available dicarboxylic acid prodrugs are prednisolone succinate (Sugiyama et al., 2001). and chloramphenicol succinate (Ambrose, 1984). In addition, Muangnoi et al. have recently developed a curcumin prodrug by using glutaric acid as a promoiety. The glutaric acids were conjugated on both phenolic hydroxyl groups of curcumin via an ester bond, and the obtained prodrug, curcumin-diglutaric acid, showed higher water solubility and pharmacological activity than the unconjugated curcumin (Muangnoi et al., 2018). This evidence strongly suggests that the improvement of water solubility and activity of THC can be achieved by dicarboxylic acid prodrug design. THC-diglutaric acid prodrug could be a potential alternative hepatoprotective candidate for alcohol-induced liver injury.

The main objectives of this research study are as follows

1. To synthesize the prodrug of THC by conjugation with glutaric acid via an ester linkage.
2. To characterize the synthesized THC prodrug by determining its physicochemical and biopharmaceutical properties, including solubility, stability, and partition coefficient.
3. To determine the pharmacological response of THC prodrug in alleviating alcohol-induced hepatotoxicity *in vitro* using a HepG2 cell line.



CHAPTER 2 LITERATURE REVIEW

2.1 Alcoholic Liver Disease (ALD)

2.1.1 The incidence of Alcoholic Liver Disease (ALD)

One of the significant risk factors contributing to the disease and mortality is alcohol (Rehm et al., 2017; Rehm & Imtiaz, 2016). The effect of heavy and chronic alcohol consumption resulted in approximately 3 million deaths (5.3% of all global deaths) in 2016 that is higher than the mortality caused by diabetes (2.8%), tuberculosis (2.3%), HIV/AIDs (1.8%), and hypertension (1.6%) (Organization, 2018). Heavy alcohol consumption produced alcoholic liver disease (ALD), which can be characterized by a variety of disease states starting from alcoholic fatty liver (steatosis), hepatitis, fibrosis, liver cirrhosis, and even liver cancer or hepatocellular carcinoma (HCC) (Osna et al., 2017). In 2016, liver disease deaths were reported, about 1,254,000 deaths worldwide, and 588,100 deaths (46.9%) were caused by alcohol-attributable liver disease (Rehm & Shield, 2019). The recent study of disease burden in 2017 indicates that alcohol-related diseases, including liver cancer, liver cirrhosis, and other chronic liver diseases, affected 13,280,000 disability-adjusted life years (DALYs & Collaborators) or 21.4% of all DALYs for liver diseases (DALYs & Collaborators, 2018). The DALYs are represented to the total years of full, healthy life lost, and one DALYs is comparable to one year of a full healthy life. DALYs are calculated by the sum of years of life lost due to premature death and the number of years lived with illness or disability from the unhealthiness (Rehm et al., 2013). Furthermore, recent research reveals that alcohol consumption has increased over three decades (1990 – 2017) by alcohol per-capita consumption extended from 5.9 L in 1990 to 6.5 L in 2017 and is predicted to be 7.6 L in 2030 (Manthey et al., 2019). According to the alcohol consumption trend, alcohol consumption will be increased and recognized as an essential issue in the future.

2.1.2 The burden of ALD in Thailand

In 2018, WHO indicated that alcohol consumption in Thailand was the third-highest in Southeast Asia (WHO, 2021). In 2015, Wakabayashi performed a cohort study in the Thai population. They recruited 87,151 cases and found that 65% of the overall case (78% of men and 53% of women) were occasionally or regularly alcohol drinkers, and only 26% of the total cohort population never had drunk alcohol. They also reported that the odds ratios of liver disease were associated with the pattern of alcohol drinking which regular heavy drinkers were the highest odds ratio (OR = 2.0) as compared to occasional light drinkers (OR = 1.2) (Wakabayashi et al., 2015). These high levels of alcohol consumption in Thailand affected the health care costs of 5,491.2 million baht as reported in 2006 (Thavorncharoensap et al., 2010). Liver cirrhosis is one of Thailand's highest prevalence health problems, around 92,301 admissions or 24.3% of total admission of digestive system diseases in 2010 (Poovorawan et al., 2015). According to the previous research, they studied the prevalence of cirrhosis in Nakhon Nayok province in 2007. They found that there are 199 cases with a rate of 75.3 per 100,000 population. Moreover, 143 cirrhosis patients were diagnosed with alcoholic cirrhosis with a rate of 53.6 per 100,000 population (Rattanamongkolgul et al., 2010). In 2015, Poovorawan analyzed the inpatient information with liver cirrhosis from the 2010 Nationwide Hospital Admission Data. They reported that 73% of 31,423 cases of liver cirrhosis were identified as alcoholic liver disease. Therefore, the most common etiology of liver cirrhosis in Thailand is alcoholic liver disease (Poovorawan et al., 2015). Thus, liver cirrhosis is associated with the high health care costs in both direct costs (medicine and hospitalization costs) and indirect costs (work productivity and reduction in health-related quality of life) as reported in USA, 2004. They indicated that the total health care costs were estimated to be \$13.1 billion due to liver cirrhosis being a progressive disease (Neff et al., 2011). To reduce these health care costs from liver cirrhosis, developing an effective protective agent for ALD is the most attractive topic for research.

2.1.3 Pathophysiology of ALD

The amount of alcohol exposure is related to the risk of ALD development in dose-response relationships. Heavy alcohol consumption (> 40 g of pure ethanol per day) or chronic consumption (12 – 24g of pure ethanol per day) can dramatically increase the possibility of ALD as compared to non-drinkers (Rehm et al., 2010). Most heavy and chronic drinkers (90 – 100%) initiate alcoholic fatty liver, and 10% to 20% of the alcoholic fatty liver will develop to advanced ALD state (Seitz et al., 2018). In addition to alcohol consumption, some risk factors affect the ALD progression, including genetics, sex, obesity, other underlying liver disease, drugs, xenobiotic consumption, and smoking (Seitz et al., 2018).

2.1.3.1 Oxidative stress

The ethanol metabolism is important in generating oxidative stress to produce toxic metabolites that result in liver disease or ALD. In hepatocytes, alcohol dehydrogenase (ADH) is the crucial enzyme to oxidize ethanol by using nicotinamide adenine dinucleotide (NAD⁺) as a cofactor, producing reduced NAD⁺ (NADH) and acetaldehyde as shown in Figure 2 (Osna et al., 2017). Additionally, cytochrome P450 2E1 (CYP2E1) is an ethanol-inducible enzyme located in the smooth endoplasmic reticulum (ER) of hepatocytes that metabolized ethanol via oxidation to acetaldehyde and converts reduced NAD phosphate (NADPH) to its oxidized form (NADP⁺) (Osna et al., 2017). Another metabolic pathway associated with ethanol metabolism is the catalase enzyme that can metabolize ethanol to acetaldehyde using hydrogen peroxide (H₂O₂) (Osna et al., 2017). This pathway is identified as a minor pathway (Osna et al., 2017). Furthermore, acetaldehyde was produced and accumulated in the hepatocyte cells, which is a highly reactive and toxic compound that can bind to the protein and impair the cell's structure and function (Setshedi et al., 2010). However, the toxicity of acetaldehyde is minimized when oxidized to acetate via mitochondrial aldehyde dehydrogenase (ALDH) and a cofactor NAD⁺ (Osna et al., 2017). The accumulation of NADH resulting from ADH and

ALDH oxidation decreases the NAD^+/NADH ratio, affecting several biochemical pathways using NAD^+ as a cofactor, including fatty acid oxidation and resulting in hepatic steatosis (Ceni et al., 2014).

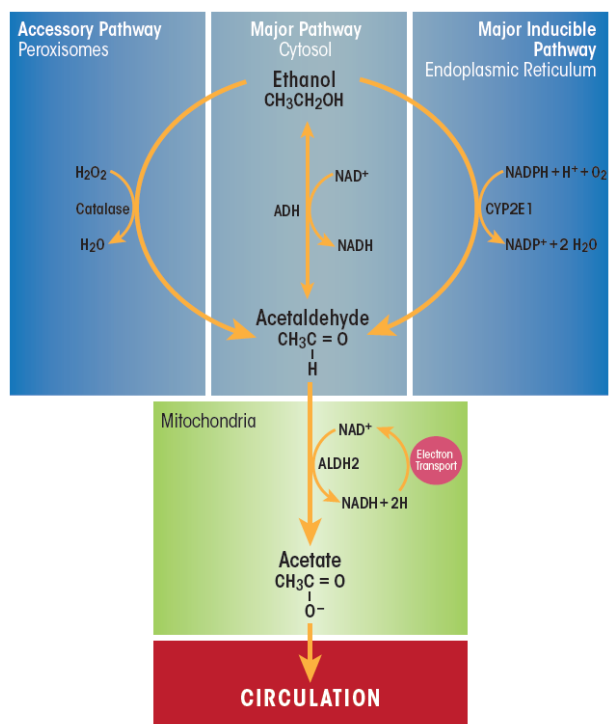


Figure 2 The metabolizing pathway of ethanol via oxidized enzymes including catalase, ADH, and CYP2E1 (Osna et al., 2017).

To re-oxidize NADH to NAD^+ , mitochondria are responsible for cellular organelle through electron transfer chain that leads to the generation of reactive oxygen species (ROS) by transferring an electron to oxygen molecule such as superoxide anion (O_2^-), hydrogen peroxide (H_2O_2), and the hydroxyl radical (OH^\bullet) (Ceni et al., 2014). Then, mitochondria are identified as a significant source of ROS within the cell (Figure 3).

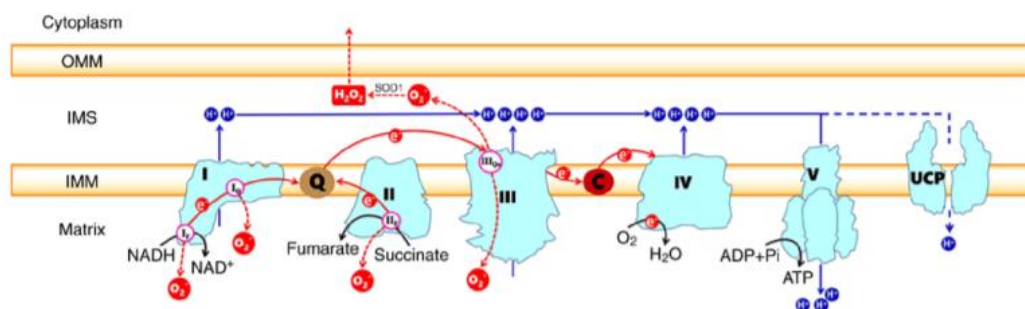


Figure 3 The reactive oxygen species are generated from the complex series of enzymes in the electron transport chain in the cristae membrane of mitochondria (Zhao et al., 2019).

In addition to acetaldehyde generation via CYP2E1 metabolism, the oxidation of ethanol through CYP2E1 requires oxygen in the reaction, resulting in reactive ROS generation as a byproduct (Figure 4) (García-Suástegui et al., 2017; Linhart et al., 2014). ROS are reactive toxic substances that react with protein causing cellular and DNA damage and lipid peroxidation by free radicals and their interaction with unsaturated fatty acids. Lipid peroxidation affects the integrity of cellular membranes, especially mitochondria, which also damages proteins and DNA (Leung & Nieto, 2013). Moreover, CYP2E1 is an inducible enzyme that can be upregulated by heavy alcohol consumption and elevates ROS generation (Jimenez-Lopez & Cederbaum, 2005; Lu & Cederbaum, 2008).

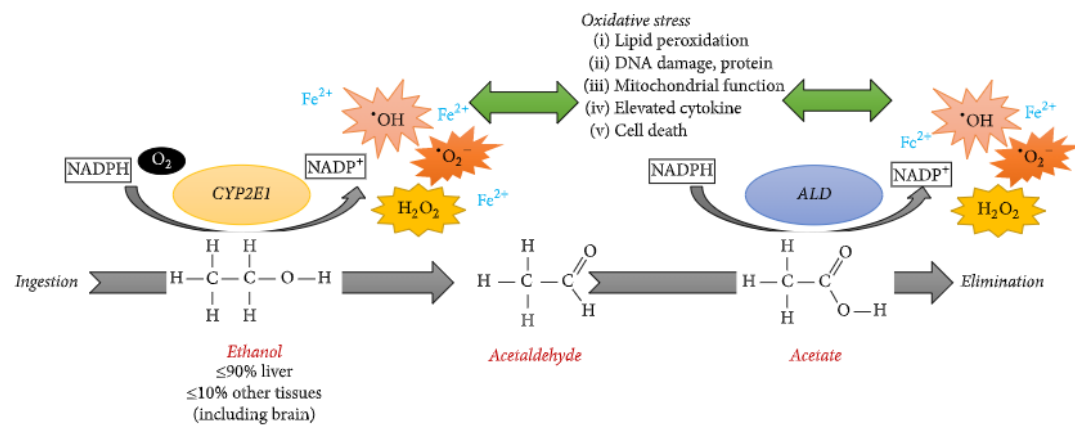


Figure 4 The ethanol metabolism through CYP2E1 enzyme using NADPH and oxygen as a cofactor that generated ROS as a byproduct (García-Suástegui et al., 2017).

To minimize ROS toxicity, our body has enzymatic and non-enzymatic antioxidant mechanisms as shown in Table 1 (Cichoż-Lach & Michalak, 2014; Leung & Nieto, 2013). Unfortunately, under oxidative stress conditions resulting from excessive ethanol consumption, the amounts of ROS generation are higher than the capacity of the liver's antioxidant mechanisms, which results in liver damage (Cederbaum et al., 2009; Cichoż-Lach & Michalak, 2014; Osna et al., 2017). Moreover, the increase of ROS level also triggered cell death through the apoptotic pathway (Matés et al., 2012). To improve the intracellular antioxidant defense system, scientific research revealed that the nuclear factor erythroid 2 (NFE2)-related factor 2 (Nrf2) plays a crucial role in protecting the cell from oxidative stress by regulating the expression of the antioxidant gene.

Table 1 Lists intracellular enzymatic and non-enzymatic antioxidants (Cichoż-Lach & Michalak, 2014; Leung & Nieto, 2013).

Enzymatic antioxidant	Non-enzymatic antioxidant
heme oxygenase	Glutathione (GSH)
Ceruloplasmin	ferritin
glutathione peroxidase	vitamin A
glutathione transferase	vitamin C
catalase	vitamin E
superoxide dismutase (SOD)	-----

2.1.3.1.1 The nuclear factor erythroid 2-related factor 2 (Nrf2)

Nrf2 is a transcription factor located in the cytoplasm that forms a complex with an inhibited protein, Kelch-like ECH associated protein-1 (Keap-1), which restrains the Nrf2 activity by promoting the degradation of Nrf2 via ubiquitination (Taguchi et al., 2011). Under stress conditions, ROS interrupts the Nrf2-Keap-1 complex that can unbind Nrf2 from Keap-1. Then, free Nrf2 translocates into the nucleus and binds to a DNA sequence at antioxidant responsive elements (ARE) (Figure 5) (Keleku-Lukwete et al., 2017). Nrf2 regulates the expression of several antioxidant enzymes, including NAD(P)H quinone oxidoreductase (NQO1), glutathione peroxidase (GPx), glutathione S-transferase, glutathione reductase (GR), UDP-glucuronosyltransferase, SOD, glutamate-cysteine ligase (GCLC and GCLM), and heme oxygenase (HO-1) (Ma, 2013). Therefore, the stimulation of the Nrf2-Keap-1 pathway can increase the capacity of the liver's antioxidant mechanisms and enhance the protective effect against alcohol-induced hepatotoxicity.

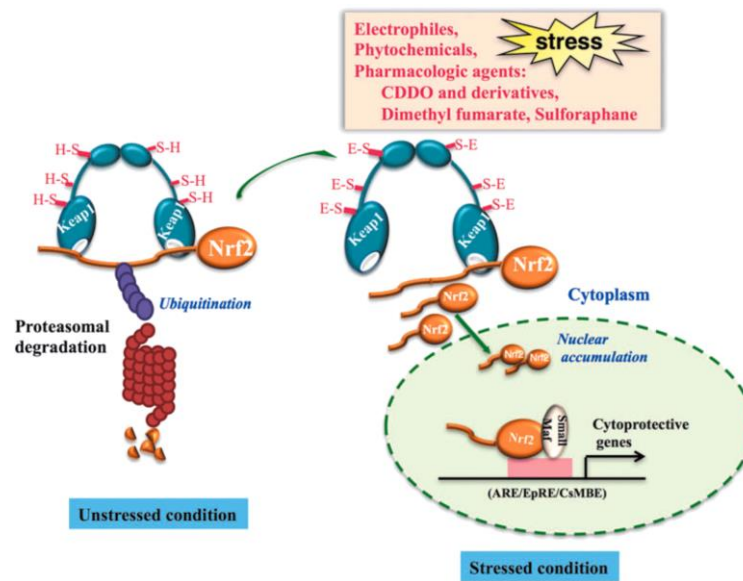


Figure 5 The Nrf2-Keap-1 formation under normal and stress conditions. Nrf2 formed a complex with Keap-1 protein that is involved in the degradation of Nrf2 under unstressed conditions. In stress conditions, ROS, or electrophilic reagents (E) interact with the thiol group of amino acid “cysteine” on Keap1 and modify the structure of Keap1, where Nrf2 will be released and translocated into the nucleus (Keleku-Lukwete et al., 2017).

Several phytochemical compounds exert hepatoprotective effects by inducing the expression of Nrf2 protein and mRNA in alcohol-induced toxicity in both *in vitro* and *in vivo* models. In 2019, Lee S et al. studied the protective effect of quercetin, quercetin-3-glucoside, and rutin in alcohol-induced hepatic damage. HepG2 cell line was used as *in vitro* model inducing by ethanol 5% for 24 h. The results showed that ethanol 5% could significantly decrease the expression of Nrf2 in the nucleus compared with the control group. For quercetin, quercetin-3-glucoside, and rutin treatment group, the expression of nuclear Nrf2 was increased as well as antioxidant enzymes including HO-1, NQO-1, and GCLC (Lee et al., 2019). Furthermore, Yan was studied the hepatoprotective effect of cinnamic and syringic acids in alcohol-fed mice. Cinnamic and syringic acids can restore the expression of Nrf2 level and promote the

translocation of Nrf2 into the nucleus (Yan et al., 2016). These research studies suggest that the Nrf2-Keap1 signaling pathway is a crucial transcription factor in protecting the liver from alcohol toxicants.

2.1.3.2 Apoptosis

Apoptosis has been accepted as the important mode of programmed cell death controlled by a genetic determination to eliminate the cells (Elmore, 2007). It is identified as a natural physiologic process in multicellular organisms required to maintain normal tissue development and homeostasis by killing aged or unwanted or damaged cells when cells are exposed to noxious agents (Elmore, 2007; Singh & Bose, 2015). The apoptosis cells are characterized by the change of cell morphology including cell shrinkage, plasma membrane blebbing, chromatin condensation, and DNA fragmentation (Matés et al., 2012; Singh & Bose, 2015). As a result, the apoptotic cells are separated into cell fragments or apoptosis bodies that are rapidly phagocytosed by immune cells such as macrophages without any induction of inflammatory response (figure 6) (Elmore, 2007; Singh & Bose, 2015; Zimmermann & Green, 2001). To initiate cell death through the apoptosis pathway, several stimuli trigger apoptosis, including ROS, damaged DNA, and viral infection (Elmore, 2007; Matés et al., 2012). The mechanisms of apoptosis are complex, consisting of several cascades of molecular events that can be separated into 2 main pathways: extrinsic pathway or death receptor pathway and intrinsic pathway of mitochondria pathway (Elmore, 2007). At the terminal of the process, both pathways converge on the executioner caspase, in which intracellular organelles are degraded by the cleavage of caspase-3 and then digested by macrophage (Elmore, 2007).

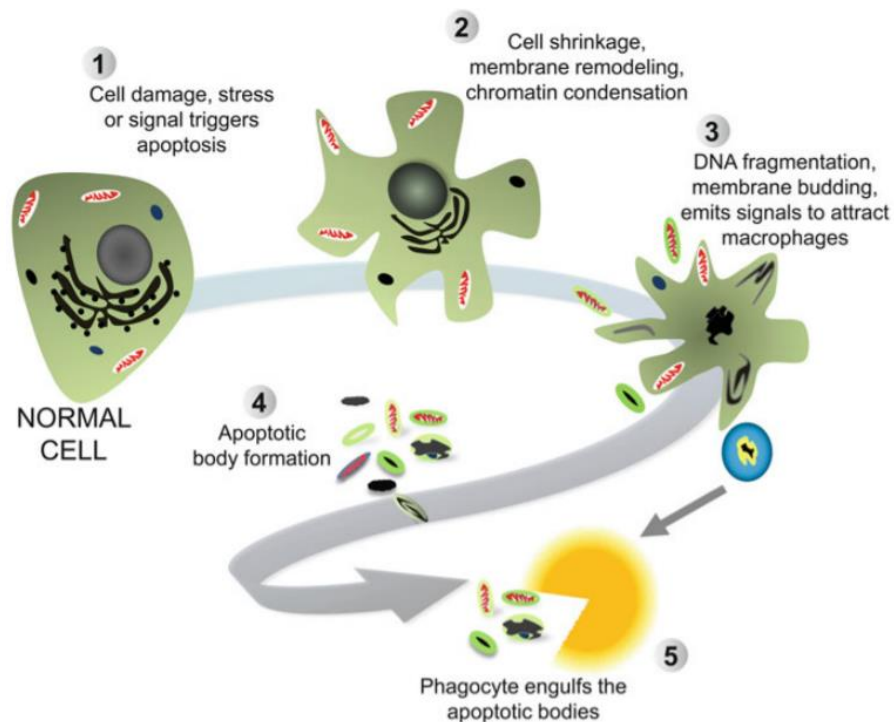


Figure 6 The schematic of cellular morphologic changes during the apoptosis death process (Singh & Bose, 2015).

2.1.3.2.1 Extrinsic pathway

The extrinsic signaling pathways are activated through death receptors, which are members of the tumor necrosis factor receptor (TNF-R) superfamily (Redza-Dutordoir & Averill-Bates, 2016). These ligands and receptors include FasL/FasR, TNF- α /TNFR1, Apo3L/DR3, Apo2L/DR4 and Apo2L/DR5 (Elmore, 2007). Apoptosis pathway is induced when ligand bind to its receptor and generates the signaling to recruit adaptor protein such as Fas-associated death domain (FADD) or TNF receptor-associated death domain (TRADD) depending on ligand and receptor model and form death-inducing signaling complex (DISC) (Redza-Dutordoir & Averill-Bates, 2016; Samira Goldar, 2015; Zimmermann & Green, 2001). Then, procaspase-8 or -10 is also recruited to interact with adaptor protein via dead effector domain and led to be activated into caspase-8/-10 which plays a role to activate the downstream executioner caspase including caspases-3 and -7 and hence apoptosis (figure 7) (Redza-Dutordoir & Averill-Bates, 2016; Samira Goldar, 2015).

2.1.3.2.2 Intrinsic pathway

The initiation of the intrinsic signaling pathway is emerged through mitochondrial by several stimuli as mentioned previously (Elmore, 2007). In addition to the caspase, the Bcl-2 (B-cell lymphoma 2) family of proteins controls and regulates the apoptotic mitochondrial pathway (Singh & Bose, 2015). The Bcl-2 family members can be separated into pro-apoptotic and anti-apoptotic members such as pro-apoptotic; Bcl-10, Bax, Bak, Bid, Bad, Bim, Bik, and Blk and anti-apoptotic; Bcl-2, Bcl-x, Bcl-XL, and Bcl-XS (Elmore, 2007). Additionally, the regulation of these proteins such as Bax and Bcl-2 initiates through the tumor suppressor protein p53 (Elmore, 2007). Under normal conditions, anti-apoptotic proteins are localized on the outer mitochondrial membrane (OMM) that inhibit the activity of pro-apoptotic (Redza-Dutordoir & Averill-Bates, 2016). However, the stress condition can upregulate the expression of pro-apoptotic proteins and then activate them to induce apoptosis (Redza-Dutordoir & Averill-Bates, 2016). The activation of Bax or Bak can increase the membrane permeability of mitochondrial that leads to the release of cytochrome c into the cytosol (Lopez & Tait, 2015; Zimmermann & Green, 2001). After that, the formation of the apoptosome, consisting of cytochrome c and apoptotic protease activating factor -1 (Apaf-1), is generated in the cytosol (Lopez & Tait, 2015). Subsequently, procaspase-9 is recruited to the apoptosome, followed by the activation of procaspase-9 (figure 7). The apoptosome also recruits the executioner caspase-3 and -7, which are activated by active caspase-9 (Lopez & Tait, 2015; Zaman et al., 2014).

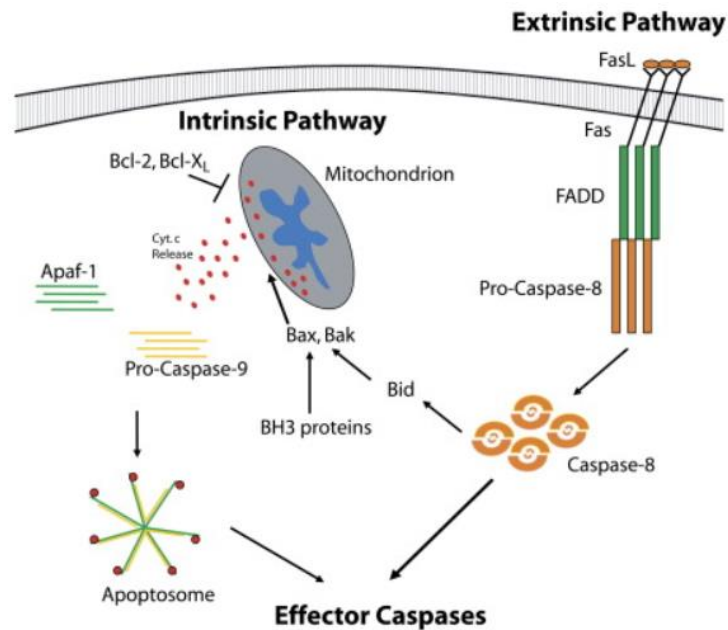


Figure 7 The intrinsic and extrinsic pathway of apoptosis (Schafer & Kornbluth, 2006)

2.1.3.2.3 Ethanol and apoptosis

As mentioned in the pathophysiology of ALD, the metabolism of ethanol through alcohol dehydrogenase enzyme (ADH) decreases the ratio of $NAD^+/NADH$ that involves to dysfunction of the mitochondrial respiratory chain and then promotes the leakage of ROS from mitochondria (Wang et al., 2016). Additionally, chronic alcohol consumption can also upregulate the expression of CYP2E1, resulting in the overproduction of ROS and promoting oxidative stress (Hoek et al., 2002). It was found that ROS can impair mitochondrial protein and mitochondrial DNA and activate the mitochondrial permeability transition (MPT) by direct oxidation of the pore complex. Subsequently, the cytochrome c was released from mitochondrial to the cytosol via opening pore and triggered the apoptosis of liver cells (Hoek et al., 2002; Wang et al., 2016). According to Morio et al. 2013, ROS generating from ethanol metabolism can also trigger apoptosis via the MAPKs pathway by stimulating the phosphorylation of JNK and p38. JNK and p38 further downregulate the expression of Bcl-2 protein and upregulate the expression of Bax

protein, resulting in promoting cytochrome c release and caspase activation, respectively (Morio et al., 2013).

2.1.4 The current management of ALD

According to the pathophysiology of ALD, it involved uncontrol alcohol consumption that leads to change the behavior and cognition of patients including craving alcohol and alcohol withdrawal symptoms (Leggio & Lee, 2017; Mosoni et al., 2018). This sign of this illness condition is called alcohol use disorder or AUD. The most effective treatment of ALD is alcohol abstinence. However, sudden stop drinking alcohol can induce withdrawal symptoms including headache, anxiety, and tonic-clonic seizures (Muncie et al., 2013). The primary medication for alcohol withdrawal syndrome is long-acting benzodiazepines such as chlordiazepoxide and diazepam (Muncie et al., 2013). Benzodiazepines can reduce symptoms and prevent seizures. However, anticonvulsants can be used as an alternative treatment for alcohol withdrawal syndrome, but they cannot prevent seizures (Muncie et al., 2013). Moreover, some medications, including acamprosate, disulfiram, and naltrexone, were approved by the US FDA to support the alcohol abstinence of patients who are addicted to alcohol (Leggio & Lee, 2017; Williams, 2005). In AUD patients with advanced liver disease, the literature review of Mosoni C et al. indicated that baclofen, a selective GABA-B receptor agonist, can be used as medicine for AUD and advanced liver disease. They revealed that baclofen has efficacy to prevent alcohol relapse and reverse the progression of hepatitis as well as it has a safety profile (Mosoni et al., 2018).

As mentioned before, ALD is a chronic disease with a broad spectrum of hepatic lesions. For hepatitis or liver cirrhosis, corticosteroid was widely used as an anti-inflammatory medicine to suppress the immune response and proinflammatory cytokine response. The recommendation regimen from the guideline is prednisolone 40 mg orally per day for 4 weeks or methylprednisolone 32 mg per day by intravenous injection (Singal et al., 2018). Although corticosteroids can improve the

hepatitis condition and provide short-term survival benefits for severe hepatitis patients, several contraindications include gastrointestinal bleeding and active infection (Barve et al., 2008). Pentoxifylline is an alternative drug for hepatitis patients with renal failure. It is a nonselective phosphodiesterase inhibitor that can improve the amount of adenosine 3',5'-cyclic monophosphate (cAMP) and follow by decreasing the production of the pro-inflammatory cytokine, tumor necrosis factor (TNF) (Barve et al., 2008). The clinical data from meta-analysis revealed that pentoxifylline showed a benefit to reducing the risk of renal failure and death from hepatorenal syndrome (Singal et al., 2018). However, there is no FDA-approved medicine to treat ALD directly and efficiently (Leggio & Lee, 2017; Osna et al., 2017). Therefore, the research study for developing a new medication approach to ameliorate the progression of ALD is necessary for ALD patients who suffer from hepatic lesions.

2.2 Tetrahydrocurcumin

2.2.1 The overview of tetrahydrocurcumin

Tetrahydrocurcumin (THC; 1,7-bis (4-hydroxy-3-methoxyphenyl) heptane-3,5-dione) is one of the major active hydrogenated metabolites of curcumin that was first identified in 1978 by Holder et al. (Pan et al., 1999); (Holder et al., 1978). The chemical structure of THC consists of a phenolic hydroxyl functional group and β -diketone moiety that can be tautomerized into keto and enol forms as shown in Figure 8 (Lee et al., 2005). The keto form of THC is predominantly seen in the polar solvent at acidic conditions, but when the amount of organic solvent is increased and under basic conditions, THC will be converted to its enol form (Bhatia et al., 2016). The pharmacological activities of THC are similar to curcumin, including anti-inflammatory, anticancer, and especially antioxidant (Aggarwal et al., 2014). However, THC provides a more significant antioxidant effect than curcumin due to its phenolic hydroxyl and β -diketone moieties that act as a radical scavenger (Osawa et al., 1995). Moreover, THC has higher stability than curcumin in phosphate buffer pH

7.2 at 37 °C (Pan et al., 1999). Curcumin is a basic labile compound decomposing more than 90% after incubation under this condition by breaking the heptadienedione chain into ferulic acid, vanillin, and feruloylmethane (Jankun et al., 2016). However, THC was very stable because there was no α , β dienes (Pan et al., 1999). In a pharmacokinetic study, Okada et al. reported that THC has a greater oral bioavailability than curcumin in the mice model (Okada et al., 2001). For the toxicity profile of THC, Majeed M et al. investigated the subchronic toxicity for 90 days and reproductive and developmental toxicity in Wistar rat. The results showed that THC was safe at doses of up to 400 mg/kg which it was 10 times higher than effective dose of THC without any adverse effect (Majeed et al., 2019).

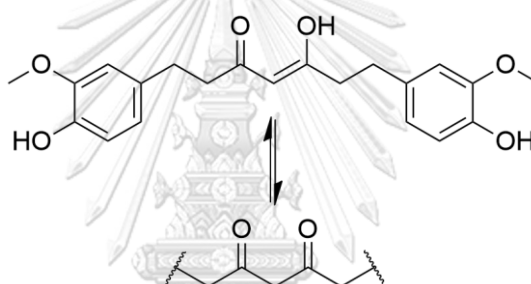


Figure 8 The chemical structure of tetrahydrocurcumin (THC) and its tautomerization

2.2.2 The pharmacological activity of THC

From an extensive literature review, several publications addressed the preventive effect of THC against oxidative stress conditions by chemical inducers *in vitro* and *in vivo* as summarized in Table 2.

Table 2 Studies on the protective effect of tetrahydrocurcumin against chemical-induced oxidative stress

Author (year)	Experiment model	Research findings	Ref.
Vacek JC et al. (2018)	<i>In vitro</i> model mouse brain endothelial cells (bEnd3) cells were stimulated with Homocysteine (Hcy) 500 μ M to mimic neurodegenerative disorders	- THC 15 μ M exerted neuroprotective effects against Hcy-induced toxicity by reducing intracellular ROS generation and suppressing the apoptosis of bEnd3 cells.	(Vacek et al., 2018)
Murugan P. and Pari L. (2006)	<i>In vivo</i> model streptozotocin has been used to induce diabetic Wistar rats	- THC at 80 mg/kg exhibits the highest efficacy that can increase plasma insulin level, resulting in the reduction of blood glucose level. - TBARS and hydroperoxides in hepatic and renal tissue were reduced after being treated with THC that has a higher effect than curcumin. - Antioxidant enzymes (SOD, CAT, GPx, GST) and other antioxidants (GSH, vitamin C, and vitamin E) were increased in the THC treatment group.	(Murugan & Pari, 2006)

Author (year)	Experiment model	Research findings	Ref.
Okada K et al. (2001)	<p><i>In vivo</i> model</p> <p>Renal injury mice were induced by ferric nitrilotriacetate</p>	<ul style="list-style-type: none"> - TBARS, HNE, and 8-OHdG were reduced in the THC treatment group. - THC improved the suppression of the activity of antioxidant enzymes, including GPx, NADPH: QR, and GST. 	(Okada et al., 2001)
Li K et al. (2019)	<p><i>In vivo</i> model</p> <p>Diabetic mice were induced by streptozotocin.</p> <p><i>In vitro</i> model</p> <p>H9c2 cardiomyocyte Lines were induced diabetic cardiomyopathy by using a high glucose level</p>	<ul style="list-style-type: none"> - THC can protect H9c2 cells from glucose-induced cell death, and it can also inhibit the production of ROS in H9c2 cells by stimulating the SIRT1 signal pathway. - The cardiac hypertrophy and cardiac fibrosis in mice were improved in the THC treatment group at a dose of 120 mg/kg/day. 	(Li et al., 2019)

Author (year)	Experiment model	Research findings	Ref.
Pari L. and Murugan P. (2006)	<i>In vivo model</i> Renal injury Wistar rats were induced by chloroquine	<ul style="list-style-type: none"> - THC 80 mg/kg can significantly improve kidney function. - The level of TBARS and hydroperoxides were reduced in the THC treatment group. - The number of non-enzymatic antioxidants and enzymatic antioxidant activity was increased in the THC treatment group. 	(Pari & Murugan, 2006)
Nakmareong S et al. (2012)	<i>In vivo model</i> N-nitro-L-arginine methyl ester (L-NAME) was administered to Sprague-Dawley rats to develop hypertension and vascular remodeling	<ul style="list-style-type: none"> - 100 mg/kg per day of THC can reverse the vascular remodeling by decreasing aortic wall thickness and improving the elasticity of the thoracic aorta. - Moreover, THC can reduce the generation of superoxide radicals and plasma malondialdehyde and protein carbonyl levels. THC can also restore the level of GSH depleted by L-NAME. 	(Nakmareong et al., 2012)

Author (year)	Experiment model	Research findings	Ref.
Sangartit W et al. (2014)	<p><i>In vivo model</i></p> <p>Adult male ICR mice were treated with 100 mg/l of CdCl₂ to induce hypertension, arterial stiffness and vascular remodeling</p>	<ul style="list-style-type: none"> - 100 mg/kg/day of THC 5 days per week for 8 weeks can reverse the elevation of blood pressure in mice exposed to Cd. - The mechanism of action of THC is to upregulate eNOS and restore the level of NO, markedly decrease in MMP-2 and MMP-9 levels and restore the capacity of the antioxidant defense system. 	(Sangartit et al., 2014)
Greeshma M et al. (2015)	<p><i>In vivo model</i></p> <p>Wistar rats were administered by vincristine sulfate (75 µg/kg) to induce Peripheral neuropathy</p>	<ul style="list-style-type: none"> - THC 80 mg/kg exerted protective effects against vincristine-induced peripheral neuropathy - THC can also restore the activity of antioxidant enzymes including SOD, CAT, and GPx as well as GSH level as compared to the vincristine treated group. On the other hand, the level of lipid peroxidation and Nitric oxide was decreased. 	(Greeshma et al., 2015)

Author (year)	Experiment model	Research findings	Ref.
Song KI et al. (2015)	<p><i>In vivo</i> model Wistar rats were induced nephrotoxicity by using cisplatin.</p> <p><i>In vitro</i> model LLC-PK1 cells were induced by 25 μM cisplatin.</p>	<ul style="list-style-type: none"> - Cell viability was increased in the THC treatment group in a dose-dependent manner. - The renal histological and renal function were significantly recovered by THC treatment. 	(Song et al., 2015)
Sangartit W et al. (2016)	<p><i>In vivo</i> model Iron overload ICR mice were induced by intraperitoneal injection of iron sucrose 10 mg/kg per day for 8 weeks</p>	<ul style="list-style-type: none"> - THC 50 mg/kg can reduce the level of iron in serum and attenuate the hypertension condition. - In mice, the oxidative stress condition was improved in THC treatment by lowering superoxide anion and MDA while increasing GSH levels in the blood. - The combination of deferiprone and THC therapy exerted higher protective effects against iron overload-induced cardiovascular dysfunction than THC or deferiprone monotherapy. 	(Sangartit et al., 2016)

In addition, Park studied the neuroprotective effect of THC by using Hippocampal HT22 cells as *in vitro* model (Park et al., 2019). HT22 cell was induced by glutamate, causing the increase in ROS species affecting cell death by oxidative stress. As a result, ROS can be reduced after pretreatment of the cell with THC in a dose-dependent manner. Furthermore, THC inhibited apoptosis cell death via MAPKs blockage with ERK, JNK, and p38 reduction. In an *in vivo* study, Pari L et al. (Pari & Murugan, 2004) investigated the protective effect of THC against erythromycin estolate-induced hepatotoxicity in the Wister rat model. The results indicated that the levels of biomarker enzymes of liver damage, including AST, ALT, ALP, and bilirubin, are decreased when administered the THC to the rat for 15 days via oral administration. In the THC treatment group, the level of an oxidative compound such as thiobarbituric acid-reactive substances (TBARS) and hydroperoxides is reduced, and the level of GSH is increased compared to the negative control group. Based on their results, THC has hepatoprotection activity by restoring hepatic antioxidant capacity showing higher activity than the positive control, silymarin at doses 80 mg/kg and 200 mg/kg, respectively. THC also showed the hepatoprotection activity against chemical intoxication-induced hepatotoxicity, including chloroquine (Pari & Amali, 2005), acetaminophen (Luo et al., 2019), and arsenic (Muthumani & Miltonprabu, 2015) by scavenging free radicals, restoring hepatic antioxidation level and their activity, suppressing CYP2E1 activity, and activating of Keap-Nrf2 pathway to produce proteins or enzyme that involve in the antioxidant defense system.

A previous study also demonstrated that THC could diminish free fatty acid-induced hepatic steatosis through the HepG2 human hepatocellular carcinoma cell line model using an *in-vitro* model. The lipid droplet accumulation and triglyceride (TG) level in hepatocyte cells were improved by THC treatment. The protective effect of THC on hepatic steatosis was exerted through downregulation of lipogenesis transcription factor including sterol regulatory element-binding protein 1 (SREBP-1c), peroxisome proliferator-activated receptor gamma (PPAR- γ), and fatty acid

synthase (FAS) via activation of adenosine monophosphate-activated protein kinase (AMPK) in a dose-dependent manner. On the other hand, THC can induce lipolysis through upregulation of PPAR- α , promoting the β -oxidation of fatty acids in a dose-dependent manner (Chen et al., 2018). Therefore, THC could be an effective agent for preventing or managing hepatic steatosis. THC activity against toxic compound-induced hepatotoxicity and free fatty acid-induced hepatic steatosis indicated that THC could be a potential therapeutic agent for hepato-protection against alcohol-induced liver injury.

2.2.3 The limitation of THC

Although THC has several pharmacological activities, it cannot be used as a therapeutic agent due to THC is a lipophilic compound with a LogP value of 3.124 (Bhaskar Rao et al., 2014), resulting in its poor water solubility at 0.0067 mg/ml (Setthacheewakul et al., 2011). These physicochemical properties may limit gastrointestinal absorption resulting in low bioavailability of THC in the systemic circulation (Novaes et al., 2017). To overcome these drawbacks, the encapsulation technique was applied to improve the water solubility of THC. Setthacheewakul S et al. (Setthacheewakul et al., 2011) encapsulated THC with a solvent mixture including a surfactant, oil, and floating agent called a novel self-emulsifying floating drug delivery system (SEFDDS). The result showed that SEFDDS provides the controlled release of THC over 8 h with 80% of THC released from SEFDDS and only 30% of THC released from non-formulated THC in simulated gastric fluid (SGF) condition, indicating that the more excellent solubility of THC encapsulated with SEFDDS over free THC.

2.3 Prodrug design approach

2.3.1 Introduction of the prodrug design approach

The prodrug design approach has been used to overcome the barriers of oral drug administration. The most general barriers to oral drug delivery include

poor water solubility, poor absorption, extensive metabolism, and rapid elimination from the systemic circulation (Stella et al., 2007). A prodrug is a chemical modification of pharmacologically active compounds to improve their properties in favor of oral drug administration by conjugating with promoieties via a temporary covalent bond linkage such as ester or amide bond (Sanchez & Ferreira, 2019). A pro moiety is selected depending on the objective of prodrug design, availability of functional groups in a drug molecule, the safety profile of the conjugated prodrug and pro moiety compound, and the conversion mechanism of the prodrug *in vivo* to generate the free parent drug (Vig et al., 2013). The prodrugs are theoretically inactive compounds, which must be transformed into an active compound by a chemical or an enzymatic reaction *in vivo* to release the active compound and exhibit its pharmacological effect (Figure 9) (Huttunen et al., 2011; Vig et al., 2013).

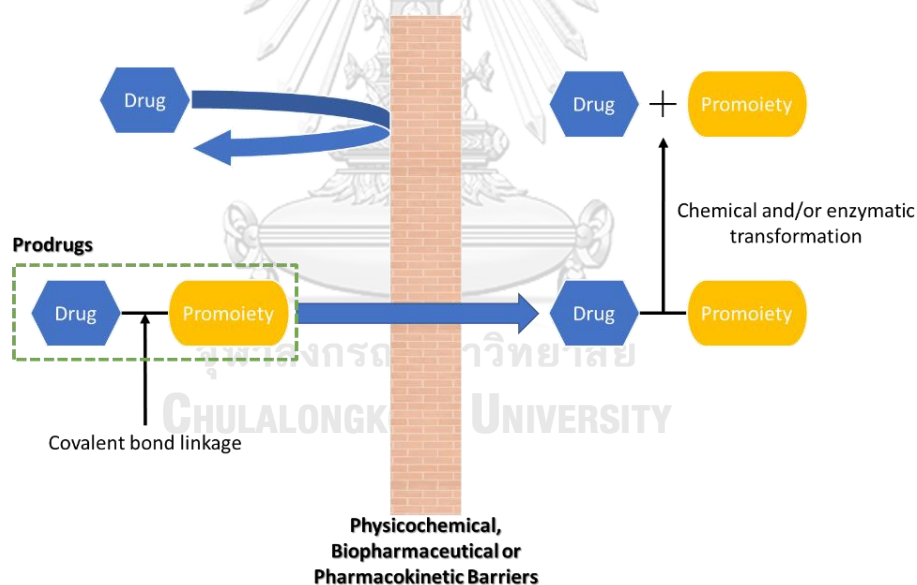


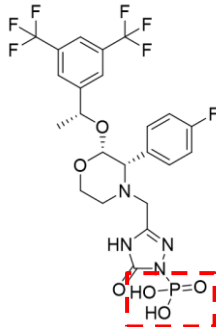
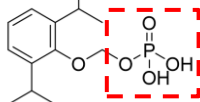
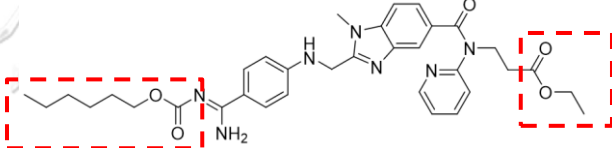
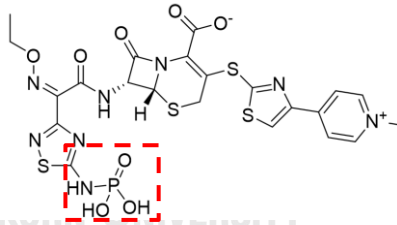
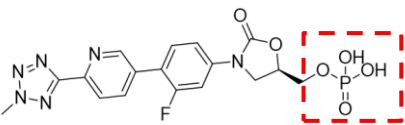
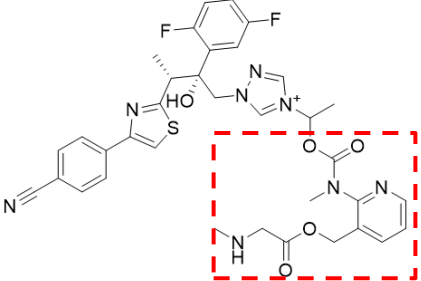
Figure 9 Schematic representation of prodrug design concept (Adapted from Ref. (Huttunen et al., 2011))

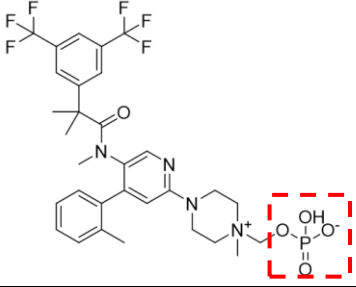
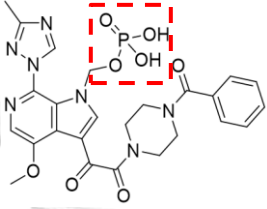
2.3.2 The enhancement of water solubility by prodrug design approach

Oral drug delivery is the most common route for drug administration. It is a non-invasive approach, administered as accurately and measured dose, and is

cheaper than another approach (Bandopadhyay et al., 2020). However, the water solubility profile of drug substances is the critical parameter for the pharmacological activity of oral drug delivery. When the drug as solid dosage form was intake through the gastrointestinal tract, it must be dissolved into a solution that was available for absorption across the intestinal membrane and then entered the systematic blood circulation (Stegemann et al., 2007). The prodrug design approach can enhance the water solubility of a lipophilic compound by conjugation with several promoiety compounds including phosphate, amino acid, and dicarboxylic acid. For instance, amprenavir is an antiretroviral drug that was classified as the Biopharmaceutics Classification System (BCS) class 2 drug, low water solubility and high permeability (Savla et al., 2017). According to its physicochemical property, the patient must be taken a high dose of the drug per day (Rautio et al., 2008). To overcome this drawback, the phosphate ester of amprenavir was developed as the fosamprenavir resulting that fosamprenavir having higher solubility than the parent compound (3 mg/ml vs. 0.04 mg/ml) (Furfine et al., 2004). As a result, fosamprenavir can be formulated as a tablet dosage form with tablet size reduction. The success of prodrug design is demonstrated by the last twelve years, 2008-2020, that there are 8 FDA-approved prodrugs designed to improve water solubility as shown in table 3 (Mullard, 2021; Sanches & Ferreira, 2019).

Table 3 The lists of FDA-approved prodrugs during 2008-2020 whose objective is to enhance water solubility.

Prodrug name	Chemical structure	year
Fosaprepitant dimeglumine		2008
Fospropofol disodium		2008
Dabigatran etexilate		2010
Ceftaroline fosamil		2010
Tedizolid phosphate		2014
Isavuconazonium		2015

Prodrug name	Chemical structure	year
Fosnetupitant		2018
Fostemsavir		2020

2.3.2.1 Dicarboxylic acid

Dicarboxylic acid compounds, namely succinic and glutaric acid, are widely used as a promoiety or carrier to improve the aqueous solubility of the parent compound via conjugation with an ester bond linkage that has a free terminal carboxylic group (Muangnoi et al., 2018; Muangnoi et al., 2021). The ionization and polarity of the free terminal carboxylic group play a key role in modulating the physicochemical properties of the parent compound in the form of a prodrug. According to the ability of dicarboxylic acid to enhance water solubility, paclitaxel and docetaxel are widely used as anticancer agents with low water solubility profiles. To improve the physicochemical property, they were conjugated with malic acid. As a result, the malyl prodrugs have higher water solubility than the parent compound 20 to 90 times, especially to their salts formed. The anticancer activity was also determined using an in vivo model. The results demonstrated a higher effect in paclitaxel prodrug (Damen et al., 2000) and a similar effect in docetaxel prodrug compared with their parent compounds (Du et al., 2007) as shown in Figure 10.

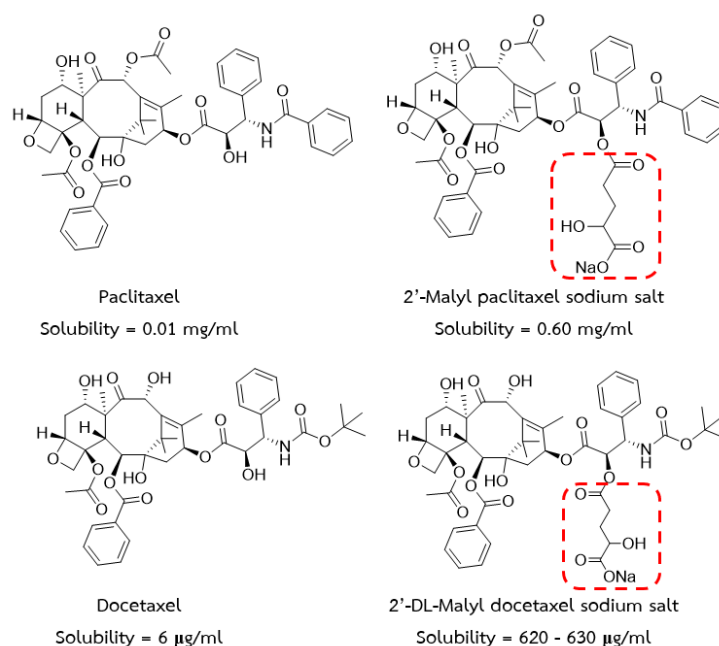


Figure 10 the chemical structure of paclitaxel and docetaxel malyl prodrug sodium salt.

Recently, Muangnoi et al. have modified the chemical structure of curcumin by conjugating with glutaric acids via ester bond linkage giving the curcumin-diglutaric acid as a diglutaric prodrug as shown in Figure 11 (Muangnoi et al., 2018). The ester bond linkage of the curcumin prodrug was broken down under alkaline conditions, and the free curcumin was released entirely within 2 hours. This study reveals that the water solubility of the prodrug was approximately 100 times higher than curcumin (7.48 µg/mL vs. 0.068 µg/mL). In addition, the lipophilicity of the prodrug was lower than curcumin with a Log P value of 1.79 and ranging from 2.56 to 3.29, respectively. The antinociceptive effect of curcumin-diglutaric acid was also evaluated in the mice model, and this study compared with curcumin, the parent compound. The mice were pre-treated with curcumin or curcumin-diglutaric acid in various doses through oral administration. The hot plate method was used to monitor the behavior response of mice. The results showed that curcumin-diglutaric acid exhibits a higher antinociceptive effect than curcumin regarding the increased water solubility that may enhance drug absorption. In 2021, Muangnoi et al. also

developed the ester derivative of lutein by using the same promoiety compound, glutaric acid. The lutein-diglutaric acid exhibits more potent than lutein for protecting against hydrogen peroxide-induced retinal pigment epithelial cells injury (Muangnoi et al., 2021). These indicate that glutaric could be used as a potential promoiety compound to improve physicochemical properties and pharmacokinetic of an interesting molecule.

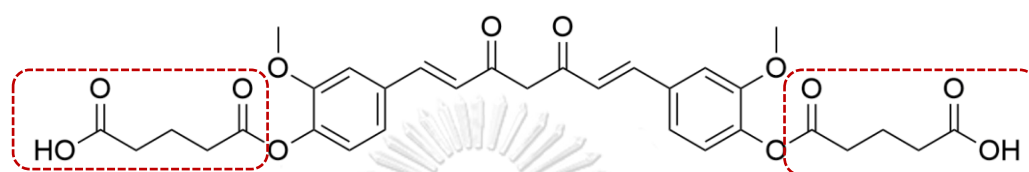


Figure 11 The chemical structure of curcumin-diglutaric acid prodrug

2.4 Cell-based model for ethanol-induced hepatotoxicity

To predict the pharmacological response of substances, competent cell lines have been used to explore the pharmacodynamic or efficacy of substances. The results from *in vitro* study can be used to assume the pharmacodynamic effect in animals or humans. The cell-based models are widely used for pharmacological evaluation prior to the animal models because the cell-based model is easier to handle the experimental. It is also lower cost and less time-consuming compared to animal or human clinical study. Furthermore, the mechanism of action of treated substances can be elucidated by tracking the alteration of targeted molecular and cellular biomarkers (Welsh et al., 2009). Although the human primary hepatocytes are the most excellent *in vitro* model comparable to *in vivo* for drug-induced hepatotoxicity studies, their scarce availability of suitable human liver, limited life span, and phenotypic instability that CYP gene and other enzymes change their expression pattern during cell culture limit their use as *in vitro* model for hepatotoxicity study (Castell et al., 2006). To overcome these drawbacks, immortalized liver-derived cell lines or human hepatocellular carcinoma cell lines, HepG2, are favorable for hepatotoxicity study (Gerets et al., 2012). These cells have

the advantage of high proliferation, easy handling, stable phenotype, and suitable experimental reproducibility (Gómez-Lechón et al., 2014). However, there is also some limitation of using these cells like its lower CYP enzyme expression than human primary hepatocytes, causing the poor response of toxicants (Westerink & Schoonen, 2007). Nevertheless, several pieces of evidence indicate that HepG2 can be used as an in vitro model to study the effect of protective agents against ethanol-induced liver damage as shown in table 4.

Table 4 the summarize of research studies that have been used HepG2 cell line as an in vitro model for ethanol-induced hepatotoxicity

Author (year)	Cell culture condition	Active compound	Concentrations of ethanol and incubation time	Ref.
Farshori NN et al. (2015)	DMEM supplemented with 10% FBS, 0.2% sodium bicarbonate and antibiotic-antimycotic solution (100x, 1 ml/100 ml of medium) Incubation at 37 °C under 5% CO ₂ .	<i>L. coronopifolia</i> extract (Pretreated 24 h)	400 mM, 24 h	(Farshori et al., 2013)
Herath KHINM et al. (2018)	DMEM supplemented with 10% FBS and 1% antibiotics (100 U/ml of penicillin and 100 µg/ml of streptomycin) Incubation at 37 °C under 5% CO ₂ .	<i>S. quelpaertensis</i> leaves 80% ethanol extract	800 mM, 24 h	(Madushani Herath et al., 2018)

Author (year)	Cell culture condition	Active compound	Concentrations of ethanol and incubation time	Ref.
Sun X et al. (2018)	DMEM supplemented with 10% FBS and 1% antibiotics (100 U/ml of penicillin and 100 µg/ml of streptomycin) Incubation at 37 °C under 5% CO ₂ .	Paeonol (Pretreated 24 h)	300 mM, 24 h	(Sun et al., 2018)
Zhang Y et al. (2018)	DMEM supplemented with 10% FBS and appropriate antibiotics Incubation at 37 °C under 5% CO ₂ .	Gastrodin (Pretreated 4 h)	600 mM, 24 h	(Zhang et al., 2018)
Yuan R et al. (2018)	DMEM supplemented with 10% FBS and 1% antibiotics (100 U/ml of penicillin and 100 µg/ml of streptomycin) Incubation at 37 °C under 5% CO ₂ .	Schisandra chinensis acidic polysaccharide	3% v/v, 24 h	(Yuan et al., 2018)

Author (year)	Cell culture condition	Active compound	Concentrations of ethanol and incubation time	Ref.
Rabelo ACS et al. (2018)	DMEM supplemented with 10% FBS, 1% glucose, 1% glutamine, and 1% antibiotics (100 U/ml of penicillin and 100 µg/ml of streptomycin) Incubation at 37 °C under 5% CO ₂ .	Hydroethanolic extract of <i>B.</i> <i>trimera</i> (Pretreated 3 h)	200 mM, 24 h	(Rabelo et al., 2018)
Nagappan A et al. (2018)	DMEM supplemented with 10% FBS and 1% antibiotics (100 U/ml of penicillin and 100 µg/ml of streptomycin) Incubation at 37 °C under 5% CO ₂ .	Gomisin N (Pretreated 3 h)	50 mM, 24 h	(Nagappan et al., 2018)
Yang S et al. (2020)	DMEM supplemented with 10% FBS and 1% antibiotics (100 U/ml of penicillin and 100 µg/ml of streptomycin) Incubation at 37 °C under 5% CO ₂ .	D-isofloridoside (Pretreated 2 h)	500 mM, 24 h	(Yang et al., 2020)

Author (year)	Cell culture condition	Active compound	Concentrations of ethanol and incubation time	Ref.
Sabitha R et al. (2020)	DMEM culture and maintained at 37°C, 5% CO ₂ and 95% air environment.	p-Coumaric acid (Pretreated 1 h)	100 mM, 24 h	(Sabitha et al., 2020)

Based on the previous research as shown in table 4, the HepG2 cells were incubated for 24 h with ethanol at concentrations ranging from low concentration 50 mM to high concentration 800 mM. Most of them used ethanol higher than 100 – 200 mM, which was reported as the physiological blood of binge drinkers since high concentration significantly promotes cell response (Henzel et al., 2004; Zhang et al., 2018). Consequently, HepG2 cells died and biomarkers of oxidative stress were changed. The modulation of biomarkers of oxidative stress includes the decreasing of enzymatic antioxidant activity (SOD, CAT, and GPx), the decreasing of GSH level, and the increase of lipid peroxidation or malondialdehyde (MDA) (Lowe, 2014). The antioxidant agent can reverse the alteration of these biomarkers resulting in increased cell viability of HepG2 cells. Therefore, the HepG2 cell line could be used as an *in vitro* model to study the hepatoprotective effect of THC and TDG against ethanol-induced hepatotoxicity.

Hence, the THC prodrug containing glutaric acid as a promoiety will be an interesting approach to enhance the water solubility of THC. In the present study, THC-diglutaric acid (TDG, Figure 11) was synthesized via an esterification reaction. The physicochemical properties, including water solubility, Log P value, stability, and drug release, were determined. The protective effect against alcohol-induced hepatotoxicity was also evaluated in the human hepatocarcinoma cell line.

CHAPTER 3 RESEARCH METHODOLOGY

3.1 Chemicals, Cell lines, Media, and Equipment

- 1) Tetrahydrocurcumin, Zhonglan Industry, China
- 2) Glutaric anhydride, TCI, Japan
- 3) N, N-Diisopropylethylamine (DIPEA), Oakwood chemical, USA
- 4) Dichloromethane, Carlo Erba, France
- 5) Hexane, RCI Labscan, Thailand
- 6) Acetonitrile, Thomas Baker, India
- 7) Chloroform-D (CDCl_3), Cambridge Isotope Laboratory, Inc., USA
- 8) Silica gel 60 – 200 μm (70 – 230 mesh), SiliCycle Inc., Canada
- 9) Formic acid, Carlo Erba, France
- 10) UHQ Water System, Milli-Q, USA
- 11) Nuclear Magnetic spectrometer 500 MHz, Jeol, Japan
- 12) High-performance liquid chromatography-mass spectrometry (HPLC/MS) consisting of Dionex Ultimate 3000 HPLC, The Thermo Fisher Scientific, USA, coupled with MicrOTOF-QII mass spectrometer, Bruker, Germany
- 13) Bruker/Alpha platinum ATR, Bruker, USA
- 14) Differential scanning calorimeter (DSC 8000), PerkinElmer, USA
- 15) Shimadzu Nexera XR UHPLC system, SHIMADZU SCIENTIFIC INSTRUMENTS, USA
- 16) Human hepatocellular carcinoma (HepG-2, ATCC), USA
- 17) Dulbecco's Modified Eagle Medium (DMEM) (Gibco, 12800), USA
- 18) Fetal bovine serum (FBS) (Gibco, 16000-044), USA
- 19) Penicillin-Streptomycin (Gibco, 15140-122), USA
- 20) Vortex mixer, Model: Vortex-Genie 2, Scientific Industries, USA
- 21) pH meter, Model: SevenEasyTM, METTLER TOLEDO, Italy
- 22) Stirrer, Model: IKA® C-MAG HS-7

- 23) Centrifuge (Hettich instrument 1706-01 Rotina 380R Benchtop), USA
- 24) Microplate reader (CLARIOstar, BMG LATECH, Germany)
- 25) 96-well plates for cell culture (Corning), USA
- 26) 48-well plates for cell culture (Corning), USA
- 27) 96-well black/clear bottom plates for cell culture (Corning), USA
- 28) 6-well plates for cell culture (Corning), USA



Methodology of study

The methodology of this study is demonstrated in Figure 12.

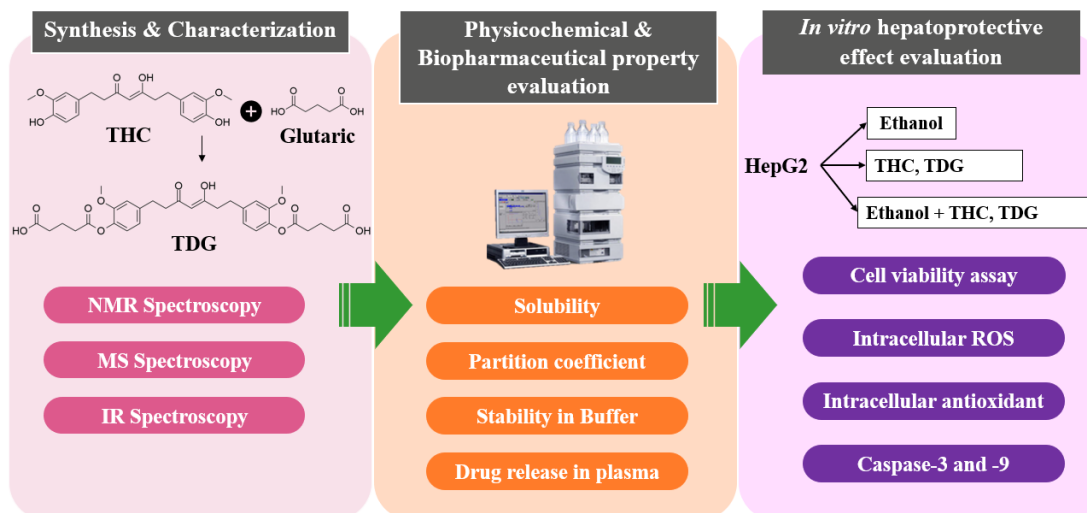


Figure 12 Methodology of the study



3.2 Synthesis of tetrahydrocurcumin-diglutaric acid conjugate

The synthesis scheme of TDG is depicted in Figure 13. In brief, a solution of THC (1.00 g, 2.69 mmol) in 5 mL anhydrous dichloromethane was added in the round-bottom flask containing a mixture of glutaric anhydride (1.23 g, 10.74 mmol) and DIPEA (0.73 mL, 5.37 mmol). The reaction was set for stirring under a nitrogen atmosphere at room temperature for 3 h. After that, the completeness of the reaction was monitored using TLC (hexane: dichloromethane: acetone = 4:4:2 with 1% formic acid) by observing the disappearance of the THC spot. The mixture solution was concentrated under reduced pressure using a rotary evaporator, and the residual was re-dissolved with ethyl acetate. The ethyl acetate solution was performed liquid-liquid extraction using 0.1 M HCl and DI water successively to remove water-soluble compounds such as DIPEA and excess free glutaric acid. The ethyl acetate layer was collected, and the residual water was adsorbed using anhydrous sodium sulfate. Then, the dried ethyl acetate layer was concentrated under reduced pressure. The obtained crude product was purified by column chromatography on silica gel 60 – 200 μm (70 – 230 mesh) using hexane, dichloromethane, and acetone as a mobile phase system at ratio 1:0:0 to 6:2:2 with 1% formic acid. Additionally, all purified fractions were collected in one container and subjected to further purification crystallization in a mixture of dichloromethane and hexane. The product TDG was obtained as a light-yellow solid. The chemical structure of TDG was identified by NMR spectroscopy, mass spectrometer, and IR spectroscopy. For NMR spectroscopy, the sample was dissolved in CDCl_3 . Chemical shifts of ^1H and ^{13}C were given as δ values in parts per million (ppm) relative to the CDCl_3 peak at $^1\text{H} = 7.26$ ppm and $^{13}\text{C} = 77.0$ ppm, and coupling constants were reported as J values in Hertz (Hz).

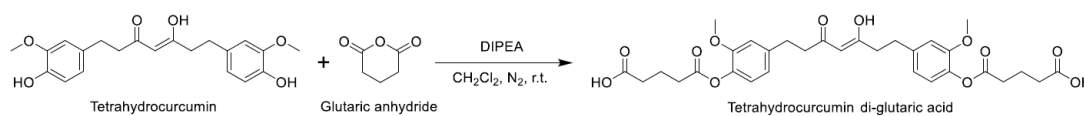


Figure 13 Synthesis scheme of tetrahydrocurcumin-di-glutaric acid (TDG) conjugate via an ester bond linkage.

3.3 Physicochemical properties evaluation

3.3.1 Preparation of buffer solutions

In this study, pH 1.2, 4.5, 6.8, and 7.4 buffer solutions were prepared according to the United States Pharmacopeia (USP) as described below:

Hydrochloric acid buffer (pH 1.2) was prepared by dissolving 0.7455 g of potassium chloride (KCl) in water 50 ml to make 0.2 M KCl. After that, 50 ml of 0.2 M KCl was mixed with 85 ml of 0.2 M HCl in a 200 ml volumetric flask followed by adjusting to volume with water.

Acetate buffer (pH 4.5) was prepared by dissolving 2.99 g of sodium acetate ($\text{NaC}_2\text{H}_3\text{O}_2 \cdot 3\text{H}_2\text{O}$) 2.99 g with 14 ml of 2 N acetic acid solution in a 1000 ml volumetric flask followed by adjusting to volume with water.

Phosphate buffers (pH 6.8 and 7.4) were prepared by first dissolving 27.22 g of monobasic potassium phosphate (KH_2PO_4) in water in a 1000 ml volumetric flask to make 0.2 M KH_2PO_4 . Then, 50 ml of 0.2 M KH_2PO_4 were added to 22.4 and 39.1 ml of 0.2 M sodium hydroxide solution (NaOH) in a 200 ml volumetric flask, then adjusted to volume with water to obtain pH 6.8 and 7.4 buffered solutions, respectively.

3.3.2 Solubility test

The solubility of TDG was measured and compared with THC by using the standard shake flask method as described in the OECD guideline. The excess amount of solid THC and TDG (around 5.0 mg) was dissolved in water, buffer solution pH 1.2 (0.2 M HCl), pH 4.5 (acetate buffer), pH 6.8 (phosphate buffer), and pH 7.4

(phosphate buffer) 2 ml, individually prepared in triplicate. For water solubility testing, it was continuously shaken using a controlled temperature water bath at 100 rpm for 24 h at 30 °C. After the shaking process, the samples were left for 24 h at 25 °C to equilibrate. In buffer solubility testing, they were continuously shaken using a controlled temperature water bath at 100 rpm for 24 h at 37 °C. After that, the samples were centrifuged, then an aliquot of the supernatant was taken to measure the concentration of THC or TDG in the water using the calibration curves generated from UHPLC-UV analysis. The dilution factors of TDG in buffer solution pH 6.8 and THC in all conditions were 100 and 10, respectively.

3.3.3 Partition Coefficient

The partition coefficients ($\log P_{o/w}$) of THC and TDG were measured by the shake-flask method as described in the OECD guidelines for testing samples. The saturated solution of two immiscible solvents, *n*-octanol and pH 1.2 buffer, was used to measure the $\log P_{o/w}$ of TDG at 25 ± 1 °C. They were mixed in three ratios (*n*-octanol: pH 1.2 buffer ratio = 1:1, 2:1, and 1:2), with each experiment performed in duplicate to obtain 6 $\log P_{o/w}$ values. Then, the mixtures were shaken at 180° rotation through its transverse axis at approximately 100 times in 5 min at 25 ± 1 °C by hand followed by centrifugation at 25 °C at 14,000 rpm for 10 minutes to separate the two phases. The concentration of TDG in each phase was measured using the calibration curves from the UHPLC-UV analysis. The dilution factor of TDG and THC in the *n*-octanol phase was 250. The $\log P_{o/w}$ values were calculated using the equation below:

$$\log P_{o/w} = \text{Log} [(\text{conc. of compound in } n\text{-octanol}) / (\text{conc. of compound in water})]$$

3.3.4 Stability study

Each stock acetonitrile solution of THC and TDG was prepared at a concentration of 400 µM. Then, the stock solution of each compound was diluted with buffer solution pH 1.2, pH 4.5, pH 6.8, and pH 7.4 to obtain a final concentration

of 20 μM , with each experiment performed in triplicate. The solutions were incubated at a temperature of 37 $^{\circ}\text{C}$ for 36 h. After that, THC and TDG were analyzed at appropriate time intervals using the UHPLC-UV method, as shown in Table 5:

Table 5 The time interval for stability study in pH 1.2, 4.5, 6.8, and 7.4

Buffer solution	Time interval (h)											
	0	0.17	0.33	0.5	1	2	4	8	12	18	24	36
pH 1.2 and 4.5	✓	-	-	✓	✓	✓	✓	✓	✓	✓	✓	✓
pH 6.8 and 7.4	✓	✓	✓	✓	✓	✓	✓	✓	✓	✓	✓	✓

✓ = conducted, - = Not conducted

The degradation pathway of TDG follows a pseudo-first-order kinetic according to the two ester bond linkages in its chemical structure. In solution, TDG was degraded into tetrahydrocurcumin-monoglutaric acid (TMG) with a rate constant of k_1 . Then, TMG was further degraded into THC with a rate constant k_2 , as shown in Figure 14. To calculate the degradation rate constant and half-life of TDG in each buffer solution, the % of TDG remaining in the solution was plotted versus time to generate the non-linear curve. This non-linear curve was fitted with the estimated value calculated from the consecutive pseudo-first-order equation, as shown in Figure 14. Then, the non-linear regression analysis was conducted by using the SOLVER function in the Excel program to improve the fit and generate the rate constant (k_{obs}) and half-life ($t_{1/2}$) of TDG in the buffer solutions.

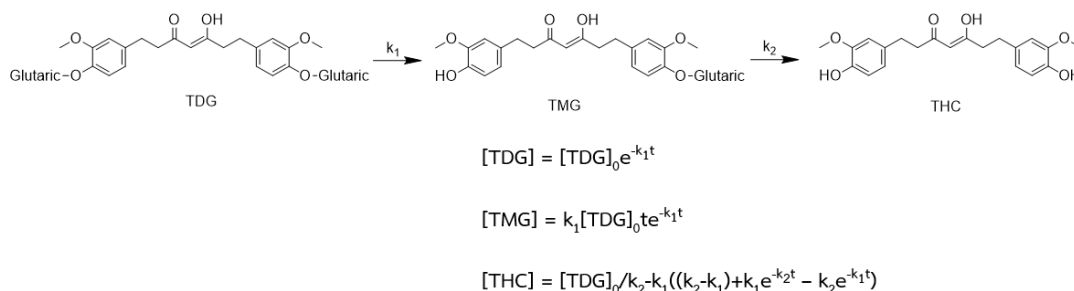


Figure 14 The degradation pathway of tetrahydrocurcumin-diglutaric acid (TDG) and the equation formula of consecutive kinetic to estimate the concentration of each compound at each time point.

3.3.5 Drug release kinetics study

Human plasma was added with a stock solution of tetrahydrocurcumin-diglutaric acid to prepare the final concentration at 80 μM . The added plasma was incubated at 37 $^{\circ}\text{C}$ for 4 h. The release profile of TDG in the plasma was determined at appropriate time intervals (0, 0.08, 0.17, 0.33, 0.67, 1, 2, 3, 4 h) by adding 10% w/v zinc sulfate followed by acetonitrile to precipitate the proteins followed by the analysis using the UHPLC. A non-linear curve was generated by plotting the % of TDG remaining in the plasma versus time to determine the rate constant and half-life of TDG in plasma. This non-linear curve was fitted with the estimated value from the consecutive pseudo-first-order equation, as shown in Figure 14. Then, the non-linear regression analysis was conducted by using the SOLVER function in the Excel program to improve the fit and generate the rate constant (k_{obs}) and half-life ($t_{1/2}$) of TDG in plasma.

3.4 Chromatographic UHPLC system for THC and TDG analysis

3.4.1 UHPLC instrumentation

A previously published HPLC analytical method of tetrahydrocurcumin was adapted with some modifications (Novaes et al., 2017). In this study, the Shimadzu Nexera XR UHPLC system (SHIMADZU SCIENTIFIC INSTRUMENTS, USA), consisting of an LC-20AD binary pump equipped with a DGU-20A degasser and SIL-

20AC thermostat autosampler, was used to analyze THC and TDG. They were carried out in a HALO C18 column (50 × 4.6 mm, 2.7 μm) with UV detection at 280 nm.

3.4.2 Chromatographic condition

The chromatography was performed using an isocratic system. The autosampler and column chamber temperatures were set at 25 °C and 35 °C, respectively. The flow rate was fixed at 1.0 mL/min, and UV detection was used at a wavelength of 280 nm. For the mobile phase, isocratic elution was eluted with mobile phase A (1.0% v/v formic acid in water) and B (1.0% v/v formic acid in acetonitrile) at a ratio of 60:40, injection volume 10 μl, and total analysis time of 9 min per injection.

3.5 Pharmacological activity evaluation

3.5.1 Cell Culture

The HepG2 cell lines were purchased from the American Type Culture Collection (ATCC, Rockville, MD, USA). The cells were cultured in DMEM media containing 10% FBS, 100 U/mL penicillin, and 100 μg/mL streptomycin in an atmosphere under 5% CO₂ at 37 °C (Madushani Herath et al., 2018; Sun et al., 2018).

3.5.2 Cell viability assay

The colorimetric MTT (3-[4,5-di-methyl-thiazol-2-yl]-2,5-diphenyl tetrazolium bromide) assay was used to evaluate cell viability. Briefly, HepG2 cells were cultured in 96 well-plates at cell density 5×10^4 cells/well with various concentrations of TDG or THC (1 – 50 μM) or ethanol (200 – 1,000 mM) for 24 h to determine the cytotoxic concentration of THC, TDG, and ethanol. The hepatoprotective effects of THC and TDG against ethanol-induced liver cell death were evaluated by incubating the THC and TDG at concentrations of 12.5 and 25 μM with HepG2 cells at a density 1×10^5 in 48-well plates for 24 h followed by adding 600 mM of ethanol to induce cell death for 24 h. In this experiment, 0.5% DMSO solution was used as vehicle control. After incubation, the MTT reagent (0.5 mg/mL)

was added and incubated at 37 °C for 4 h. Then, the medium solution was removed, and formazan crystals were dissolved by DMSO to obtain the purple-colored solution. The cell viability was monitored by measuring absorbance intensity at 540 nm via a microplate reader. The percentage cell viability was determined by the equation below (Rabelo et al., 2018):

$$\% \text{ Cell viability} = (\text{absorbance of treated cells} / \text{absorbance of control}) \times 100$$

3.5.3 Measurement of intracellular ROS

The accumulation of intracellular ROS was evaluated by fluorescence intensity using a 2',7'-Dichlorodihydrofluorescein diacetate (DCFH-DA) assay. HepG2 cells were cultured in 96-well black/clear-bottom plates at a cell density of 5×10^4 cells/well and then pre-treated with THC or TDG at concentrations 12.5 and 25 μM for 24 h. After that, the cells were induced with 600 mM of ethanol for 24 h. In this experiment, 0.5% DMSO solution was used as vehicle control. After that, the treated cells were rinsed with phosphate-buffered saline (PBS), and 10 μM DCFH-DA in PBS was added into the cells and then incubated at temperature 37 °C for another 20 min (Senthil Kumar et al., 2012). DCFH-DA permeated into cells and was transformed into non-fluorescent 2',7'-dichlorodihydrofluorescein (DCFH) by cellular esterase through deacetylation reaction. Subsequently, ROS was rapidly oxidized nonfluorescent to 2',7'-dichlorofluorescein (DCF), which has a highly fluorescent capacity (Lee et al., 2017). After incubation, intracellular ROS content was examined using a fluorescence microplate reader at 485/530 nm. The percentage of DCF fluorescence was calculated by comparing it with the untreated control group assigned to be 100%.

3.5.4 Investigation of antioxidant enzyme activities and reduced glutathione (GSH) level

HepG2 cells were cultured in 6-well plates with cell density 1.0×10^6 cells/well and then incubated with THC or TDG for 24 h at concentrations of 12.5 or

25 μM . After that, the cells were induced with ethanol 600 mM for 24 h. In this experiment, 0.5% DMSO solution was used as vehicle control. After incubation, cells were lysed by incubating with PBS containing 0.5% (v/v) triton-x100. The cell lysate was centrifuged at 14,000 rpm at 4°C for 10 min to acquire the supernatant to evaluate the activities and level of antioxidant molecules. The activities of CAT and GPx and the level of GSH were measured using commercially available assay kits. In brief, catalase activity was evaluated using methanol as a substrate to produce formaldehyde. Then, formaldehyde was reacted with 4-amino-3-hydrazino-5-mercapto-1,2,4 triazole (Purpald[®]) to obtain a purple-colored solution. The intensity of color was directly proportional to the CAT activity (Johansson & Håkan Borg, 1988). The GPx activity was evaluated indirectly using glutathione reductase (GR) as a coupled reaction. GPx enzyme plays a key role in reducing hydroperoxide into water and alcohol by using GSH as a reducing agent to form oxidized glutathione (GSSG). Then, GSSG was reduced by GR and NADPH converting back to its reduced state. Therefore, the decreasing of NADPH was used to determine the activity of GPx by measuring the absorbance at 340 nm (Baumber & Ball, 2005). In a reduced glutathione assay, glutathione reductase (GR) will reduce GSSG forming GSH. Then total GSH (GSH and GSSG) will be reacted with Ellman's reagent or 5,5'-dithio-bis (2-nitrobenzoic acid) (DTNB) to generate the yellow substance named 5'-thio-2-nitrobenzoic acid (TNB), which can be monitored at absorbance 412 nm (Rahman et al., 2006).

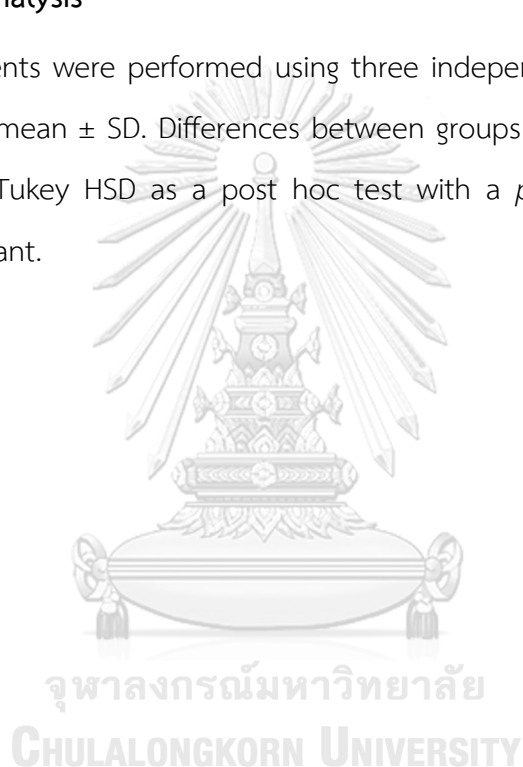
3.5.5 Evaluation of caspase-3 and -9 activities

HepG2 cells were cultured in 6-well plates with cell density 1.0×10^6 cells/well and then incubated with THC or TDG for 24 h at concentrations of 12.5 or 25 μM . After that, the cells were induced with ethanol 600 mM for 24 h. In this experiment, 0.5% DMSO solution was used as vehicle control. A hypotonic buffer consisting of 20 mM Tris-HCl pH 7.5, 1 mM ethylenediaminetetraacetic acid, 100 μM phenylmethanesulfonyl fluoride, 2 $\mu\text{g/mL}$ aprotinin, pepstatin, and leupeptin was

used to lyse the treated cells. Then, the supernatant was separated from the cell lysate to determine the activities of caspases by adding the specific substrates of caspase-3 and -9 (N-acetyl-Asp-Glu-Val-Asp p-nitroanilide or N-acetyl-Leu-Glu-His-Asp p-nitroanilide, respectively) at a concentration of 100 μ M followed by incubation at 37 °C for 1 h. The activities of the caspases were measured using the absorbance values at 405 nm with a microplate reader.

3.6 Statistical analysis

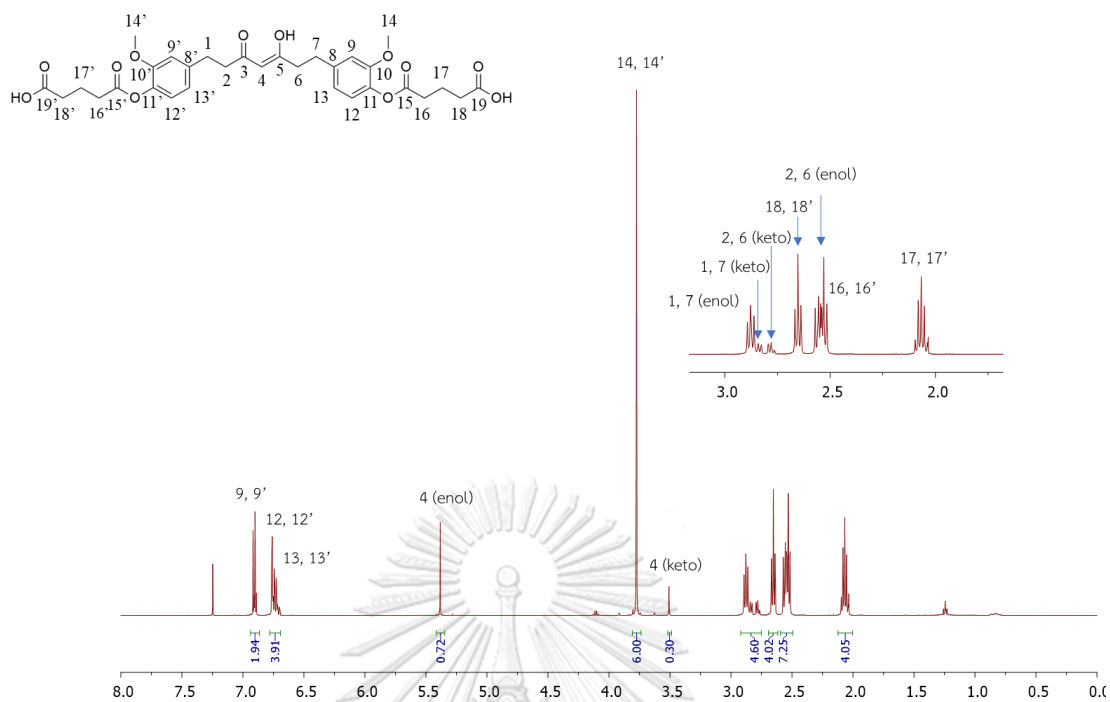
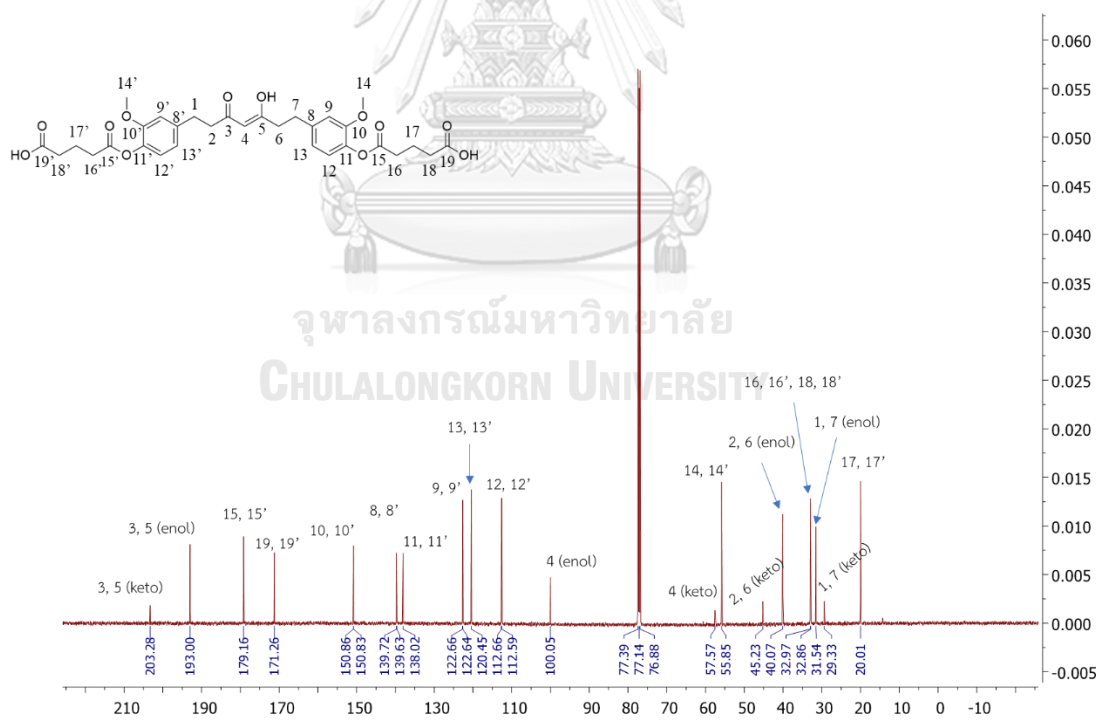
All experiments were performed using three independent replicates, and data were reported as mean \pm SD. Differences between groups were analyzed using one-way ANOVA and Tukey HSD as a post hoc test with a p -value < 0.05 considered statistically significant.



CHAPTER 4 RESULTS

4.1 Synthesis and Characterization of tetrahydrocurcumin-diglutaric acid

According to TLC results for monitoring the progression of the reaction, the spot of starting material, THC, at an R_f value of 0.43 disappeared and only a spot at an R_f value of 0.14 occurred after 3 hours. After the crude product was purified by column chromatography and recrystallization, the light-yellow solid compound was obtained in good yield (%Yield = 84.92) with purity higher than 99% resulting from HPLC chromatography. The chemical structure of TDG was characterized as following ^1H NMR (500 MHz, CDCl_3) δ (ppm): 2.03 – 2.10 (m, 4H), 2.52 – 2.57 (m, 8H), 2.65 (t, $J = 7.2$ Hz, 4H), 2.77-2.89 (m, 4H), 3.51 (s, 2H), 3.77 (s, 6H), 5.38 (s, 1H), 6.70 – 6.76 (m, 4H), 6.92 (m, 2H); ^{13}C -NMR (CDCl_3): 203.28, 193.00, 179.16, 171.26, 150.86, 150.83, 139.72, 139.63, 138.02, 122.66, 122.64, 120.45, 112.66, 112.59, 100.05, 57.57, 55.85, 45.23, 40.07, 32.97, 32.86, 31.54, 29.33, 20.01; HRMS calculated for $\text{C}_{31}\text{H}_{36}\text{O}_{12}$ [$\text{M} + \text{Na}^+$]: 623.2104; found 623.2111; melting point was 124.35 °C; the IR spectrum of TDG showed a broad spectrum for hydroxyl group of carboxylic acid at 2500 - 3500 cm^{-1} and a band at 1759 cm^{-1} was designated for carbonyl (C=O) of phenolate ester. The carbonyl (C=O) of carboxylic was represented by the band at 1704 cm^{-1} . The band at 1599 cm^{-1} represents the carbonyl group (C=O) of keto-enol tautomerism. The aromatic double bond was shown at 1510 and 1420 cm^{-1} . The band at 1035 cm^{-1} was assigned for the methoxy group (O- CH_3). The NMR, MS, and IR results are shown in Figures 15-18 and 34-36.

Figure 15 ^1H NMR spectrum of TDGFigure 16 ^{13}C NMR spectrum of TDG

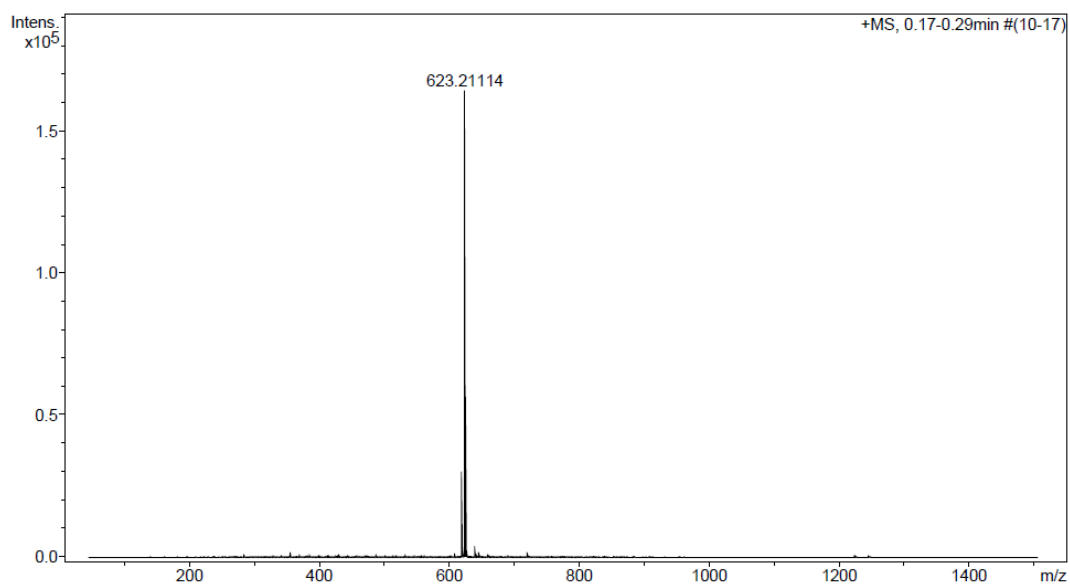


Figure 17 High-resolution mass spectrometry (HRMS) spectrum of TDG

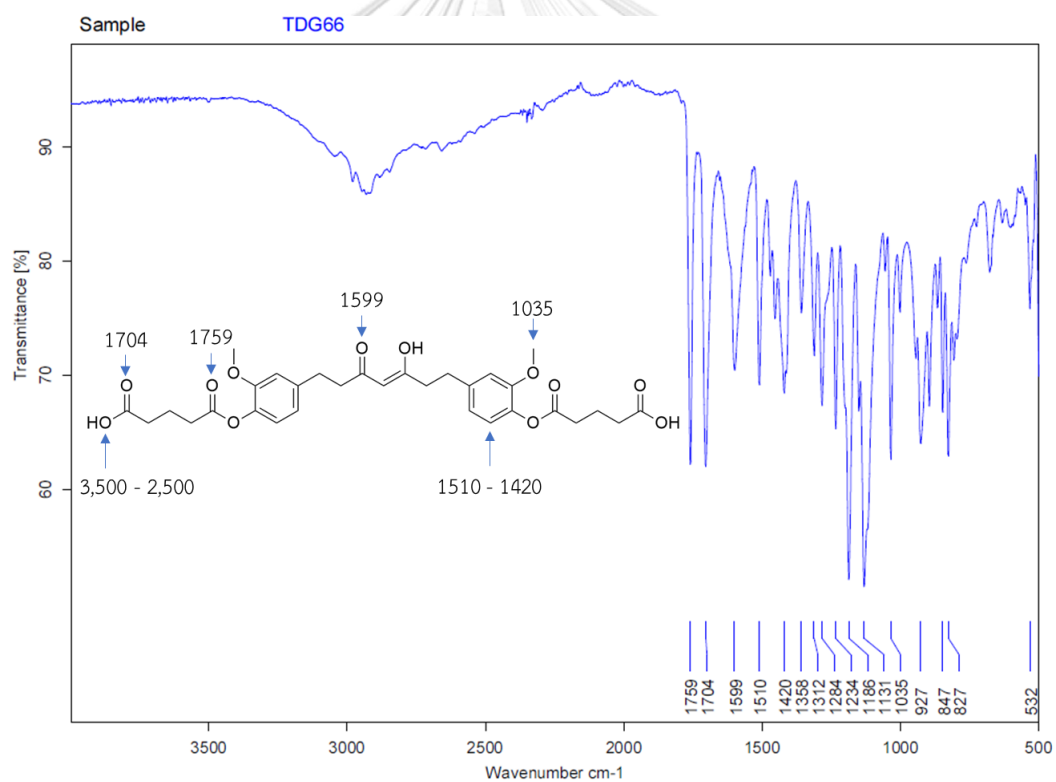


Figure 18 IR spectrum of TDG

4.2 Physicochemical and biopharmaceutical characterization

4.2.1 Solubility

The solubilities of THC and TDG in each condition are shown in Table 6. TDG had lower solubility than THC in water and acidic buffer solution pH 1.2 and 4.5. However, TDG had a solubility almost 20 times higher than THC in phosphate buffer pH 6.8.

Table 6 Solubility of THC and TDG in various conditions

Solubility condition	THC ($\mu\text{g/mL}$)	TDG ($\mu\text{g/mL}$)
water	25.83 ± 0.54	6.72 ± 0.46
HCl-KCl Buffer pH 1.2	31.88 ± 4.83	2.14 ± 0.24
Acetate Buffer pH 4.5	36.37 ± 3.90	5.93 ± 0.26
Phosphate Buffer pH 6.8	43.26 ± 4.38	792.40 ± 32.40

4.2.2 Partition coefficient (LogP)

To evaluate the lipophilicity of the compounds and estimate their ability to pass through the intestinal membrane, the Partition coefficient or LogP was investigated by using the shake flask method with buffer pH 1.2 and *n*-octanol. HPLC was used to quantify the amount of THC or TDG in each phase. The results showed that TDG had a logP value of 3.03 ± 0.26 , higher than THC (LogP = 2.68 ± 0.22). Therefore, TDG was more lipophilic than THC.

4.2.3 Stability in buffer

THC was stable in buffer pH range 1.2 to 7.4 based on a previous report (Pan et al., 1999). Similarly, TDG was found to be stable in acidic conditions at pH 1.2 and 4.5 with half-lives of 29.7 h and 22.0 h, respectively. However, TDG was unstable under basic conditions and converted into TMG and THC consecutively. The rate constant and half-life of TDG in each buffer solution are shown in Table 7.

Table 7 Rate constant (k) and half-life ($t_{1/2}$) of TDG at pH 1.2, 4.5, 6.8, and 7.4.

Buffer solution	Tetrahydrocurcumin-diglutamic acid (TDG)	
	Rate constant (k_{obs} , h^{-1})	Half-life ($t_{1/2}$, h)
HCl-KCl Buffer pH 1.2	0.023	29.7
Acetate Buffer pH 4.5	0.031	22.0
Phosphate Buffer pH 6.8	0.066	10.5
Phosphate Buffer pH 7.4	0.074	9.4

4.2.4 Kinetic drug Release in plasma

To demonstrate the degradation behavior of TDG in the systemic circulation, TDG was added into plasma and incubated at 37 °C. At appropriate time intervals, the sample was analyzed by UHPLC. The results showed that TDG was rapidly converted into TMG and THC consecutively with a rate constant of $0.758 h^{-1}$ and a half-life of 0.9 h. Furthermore, TDG was completely degraded within 4 h.

4.3 Evaluation of the hepatoprotective effects of THC and TDG against alcohol induced-oxidative damage in HepG2 cells

4.3.1 Determination of cytotoxicity in HepG2 cells

As shown in Figure 19A, the pretreated cells with various concentrations of THC and TDG for 24 h did not show any cytotoxicity effect at concentrations range 1 to 25 μM . Then, the concentration of ethanol inducing approximately 50% of cells death was investigated. The results showed that the treatment of HepG2 cells with ethanol for 24 h caused cells death in a dose-dependent manner and ethanol at 600 mM can reduce the cell viability to 50% as shown in Figure 19B. Therefore, the maximum concentration of THC and TDG for further experiments was 25 μM while ethanol was used at 600 mM with 24-h incubation to induce cell death.

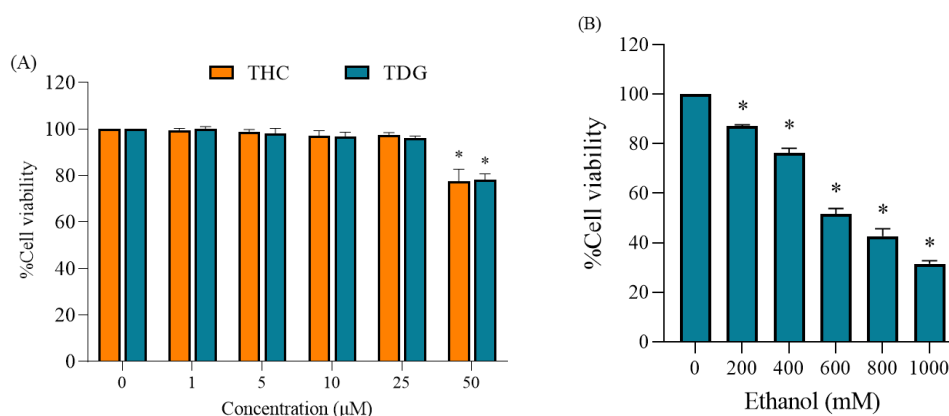


Figure 19 Cytotoxicity evaluation using MTT assay in HepG2 cells incubated with various concentrations of (A) THC and TDG and (B) ethanol for 24 h. Values are given as average % cell viability normalized to the nontreated control cells (mean \pm SD, in three independent experiments) and analyzed using One-Way ANOVA followed by Tukey post hoc test, *p < 0.05 vs. non-treated control group.

4.3.2 The protective effect of THC and TDG on alcohol-induced cell death

To determine the hepatoprotective effect against ethanol-induced cell death of THC and TDG, The MTT assay was used to determine the cell viability of HepG2 cells after ethanol incubation for 24 h. The results showed that cell viability was improved in THC and TDG pretreatment groups compared to the ethanol treatment group. Moreover, the cell viability of TDG pretreatment was effectively higher than THC as seen by the lower concentration of TDG than THC (12.5 µM vs. 25 µM) to exhibit a similar outcome as shown in Figure 20. These results indicated that TDG was more potent than THC to protect liver cells from ethanol toxicity.

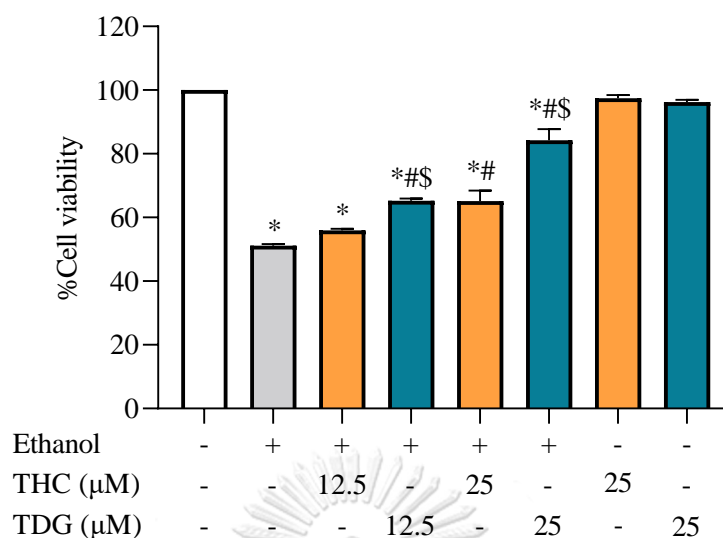


Figure 20 Hepatoprotective effects of THC and TDG on HepG2 cells. HepG2 cells were pre-incubated with THC or TDG at concentrations of 12.5 and 25 μM for 24 h. Then, cells were exposed to ethanol 600 mM for 24 h. After incubation, cell viability was evaluated by MTT assay. Values are given as average % cell viability normalized to nontreated control cells (mean ± SD values, in three independent experiments) and analyzed using One-Way ANOVA followed by Tukey post hoc test, * $p < 0.05$ compared to the nontreated control group, # $p < 0.05$ compared to the ethanol treatment group and \$ $p < 0.05$ compared to the THC treatment at corresponding concentrations.

4.3.3 Effects of THC and TDG on ROS level

As shown in Figure 21, treated HepG2 cells with ethanol exhibit an increased intracellular level of ROS compared to the control group. However, pre-treatment of cells with THC and TDG at concentration 25 μM for 24 h can suppress ROS production by 38.11% and 75.28%, respectively. TDG was more potent than THC to protect cells from alcohol-induced oxidative stress. Moreover, TDG was used at a lower concentration than THC about two times (12.5 vs. 25 μM) to show the corresponding outcome.

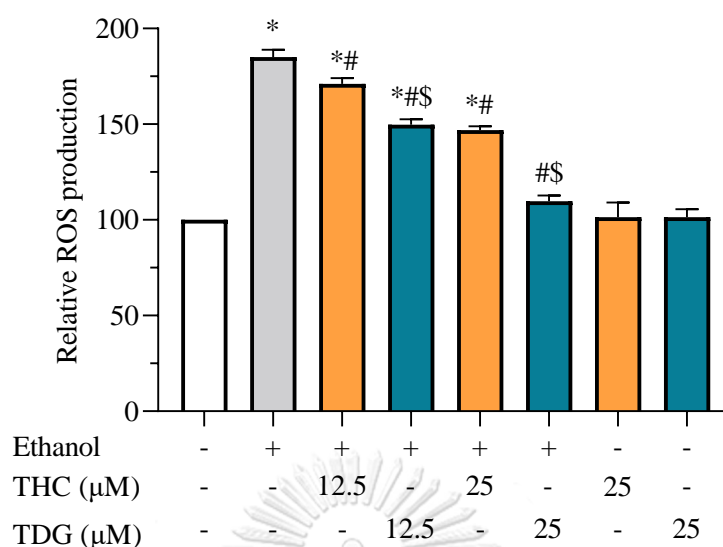


Figure 21 Effect of THC and TDG on alcohol-induced ROS generation in HepG2 cells. HepG2 cells were prior incubated with THC or TDG at concentrations 12.5 and 25 μM for 24 h. Then, cells were exposed to ethanol 600 mM for 24 h. After incubation, DCFH-DA was used to determine the ROS level. Values are given as mean ± SD values of three independent experiments and analyzed using One-Way ANOVA followed by Tukey post hoc test, * $p < 0.05$ compared to the nontreated control group, # $p < 0.05$ compared to the ethanol treatment group, and \$ $p < 0.05$ compared to the THC treatment at corresponding concentrations.

4.3.4 Effects of THC and TDG on CAT, GPx activities and GSH level

The decreasing of CAT and GPx activities and the depletion of GSH level after treated cells with ethanol 600 mM for 24 h were shown in Figure 22. These findings were consistent with the increase of intracellular ROS which represented the oxidative stress condition. The pre-treatment of cells with THC and TDG can restore the capacity of the antioxidant defense system. The results at concentration 25 μM, the CAT activity was increased by 24.13% and 36.14% and GPx was increased by 24.26% and 44.94% in THC and TDG treatment groups, respectively (figure 22A-B). Furthermore, the level of GSH was also increased by 25.29% and 44.15% in THC and TDG treatment groups, respectively (figure 22C). Notably, TDG exhibited better

antioxidant activity and higher GSH levels than THC. Nevertheless, the treated cells with TDG (TDG control group) showed the upregulation of antioxidant enzymes activities and cellular GSH level.

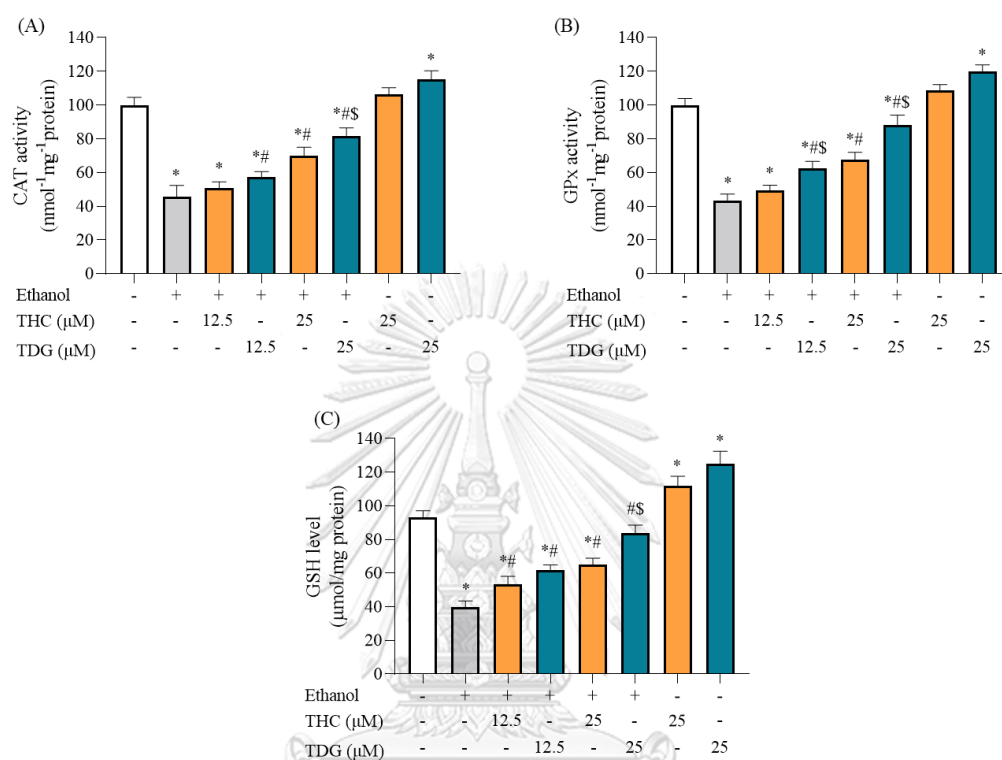


Figure 22 THC and TDG ameliorate alcohol-induced antioxidant defense depletion (A) CAT activity, (B) GPx activity, and (C) GSH level. HepG2 cells were prior incubated with THC or TDG at concentrations 12.5 and 25 μM for 24 h. Then, cells were exposed to ethanol 600 mM for 24 h. After incubation, (A) CAT activity and (B) GPx activity, and (C) GSH level were determined by kits assay. Values are given as mean ± SD values of three independent experiments and analyzed using One-Way ANOVA followed by Tukey post hoc test, * $p < 0.05$ compared to the nontreated control group, # $p < 0.05$ compared to the ethanol treatment group, and \$ $p < 0.05$ compared to the THC treatment at corresponding concentrations.

4.3.5 Effects of THC and TDG on caspase-3 and -9 activity

To determine the effect of THC and TDG on the inhibition of the apoptosis pathway induced by ethanol, the activities of caspase-3 and -9 were

evaluated. As shown in Figure 23, the activities of caspase-3 and -9 were significantly enhanced by 5.21 and 4.24-fold after incubation with ethanol 600 mM for 24 h. However, the pre-treatment of cells with THC and TDG (25 μ M) remarkably suppress the activities of caspase-3 and caspase-9. Similar to previous results, the activities of caspases in the TDG group were effectively reduced than THC at the corresponding concentration. These results indicated that TDG was more potent than THC to prevent ethanol-induced apoptosis.

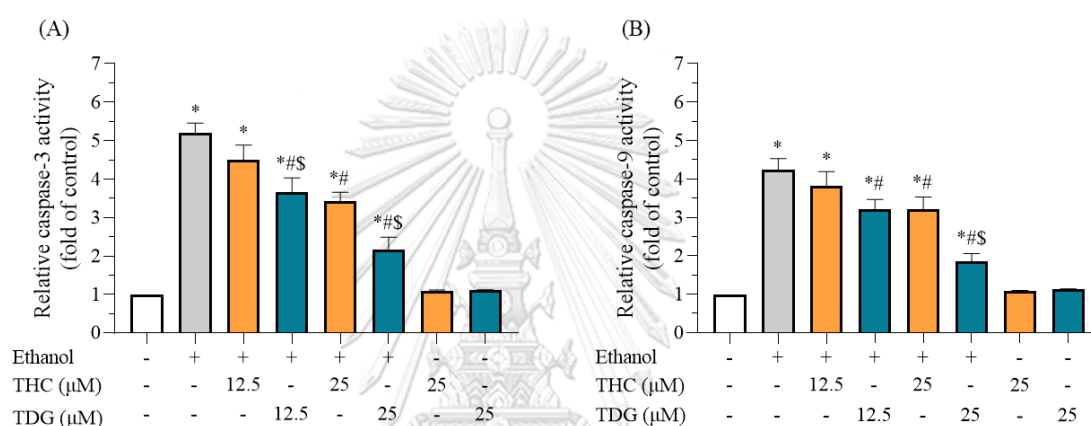


Figure 23 THC and TDG suppress alcohol-induced apoptosis on HepG2 cells. Cells were prior incubated with THC or TDG at concentrations 12.5 and 25 μ M for 24 h. Then, cells were exposed to ethanol 600 mM for 24 h. After incubation, the activities of (A) caspase-3 and (B) caspase-9 were determined by adding specific substrates of caspase -3 and -9 and measuring the absorbance at 405 nm. Values are given as mean \pm SD values of three independent experiments was analyzed using One-Way ANOVA followed by Tukey post hoc test), * p <0.05 compared to the nontreated control group, # p <0.05 compared to the ethanol treatment group, and \$ p <0.05 compared to the THC treatment at corresponding concentrations.

CHAPTER 5 DISCUSSION AND CONCLUSION

The synthesis of TDG was adapted from previous research with some modifications (Muangnoi et al., 2021). The glutaric anhydride was used as a substrate to conjugate with THC due to the more reactive cyclic acid anhydride than the free carboxylic group for one-step esterification with the phenolic group of THC (Trabelsi et al., 2017). This reaction did not use a coupling agent and was carried out at room temperature. For the reaction mechanism, the lone pair of oxygen of the phenolic group plays a role as a nucleophile to attack the carbonyl group of a cyclic acid anhydride. Then, another one of the carbonyl groups becomes the leaving group to generate the THC conjugating with glutaric acid via ester bond linkage which has free carboxylic at the terminal. The high equivalent of glutaric anhydride (4 equiv. vs. 1 equiv. of THC) was used to force the reaction to generate the di-substitution of THC with glutaric acid. The *N,N*-Diisopropylethylamine (DIPEA) was used as a proton scavenger since DIPEA is a basic compound ($pK_a = 10.90$) with a steric structure that provides non-nucleophilic property. After THC was reacted with glutaric anhydride, DIPEA will deprotonate the proton of the phenolic group (Bakhtin et al., 2018). However, DIPEA can also serve as a catalyst in the esterification by reacting with glutaric anhydride to form acylammonium intermediate. The acylammonium intermediate was then attacked by the hydroxyl group of phenolic to form an ester linkage as depicted in Figure 24 (Ren et al., 2018). Finally, THC can be conjugated with glutaric acid via an ester bond linkage. However, only the hydroxyl of the phenolic group will be able to conjugate with glutaric acid. The hydroxyl of the enolic group cannot be conjugated due to an intramolecular bond between the hydroxyl group of enolic and oxygen of ketone resulting in pi-electron resonance that will stabilize the lone pair electron of the hydroxyl group to be non-reactive (Fragoza-Mar et al., 2011). Although two purification methods including column chromatography and recrystallization were used to achieve the highest purity of TDG, the yield of the product was still greater than 80%.

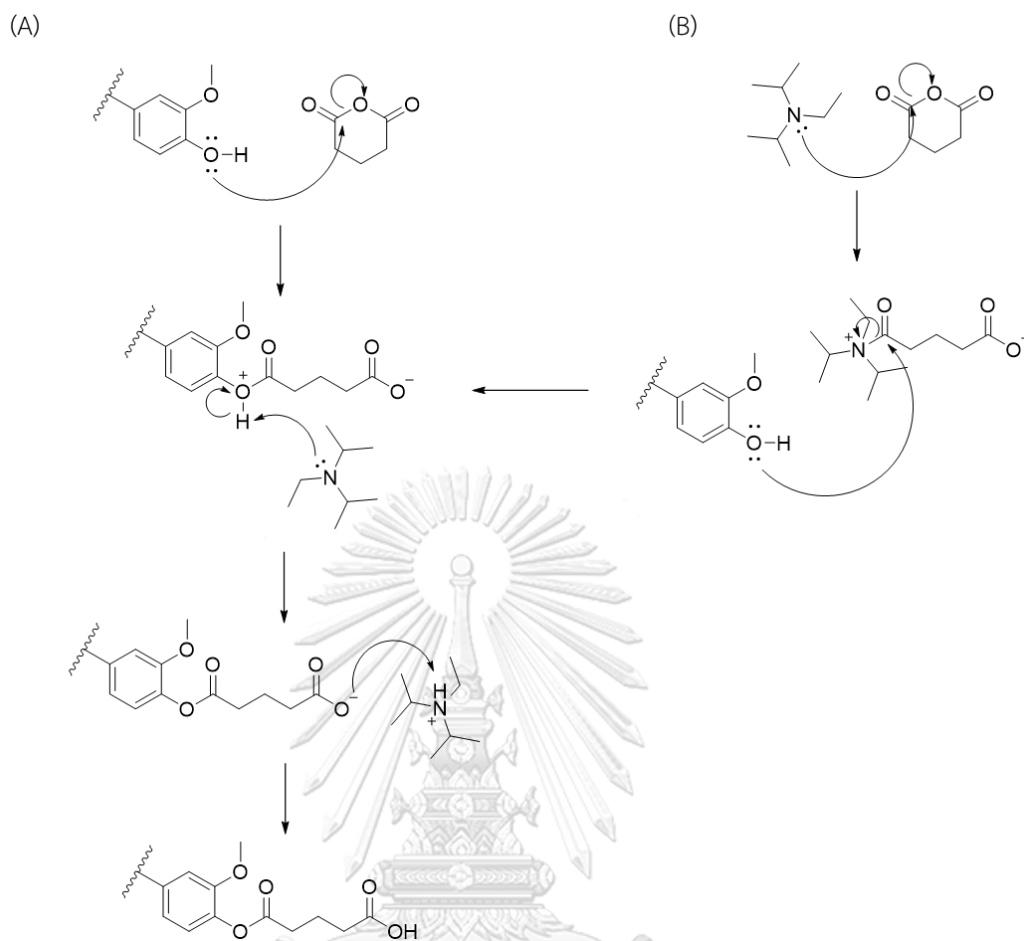


Figure 24 Proposed mechanism reaction of DIPEA, glutaric anhydride, and THC. DIPEA can serve as a (A) base by deprotonating of phenolic proton or (B) catalyst by reacting with glutaric anhydride to form acylammonium intermediate.

The chemical structure of TDG was elucidated by several well-established techniques to assure the conjugation between THC and glutaric acid including NMR, IR, and MS spectrometry. The ^1H NMR spectroscopy can distinguish THC and TDG by detecting phenolic protons at a chemical shift of 5.53 ppm reported in the previous research (Wagner et al., 2013). This study found that the phenolic proton of THC produced a broad signal at a chemical shift of 5.62 ppm. However, the NMR spectrum of TDG did not have any signals at chemical shifts 5.53 to 5.62 ppm indicating that two phenolic groups of THC were completely formed ester bond linkage. Moreover, the success of this conjugation was confirmed by MS

spectrometry. The result showed that the mass to charge ratio was observed at 623.21114 g/mol corresponding to the protonated ion of TDG [$M + Na^+$] with a mass error of 1.19 ppm. However, an attempt of synthesizing tetrahydrocurcumin-monoglutaric acid (TMG) has been made. However, the product was obtained at a low yield with contamination of THC and TDG. In addition, the product cannot be solidified after the purification process. Therefore, the focus of this study was shifted to the synthesis of TDG.

Moreover, the NMR results revealed that TDG could be tautomerized into keto-enol form by showing singlet peaks proton at 3.51 and 5.38 ppm for keto and enol form of centered carbon (H-4), respectively. In addition to the methylene carbon between β -diketone, the chemical shifts of proton at the heptane chain were also different between keto and enol form. The alkyl proton H-1 and H-7 showed 2 chemical shifts at 2.83-2.84 for keto and 2.86-2.89 ppm for enol. Similarly, the chemical shifts at 2.52-2.57 and 2.76-2.79 ppm of the alkyl proton H-2 and H-6 indicated the enol and keto form, respectively (Figure 15, 16). Therefore, the integration of 1H NMR spectrum didn't correspond to the total number of protons on these spectrum areas.

According to the limitation of THC, a poor water solubility profile is an essential factor that limits the absorption of THC through the intestinal membrane after oral administration (Boyd et al., 2019). In this study, the physicochemical and biopharmaceutical properties of TDG were determined by using a validated UHPLC chromatographic system to analyze the sample. The results of analytical method validation for quantification of TDG are shown in Table 8. The solubility of TDG in buffer pH 1.2, 4.5, and 6.8 was evaluated for simulating the gastrointestinal condition (gastric fluid, duodenal fluid, and intestinal fluid, respectively) (Hamed et al., 2016). The results showed that TDG had lower solubility in water, buffer pH 1.2 and 4.5 while enhanced in buffer pH 6.8 compared with THC corresponding to its pKa value of free terminal carboxylic groups. The calculation of pKa from MarvinSketch,

ChemAxon showed that the pKa value of free terminal carboxylic groups was 3.30 – 3.90. Therefore, TDG can be ionized completely when dissolved in buffer pH 6.8. In addition, the lipophilicity of TDG was higher than THC with logP values of 3.03 and 2.68, respectively, corresponding to the di-substitution of THC with glutaric acid, which has a greater molecular weight than THC (600.2 vs. 372.4 g/mol). In the logP evaluation, the buffer pH 1.2 was selected to examine the partition coefficient because TDG must be unionized during the examination process. These results suggest that TDG may be used orally due to its greater solubility with sufficient logP value.

The amount of a pharmacological substance to persist in biological fluids and reach its target areas is generally characterized as a stability profile under various gastrointestinal and physiological pH. Therefore, the stability of TDG in buffer solutions at different pH including 1.2 (gastric fluid), 4.5 (duodenal fluid), 6.8 (intestinal fluid) and 7.4 (blood) was determined by a validated UHPLC chromatographic system (Constable, 2009; Hamed et al., 2016). The results showed that TDG was stable under pH 1.2 and 4.5 with a half-life of over 20 hours. In contrast, TDG was susceptible to degradation at pH 6.8 and 7.4 with a half-life lower than 10 hours. As expected, the rate constant of TDG degradation under physiological pH 7.4 was highest than at lower pH because the ionized carboxyl group, which is predominant at pH 7.4 can undergo intramolecular nucleophilic attack or intramolecular cyclization on the carbonyl of ester linkage, especially to phenyl ester. These findings agree with the previous report (Fredholt et al., 1995; Muangnoi et al., 2018).

Table 8 the report of analytical method validation parameters for quantification of TDG

Parameters	Results
Linearity	
- Range ($\mu\text{g/ml}$)	0.40 to 12
- Regression equation	$y = 4,969.5558x - 41.9306$
- Correlation coefficient (r^2)	0.9999
- Lack of fit	$F_{\text{cal}} = 0.29$ (NMT $F_{(8,20)} = 2.45$) Appropriate fit for the data
LOD ($\mu\text{g/ml}$)	0.25 $\mu\text{g/ml}$
LOQ ($\mu\text{g/ml}$)	0.40 $\mu\text{g/ml}$
Accuracy (%recovery)	
- 0.40 $\mu\text{g/ml}$	101.8 %
- 8.00 $\mu\text{g/ml}$	101.0 %
- 10.00 $\mu\text{g/ml}$	100.8 %
- 12.00 $\mu\text{g/ml}$	101.5 %
Precision (Repeatability; %RSD)	
- 0.40 $\mu\text{g/ml}$	3.54
- 8.00 $\mu\text{g/ml}$	0.52
- 10.00 $\mu\text{g/ml}$	0.83
- 12.00 $\mu\text{g/ml}$	0.36
Precision (Intermediate; %RSD)	
- 0.40 $\mu\text{g/ml}$	4.97
- 8.00 $\mu\text{g/ml}$	0.50
- 10.00 $\mu\text{g/ml}$	0.38
- 12.00 $\mu\text{g/ml}$	1.06

As mentioned above, TDG was degraded as consecutive pseudo-first-order kinetic into TMG and THC, respectively. The model of degradation kinetic of TDG was determined by comparing the r^2 values among the 3 models including zero-order

kinetic, pseudo-first-order kinetic and second-order kinetic obtained from various testing conditions (Reis et al., 2016). The higher r^2 value was selected as the kinetic model for TDG. As shown in Table 9, the highest r^2 was found in pseudo-first-order kinetic indicating that pseudo-first-order kinetic is a suitable model for TDG.

The rate constant and half-life of TDG were calculated using a non-linear plot between % of TDG remaining against time and fitting to the consecutive pseudo-first-order model. After that, Microsoft Excel software was used to analyze non-linear least square analysis using equations described in Figure 14. The advantages of non-linear least-square over the linear least square are the closeness of fitting between non-linear least squares curve and hypothetical values curve providing more reliable calculation on the rate constant and half-life (Perrin, 2017).

According to the objective of this study, TDG was designed to be used as a prodrug that was expected as a pharmacologically inactive compound (Huttunen et al., 2011). Thereby, the transformation procedures of TDG including chemical and enzymatic reactions were required to release its active compound (THC). Once the prodrug reaches the systemic circulation, blood or plasma plays a significant role in the bioconversion of the ester-based prodrug. Then, plasma was chosen to investigate the release study of TDG. The results found that TDG was rapidly degraded in human plasma containing various esterase enzymes combined with intramolecular cyclization to accelerate the hydrolysis of the ester bond (Williams, 1985). Consequently, it was found that the rate constant in human plasma was 10 times higher than physiological pH 7.4. Similar to the degradation of TDG in buffer solution, the hydrolysis of TDG in human plasma converted TDG into intermediate compound or TMG and active compound or THC, consecutively. Therefore, TDG could be used as a potential prodrug of THC with improved physicochemical and biopharmaceutical properties for oral drug delivery.

Table 9 The r^2 value of different kinetic models for TDG degradation

Testing condition	r^2 value		
	<i>Zero-order</i>	<i>Pseudo-first order</i>	<i>Second-order</i>
Buffer pH 1.2	0.9907	0.9999	0.9871
Buffer pH 4.5	0.9880	0.9998	0.9856
Buffer pH 6.8	0.9456	0.9984	0.9658
Buffer pH 7.4	0.9327	0.9974	0.9608
plasma	0.9334	0.9824	0.9217

THC has been shown as a protective agent against several xenobiotic induced-oxidative stress in different experimental models (Li et al., 2019; Murugan & Pari, 2006; Pari & Murugan, 2006; Vacek et al., 2018). Notably, the previous research found that THC was more effective than curcumin and silymarin to prevent liver tissue from drug-induced oxidative damage in animal models (Pari & Amali, 2005; Pari & Murugan, 2004). Based on the concept of the prodrug design approach, we hypothesized that TDG would exert a hepatoprotective effect equivalent to its parent compound. TDG might be converted to THC via chemical hydrolysis or enzymatic hydrolysis through esterase(s) located in the hepatocytes (Li et al., 2017). In this study, silymarin was used as a positive control in the evaluation of hepatoprotective effects of THC and TDG. Silymarin at 10 μ M exhibited hepatoprotective effects by improving cell viability after exposure to ethanol as shown in Figure 37. The hepatoprotective effect of silymarin is consistent with the previous research, indicating that the cell-based assay used in this study was valid as an in vitro model for evaluating hepatoprotective effects of THC and TDG (Lee et al., 2019). Moreover, pretreatment of THC and TDG significantly improved the cell viability of HepG2 cells compared to the ethanol-treated group.

Moreover, the cell viability of TDG was remarkably higher than THC by using a lower concentration at 12.5 μ M to show a similar effect to THC at concentration 25

μM . These results indicated that TDG exerted more potent protective effects against alcohol-induced cell death. The higher efficacy of TDG over THC may be resulting from the conjugation with glutaric acid that provides the free terminal carboxylic group. Several drugs containing carboxylic groups such as atorvastatin, enalapril, and valsartan are identified as substrates of organic anion transporter polypeptide (OATP) (Kalliokoski & Niemi, 2009). OATP is an influx transporter that plays a role in governing the cellular uptake (Kalliokoski & Niemi, 2009). The most relevant members in the OATP family that impact the pharmacokinetics of drugs are OATP1B1, 1A2, 1B3, and 2B1 (Kalliokoski & Niemi, 2009). They are mainly located on the hepatocyte membrane, except OATP1A2 (Kalliokoski & Niemi, 2009). Therefore, TDG might be a substrate of OATP, which enhances cellular uptake and increases the hepatoprotective effect. Further experiments should be performed to validate the cellular uptake mechanism of TDG. In addition to the improvement of intracellular uptake of TDG, the increase of TDG stability may assist in maintaining the availability of TDG at the target site. The previous study indicated that the phenolic group on the chemical structure was related to the instability profile of curcuminoids (Vijaya Saradhi et al., 2010). Therefore, the ester conjugation of THC with glutaric acid could retard the degradation of THC by gradually releasing THC at the target site.

Numerous research studies showed that the incubation of HepG2 cells with specific ethanol concentrations in a particular period caused an increase in intracellular ROS levels (Farshori et al., 2013; Madushani Herath et al., 2018; Sun et al., 2018). As shown in Figure 21, this study showed results consistent with the previous reports. The level of intracellular ROS has increased after incubation of HepG2 cells with ethanol concentration 600 mM for 24 h. However, the pretreatment with THC and TDG can suppress the increase of ROS and protect cells from oxidative-induced cell death since THC is an antioxidant compound that can act as a free radical scavenger according to its chemical structure containing phenolic group and β -diketone moiety (Osawa et al., 1995). The phenolic group is characterized by the

attachment of the hydroxyl group to a benzene ring. In the presence of free radicals, this hydroxyl group will be broken down and react with free radicals (Malik & Mukherjee, 2014). β -diketone can also scavenge the free radical by using active methylene carbon between two carbonyl groups. Free radical will attack the methylene carbon and the β -diketone was cleaved into dihydroferulic acid (Osawa et al., 1995; Sugiyama et al., 1996).

In addition to the directly scavenging free radical of THC, it can also improve the capacity of the intracellular antioxidant defense system by upregulating the expression of enzymatic and non-enzymatic antioxidants. Recent research showed that THC could restore the activity of SOD, CAT, and GPx and GSH levels after being restrained by arsenic-induced oxidative damage in rat models (Muthumani & Miltonprabu, 2015). SOD, CAT, and GPx are widely well-known as the first-line defense antioxidants preventing the accumulation of free radicals (Ighodaro & Akinloye, 2018). Kim et al. (2009) studied the effect of GPx and CAT deficiency in ethanol-induced liver injury in GPx and CAT double knockout mice. They found that GPx and CAT deficiency mice are more susceptible to alcohol intoxication with higher ALT and MDA levels than wild-type mice (Kim et al., 2009). Kessova et al. (2003) evaluated the effect of alcohol in SOD deficiency mice. The results indicated that SOD is necessary to ameliorate ethanol-induced oxidative damage (Kessova et al., 2003).

Moreover, ethanol consumption can cause the depletion of antioxidant defense systems, including SOD, CAT, and GPX activity and GSH level that lead to promoting liver injury in the mice model (Wang et al., 2021). In this study, the reduction of antioxidant enzyme and GSH level was initiated after incubation of HepG2 cells with ethanol for 24 h. However, the pretreatment of THC and TDG can reverse the activity of antioxidant enzymes and GSH levels. Therefore, the decreasing of intracellular ROS may involve the protective effect of THC on the upregulation of the antioxidant defense system. However, the increase of the antioxidant defense

system of THC might be involved in the Nrf2-Keap1 pathway. The nuclear factor erythroid 2-related factor 2 (Nrf2) is a transcription factor that modulates the expression of the antioxidant defense system to protect cells from oxidative stress (Ma, 2013; Taguchi et al., 2011). The previous research found that THC can upregulate the expression of Nrf2 protein and mRNA, resulting in restoring antioxidant activities and alleviating oxidative damage (Luo et al., 2019; Wei et al., 2017).

Although, apoptosis is a normal cellular process to maintain the homeostasis of the cellular population by eliminating the injured cells (Elmore, 2007). However, the overwhelming trigger of apoptosis can cause a broad spectrum of diseases, including ALD (P. Chen et al., 2019). Therefore, the inhibition or suppression of apoptosis could be used as a therapeutic strategy for ALD. The expression of caspase-3 and caspase-9 protein and caspase-3 activity has been used as markers for apoptosis in several studies (M.-F. Chen et al., 2019; Muangnoi et al., 2019). In addition to the induction of oxidative stress by ethanol in liver tissue, it can also cause the upregulation of caspases protein levels and their activities, especially caspase-3 and -9 (P. Chen et al., 2019; Liang et al., 2021; Peiyuan et al., 2017; Sabitha et al., 2020). However, the increase of caspases was suppressed by antioxidant molecules corresponding to the reduction of oxidative stress conditions. In conjunction with the antioxidant effect results, it was found that the level of apoptosis markers, caspase-3 and -9, were reduced after treating cells with THC and TDG.

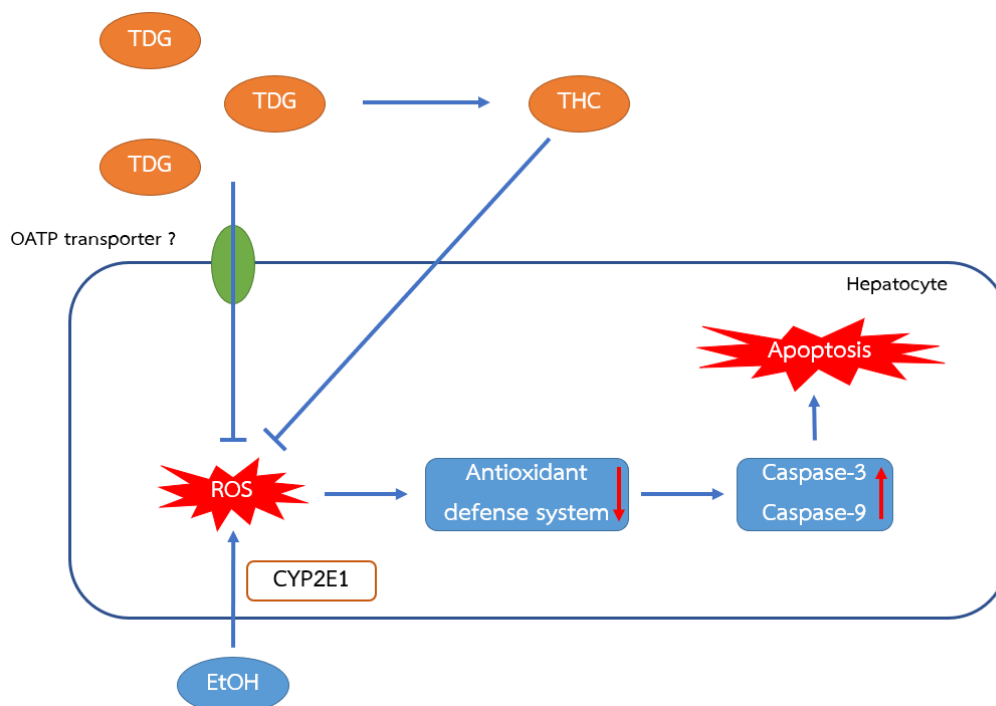


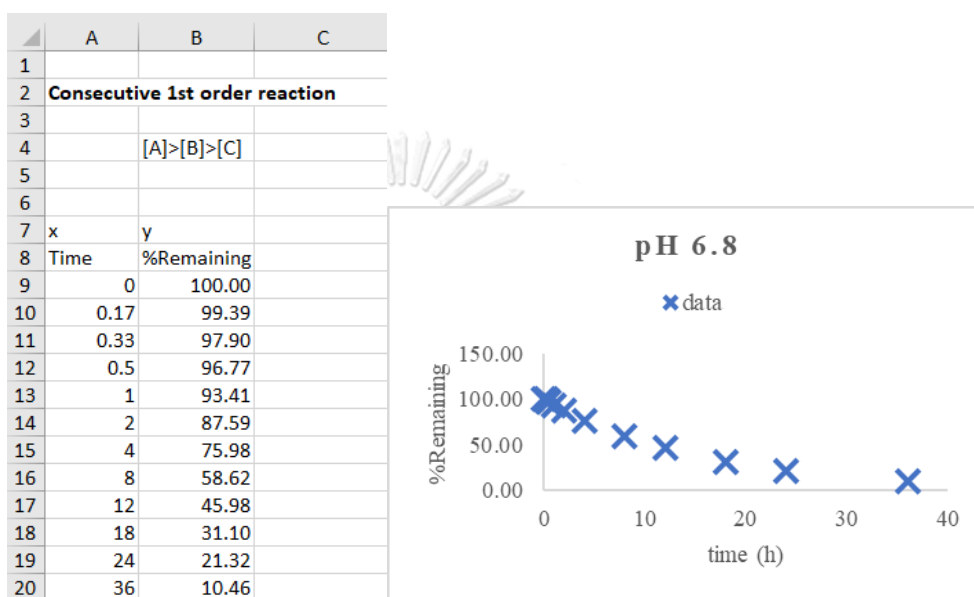
Figure 25 The proposed mechanism of TDG for protecting liver cells from alcohol-induced oxidative damage.

In summary, TDG was successfully synthesized with better hepatoprotective effects against alcohol-induced oxidative damage than THC by reducing ROS level, upregulating the expression of the antioxidant defense system, and inhibiting the apoptosis pathway. The more substantial protective effect of TDG may be resulting from the conjugation with glutaric acid that is attributed to enhance the stability of THC or increase the cellular uptake of TDG into hepatocyte cells via OATP transporter. The proposed mechanism underlying the protective effects of TDG against alcohol-induced oxidative damage is shown in Figure 25. Moreover, TDG also had higher water solubility than THC, approximately 20 times in buffer pH 6.8. Therefore, TDG could be used as a potential therapeutic agent for ALD that enabled the development of an oral drug delivery formulation (Rautio et al., 2008). Further investigation by using in vivo model would confirm the role and provide intensively about the underlying mechanism of TDG in these therapeutic functions against alcohol-induced hepatotoxicity.

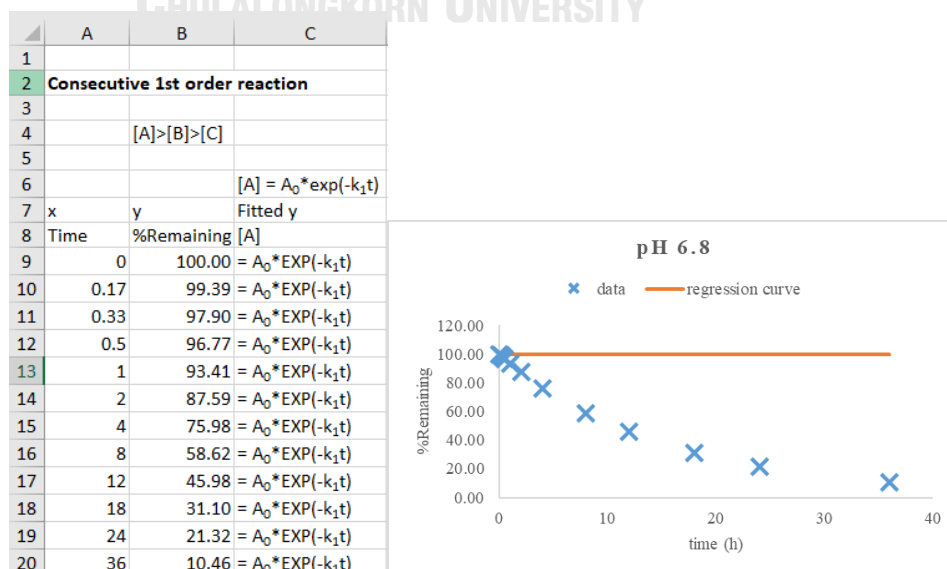
APPENDIX A

The process of calculating rate constant using SOLVER function in Excel

- Input raw data into a spreadsheet, the X column is independent variable or time, and the Y column is the dependent variable or %remaining sample. Then, raw data on X and Y were graphed in a scatter plot.



- The equation of consecutive pseudo-first-order kinetic was entered in column C. After entering the formulation and calculation, and the non-linear regression line was not fit to raw data.



3. The mean of Y was calculated by =AVERAGE(B9:B20) and the degree of freedom (df) was calculated by the total number of data minus 1.

	A	B	C	D
1				
2	Consecutive 1st order reaction			
3				
4		[A]>[B]>[C]		
5				
6			[A] = A ₀ *exp(-k ₁ t)	
7	x	y	Fitted y	
8	Time	%Remaining [A]		
9	0	100.00	100.00	
10	0.17	99.39	100.00	
11	0.33	97.90	100.00	
12	0.5	96.77	100.00	
13	1	93.41	100.00	
14	2	87.59	100.00	
15	4	75.98	100.00	
16	8	58.62	100.00	
17	12	45.98	100.00	
18	18	31.10	100.00	
19	24	21.32	100.00	
20	36	10.46	100.00	
21				
22				
23				
24				
25	k1	t1/2		
26				
27				
28		R ²		
29		Mean of y	68.21	
30		df	11	
31		S.E.		
32		t critical		
33		CI		

4. Columns D and E were calculated as residuals and squares of residuals. Residuals are the difference between data on columns B and C at the same time point. Then, the sum of square residual (SSR) was calculated.

	A	B	C	D	E
1					
2	Consecutive 1st order reaction				
3					
4		[A]>[B]>[C]			
5					
6			[A] = A ₀ *exp(-k ₁ t)		
7	x	y	Fitted y		
8	Time	%Remaining [A]		residuals	square residuals
9	0	100.00	100.00	0.00	0.00
10	0.17	99.39	100.00	0.61	0.37
11	0.33	97.90	100.00	2.10	4.41
12	0.5	96.77	100.00	3.23	10.42
13	1	93.41	100.00	6.59	43.47
14	2	87.59	100.00	12.41	154.11
15	4	75.98	100.00	24.02	576.92
16	8	58.62	100.00	41.38	1712.54
17	12	45.98	100.00	54.02	2918.02
18	18	31.10	100.00	68.90	4746.80
19	24	21.32	100.00	78.68	6189.80
20	36	10.46	100.00	89.54	8016.65
21					
22					
23				SSR	
24					24373.50
25	k1	t1/2			
26					
27					
28		R ²			
29		Mean of y	68.21		
30		df	11		
31		S.E.			
32		t critical			
33		CI			

5. Column F calculated the square of the difference between data on column B and the mean of y. Then, the sum of square of different (SuM) was calculated. After that, the R^2 was calculated as follows: $1-SSR/SuM$

	A	B	C	D	E	F
1						
2	Consecutive 1st order reaction					
3						
4		[A]-[B]>[C]				
5						
6			[A] = A ₀ *exp(-k ₁ t)			
7	x	y	Fitted y	residuals	square residuals	(y-mean of y)^2
8	Time	%Remaining [A]				
9	0	100.00	100.00	0.00	0.00	1.00
10	0.17	99.39	100.00	0.61	0.37	972.42
11	0.33	97.90	100.00	2.10	4.41	881.44
12	0.5	96.77	100.00	3.23	10.42	815.76
13	1	93.41	100.00	6.59	43.47	634.83
14	2	87.59	100.00	12.41	154.11	375.39
15	4	75.98	100.00	24.02	576.92	60.37
16	8	58.62	100.00	41.38	1712.54	92.04
17	12	45.98	100.00	54.02	2918.02	494.15
18	18	31.10	100.00	68.90	4746.80	1377.00
19	24	21.32	100.00	78.68	6189.80	2198.31
20	36	10.46	100.00	89.54	8016.65	3334.67
21						
22						
23					SSR	SuM
24					24373.50	11237.39
25	k ₁	t _{1/2}				
26						
27						
28		R ²	-1.1690			
29		Mean of y	68.21			
30		df	11			
31		S.E.				
32		t critical				
33		CI				

6. The standard error (S.E.) was calculated by the square root of SSR divided by df. T critical at a significance level of 95% was calculated as follows: =tinv(0.05/df). The confidence interval (CI) was calculated by S.E. multiplied by t critical.

	A	B	C	D	E	F
1						
2	Consecutive 1st order reaction					
3						
4		[A]-[B]>[C]				
5						
6			[A] = A ₀ *exp(-k ₁ t)			
7	x	y	Fitted y	residuals	square residuals	(y-mean of y)^2
8	Time	%Remaining [A]				
9	0	100.00	100.00	0.00	0.00	1.00
10	0.17	99.39	100.00	0.61	0.37	972.42
11	0.33	97.90	100.00	2.10	4.41	881.44
12	0.5	96.77	100.00	3.23	10.42	815.76
13	1	93.41	100.00	6.59	43.47	634.83
14	2	87.59	100.00	12.41	154.11	375.39
15	4	75.98	100.00	24.02	576.92	60.37
16	8	58.62	100.00	41.38	1712.54	92.04
17	12	45.98	100.00	54.02	2918.02	494.15
18	18	31.10	100.00	68.90	4746.80	1377.00
19	24	21.32	100.00	78.68	6189.80	2198.31
20	36	10.46	100.00	89.54	8016.65	3334.67
21						
22						
23					SSR	SuM
24					24373.50	11237.39
25	k ₁	t _{1/2}				
26						
27						
28		R ²	-1.1690			
29		Mean of y	68.21			
30		df	11			
31		S.E.	47.07			
32		t critical	2.20			
33		CI	103.60			

7. The lower and upper limits were calculated by minus data on column C with CI or plus data on column C with CI and input results on column G and H, respectively.

	A	B	C	D	E	F	G	H
1								
2	Consecutive 1st order reaction							
3								
4		[A]>[B]>[C]						
5								
6			[A] = A ₀ *exp(-k ₁ t)					
7	x	y	Fitted y					
8	Time	%Remaining [A]	residuals	square residuals	(y-mean of y)^2	Lower	Upper	
9	0	100.00	100.00	0.00	0.00	1.00	-3.60	203.60
10	0.17	99.39	100.00	0.61	0.37	972.42	-3.60	203.60
11	0.33	97.90	100.00	2.10	4.41	881.44	-3.60	203.60
12	0.5	96.77	100.00	3.23	10.42	815.76	-3.60	203.60
13	1	93.41	100.00	6.59	43.47	634.83	-3.60	203.60
14	2	87.59	100.00	12.41	154.11	375.39	-3.60	203.60
15	4	75.98	100.00	24.02	576.92	60.37	-3.60	203.60
16	8	58.62	100.00	41.38	1712.54	92.04	-3.60	203.60
17	12	45.98	100.00	54.02	2918.02	494.15	-3.60	203.60
18	18	31.10	100.00	68.90	4746.80	1377.00	-3.60	203.60
19	24	21.32	100.00	78.68	6189.80	2198.31	-3.60	203.60
20	36	10.46	100.00	89.54	8016.65	3334.67	-3.60	203.60
21								
22								
23					SSR	SuM		
24					24373.50	11237.39		
25	k1	t1/2						
26								
27								
28		R ²		-1.1690				
29		Mean of y		68.21				
30		df		11				
31		S.E.		47.07				
32		t critical		2.20				
33		CI		103.60				

8. In this step, the raw data on column B and calculated data on column C was not fit. Therefore, the SOLVER function in excel was used to improve the fit of data.

The screenshot shows the Excel Solver Parameters dialog box. The 'Set Objective' field is empty. The 'By Changing Variable Cells' field is empty. The 'Subject to the Constraints' field is empty. The 'Solving Method' is set to 'GRG Nonlinear'. The 'Options' tab is selected, showing 'Select a Solving Method' as 'GRG Nonlinear' and 'Select the LP Simplex engine for linear Solver Problems, and select the Evolutionary engine for Solver problems that are non-smooth.' The spreadsheet data is visible in the background, including columns A through H and rows 1 through 33.

9. In an objective box, enter SSR value cells. In the By Changing variable cells, enter the cells to input the kinetic constant. After finishing, click Solve to perform the fit.

Solver Parameters

Set Objective:

To: Max Min Value Of:

By Changing Variable Cells:

Subject to the Constraints:

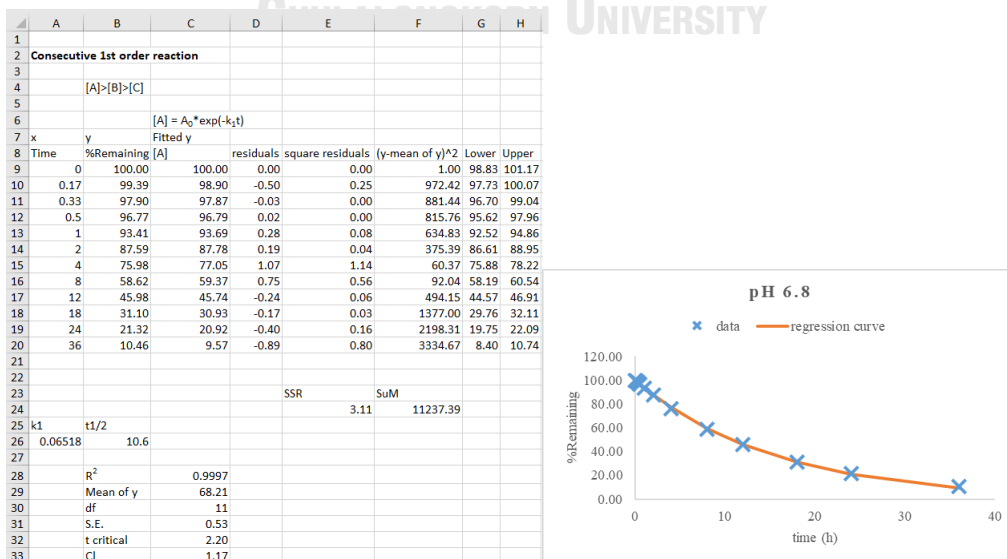
Make Unconstrained Variables Non-Negative

Select a Solving Method:

Solving Method
Select the GRG Nonlinear engine for Solver Problems that are smooth nonlinear. Select the LP Simplex engine for linear Solver Problems, and select the Evolutionary engine for Solver problems that are non-smooth.

Buttons: Add, Change, Delete, Reset All, Load/Save, Help, Solve, Close

10. The value of the kinetic constant was shown while the other values in the spreadsheet were changed. As shown in the picture below, the R^2 was 0.9997 and the SSR value was reduced to 3.11, indicating that the non-linear regression line best fitted the raw data as shown in the graph.



APPENDIX B

The non-linear regression curve of TDG stability and drug release study

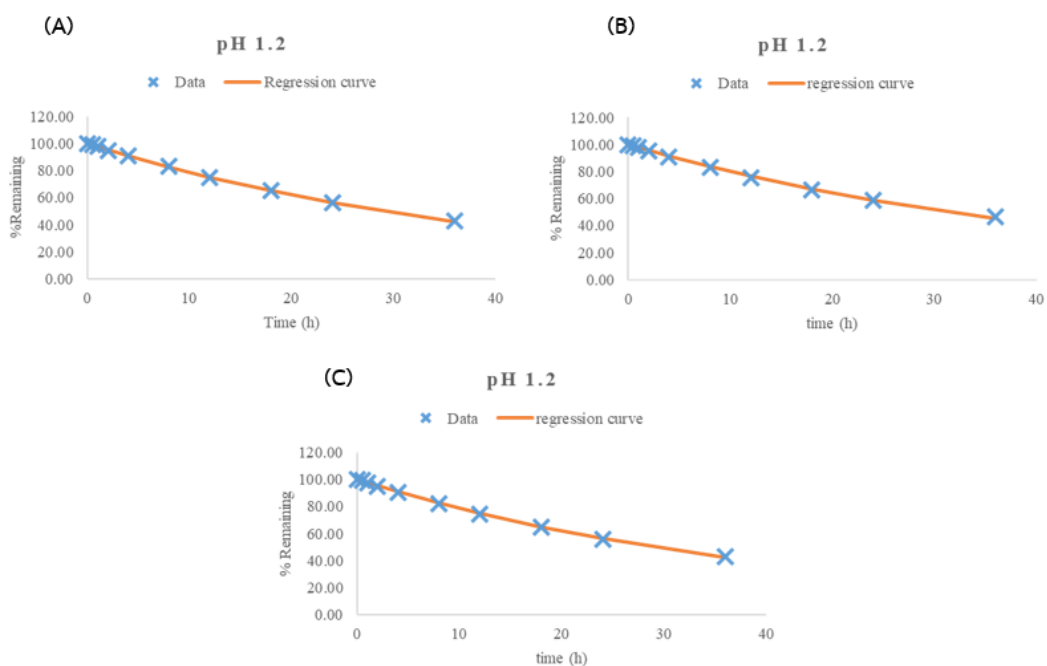


Figure 26 The kinetic plots of TDG in buffer solution pH 1.2, n = 3.

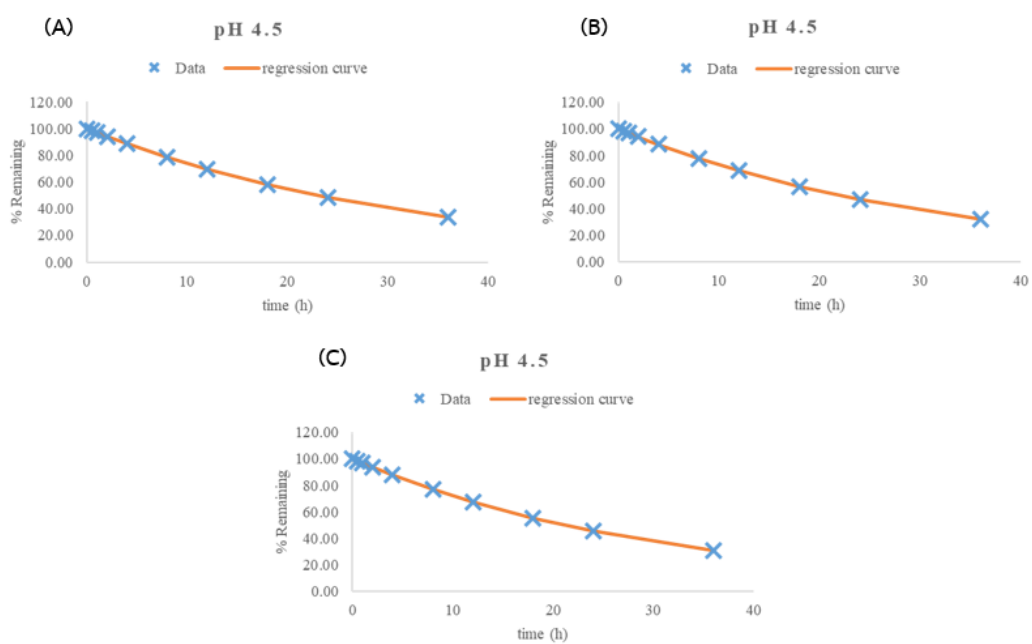


Figure 27 The kinetic plots of TDG in buffer solution pH 4.5, n = 3

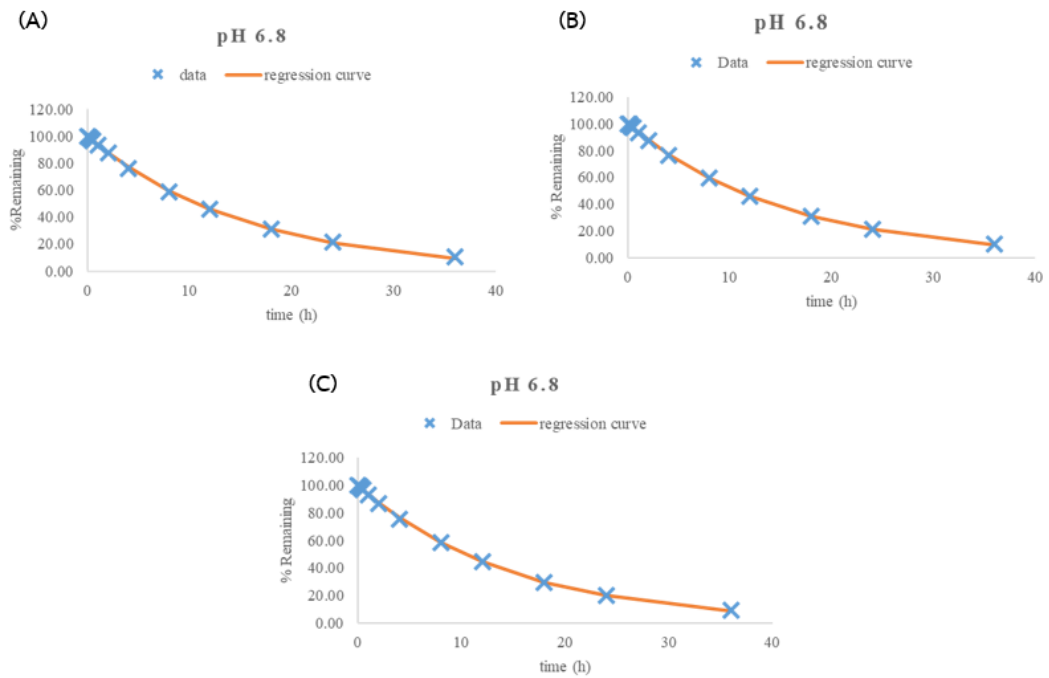


Figure 28 The kinetic plots of TDG in buffer solution pH 6.8, n = 3

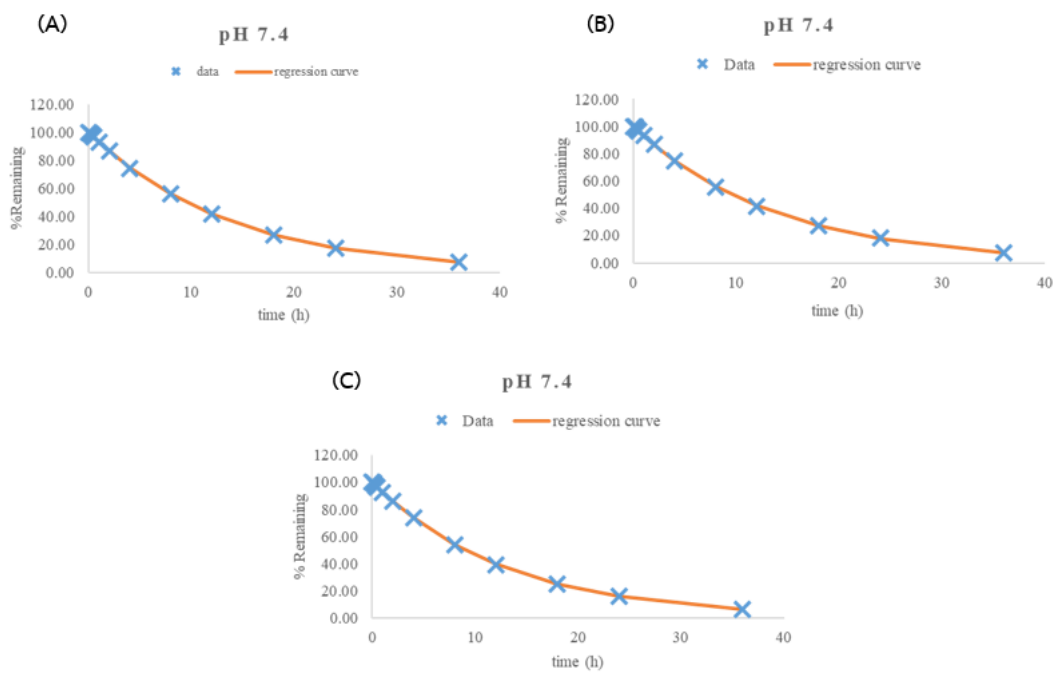


Figure 29 The kinetic plots of TDG in buffer solution pH 7.4, n = 3

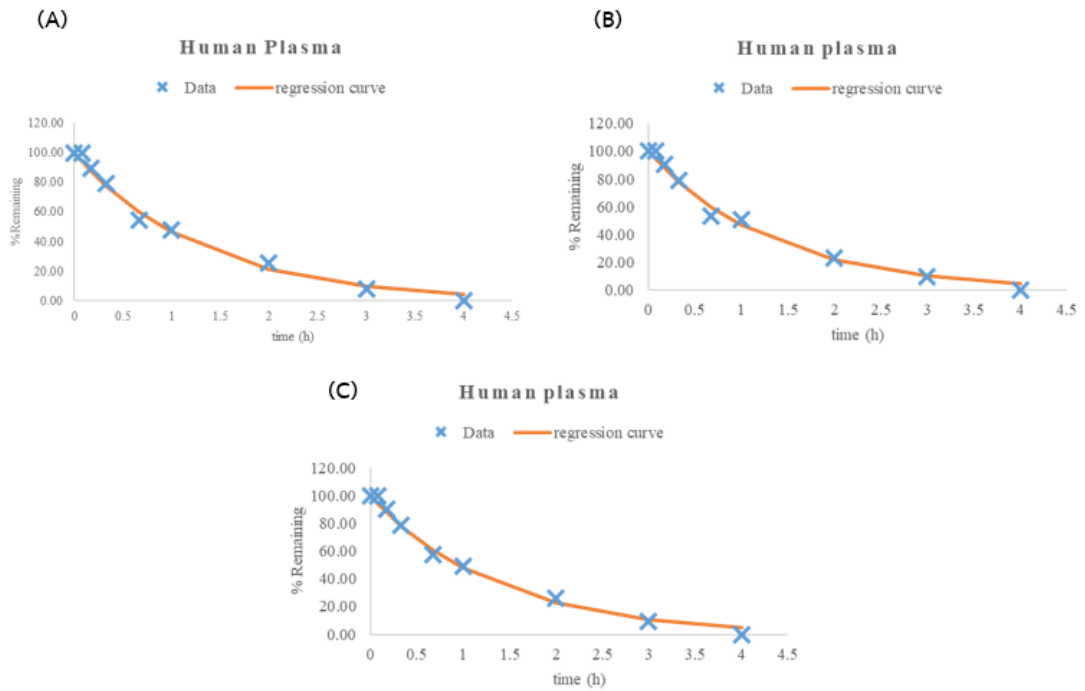


Figure 30 The kinetic plots of TDG in human plasma, n = 3



APPENDIX C

UHPLC chromatograms of THC, TMG, and TDG at 10 µg/ml

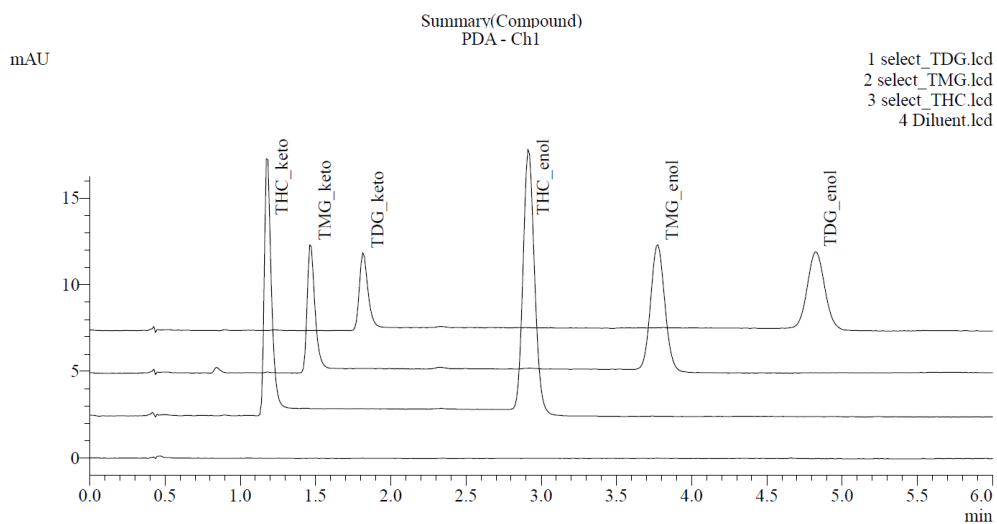
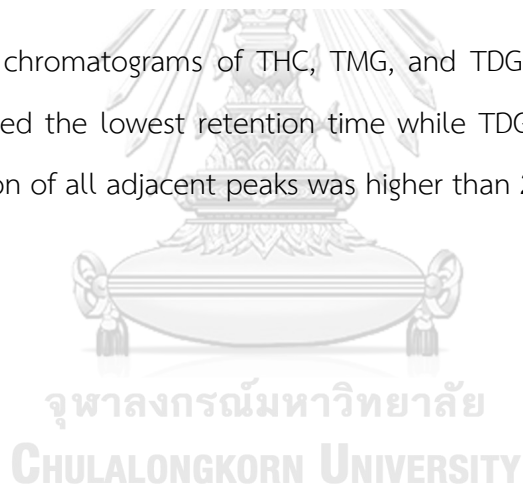


Figure 31 UHPLC chromatograms of THC, TMG, and TDG at a concentration of 10 µg/ml. THC showed the lowest retention time while TDG had the higher retention time. The resolution of all adjacent peaks was higher than 2.0.



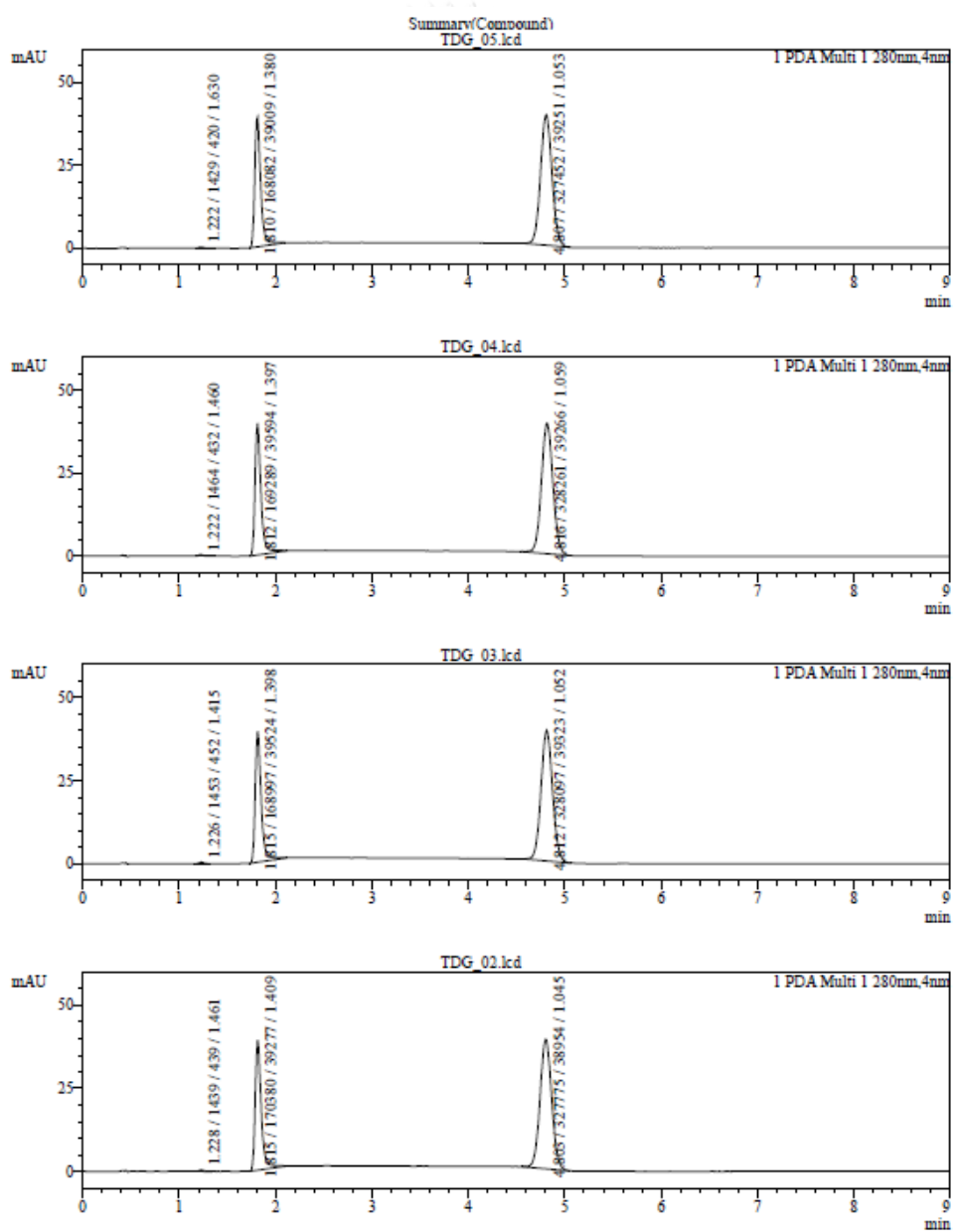
APPENDIX D

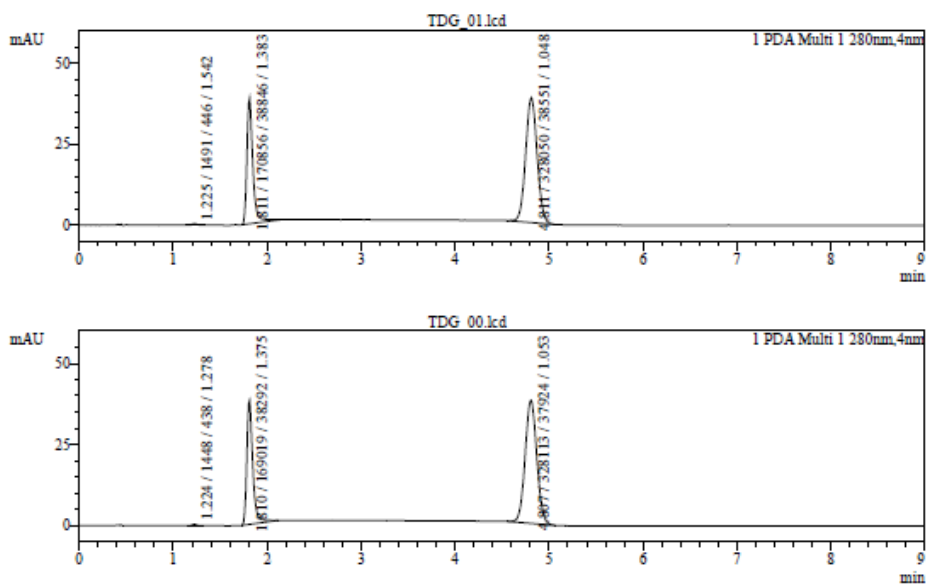
UHPLC chromatogram for evaluating the purity of TDG

1. The evaluation of %purity of TDG

The average total peak area was 498,849 and the average sum of keto and enol peak area was 497,395. Therefore, the purity of TDG was 99.71%. The equation to calculate the %purity was shown below:

$$\%Purity = [(AVG \text{ peak area of keto} + AVG \text{ peak area of enol}) / \text{total peak area}] \times 100$$





Summary(Compound)

<< PDA >>

ID#1 Compound Name: TDG keto

Title	Sample Name	Ret. Time	Area
TDG 05.lcd	TDG 05	1.810	168082
TDG 04.lcd	TDG 04	1.812	169289
TDG 03.lcd	TDG 03	1.815	168997
TDG 02.lcd	TDG 02	1.815	170380
TDG 01.lcd	TDG 01	1.811	170856
TDG 00.lcd	TDG 00	1.810	169019
Average		1.812	169437
%RSD		0.129	0.598
Maximum		1.815	170856
Minimum		1.810	168082
Standard Deviation		0.002	1013

ID#2 Compound Name: TDG enol

Title	Sample Name	Ret. Time	Area
TDG 05.lcd	TDG 05	4.807	327452
TDG 04.lcd	TDG 04	4.816	328261
TDG 03.lcd	TDG 03	4.812	328097
TDG 02.lcd	TDG 02	4.803	327775
TDG 01.lcd	TDG 01	4.811	328050
TDG 00.lcd	TDG 00	4.807	328113
Average		4.809	327958
%RSD		0.097	0.090
Maximum		4.816	328261
Minimum		4.803	327452
Standard Deviation		0.005	294

Figure 32 The UHPLC chromatogram of 100 $\mu\text{g/ml}$ of TDG analyzed with 6 replications.

APPENDIX E

The calibration curve of TDG

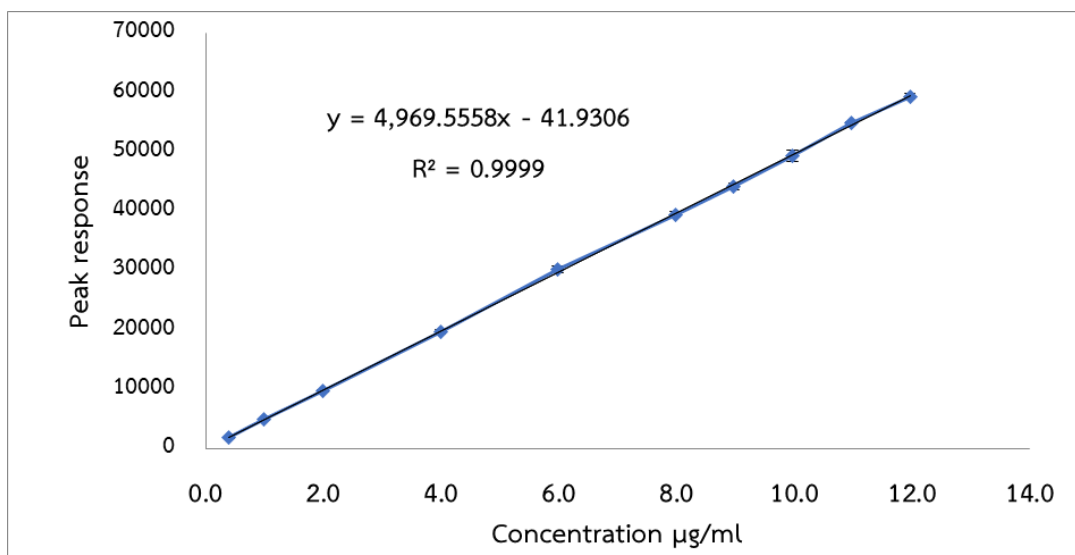
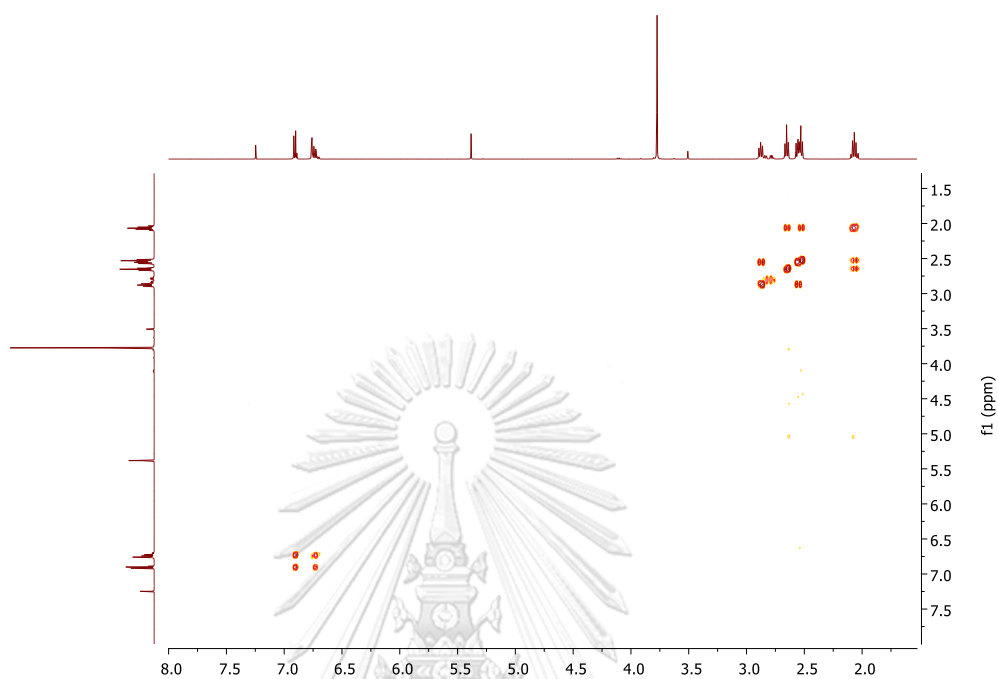
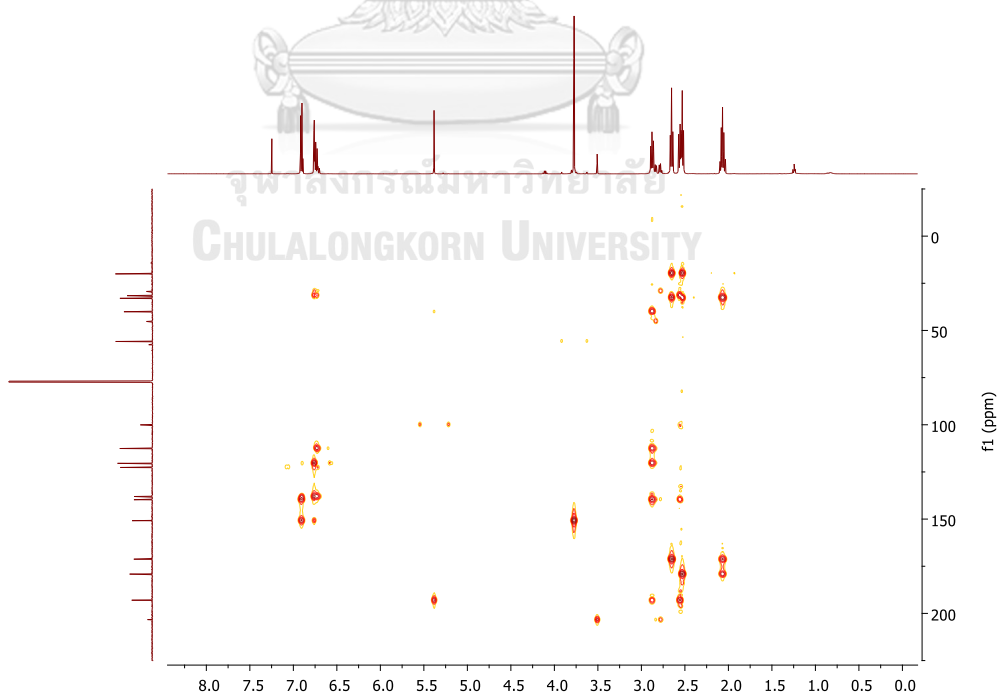


Figure 33 The calibration curve of TDG showed a good relationship between peak response and concentration with R square 0.9999.



APPENDIX F

Two-dimensional nuclear magnetic resonance (2D-NMR) spectrum

Figure 34 COSY spectrum of TDG in CDCl₃Figure 35 HMBC spectrum of TDG in CDCl₃

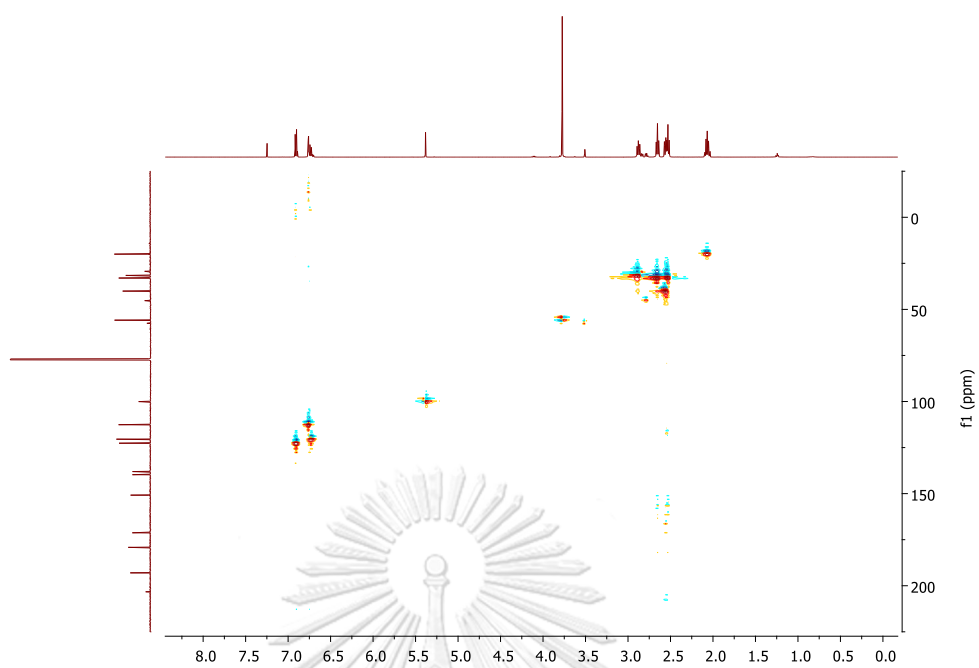


Figure 36 HSQC spectrum of TDG in CDCl_3

APPENDIX G

Hepatoprotective effect of silymarin in alcohol-induced liver cells death

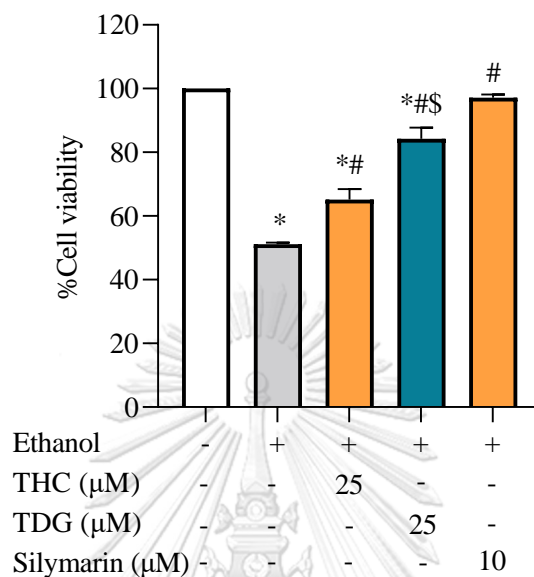


Figure 37 Effect of THC, TDG, and silymarin on ethanol-induced liver cell death. The pretreatment of cells with silymarin at 10 μM recovered cell viability to a similar level to the untreated control group. Values are given as mean \pm SD values of three independent experiments and analyzed using One-Way ANOVA followed by Tukey post hoc test, * $p < 0.05$ compared to the nontreated control group, # $p < 0.05$ compared to the ethanol treatment group, and \$ $p < 0.05$ compared to the THC treatment at corresponding concentrations.

APPENDIX H
Certificate of analysis THC



ZHONGLAN INDUSTRY CO., LTD.

Tel No.: 86-531-82956570, Fax No.: 86-531-8295657 Email ID: sale015@zhonglanindustry.com

CERTIFICATE OF ANALYSIS

Description	Tetrahydrocurcumin		
CAS	36062-04-1	Batch No.	ZL20180816
Sterilization Method	High temperature setrilization	Manufacture Date	Aug. 16, 2018
Report Date	Aug. 16, 2018	Expiry Date	Aug. 15, 2020

Item of Analysis	Specification	Results	Test Methods
Identification	99%	99.08%	HPLC
Loss on drying	5%NMT (%)	1.2%	5g/105C/5hrs
Total ash	2%NMT (%)	0.54%	5g/105C/5hrs
Residue of Solvents	None	Conform	NLS-QCS-1007
Bulk Density	45-60g/100mL	51g/100mL	CP2010IA
Heavy Metals	10ppm Max	3.7ppm	Atomic Absorption
Lead (Pb)	2ppm NMT	0.41ppm	Atomic Absorption
Arsenic (As)	2ppm NMT	0.19 ppm	Atomic Absorption
Cadmium (Cd)	2ppm NMT	0.31 ppm	Atomic Absorption
Mercury (Hg)	1ppm NMT	0.25 ppm	Atomic Absorption
Pesticide Residues	1ppm NMT	0.33 ppm	Gas Chromatography
Total Plate Count	1000cfu/g Max	363cfu/g Max	AOAC
Yeast & Mold	100cfu/g Max	Conform	AOAC
E. Coli.	Negative	Conform	AOAC
Salmonella	Negative	Conform	AOAC
Staphylococcus	Negative	Conform	AOAC

Storage: Store in tight, light-resistant containers, avoid exposure to direct sunlight, moisture and excessive heat.

Shelf Life: 24 months if store under the conditions above and stay in original packaging.

ANALYST: LIYA

CHECKER: WEICHEN

Q.C DIRECTOR: XULEILEI



REFERENCES

- Aggarwal, B. B., Deb, L., & Prasad, S. (2014). Curcumin differs from tetrahydrocurcumin for molecular targets, signaling pathways and cellular responses. *Molecules (Basel, Switzerland)*, *20*(1), 185-205. <https://doi.org/10.3390/molecules20010185>
- Ambrose, P. J. (1984). Clinical pharmacokinetics of chloramphenicol and chloramphenicol succinate. *Clinical Pharmacokinetics*, *9*(3), 222-238. <https://doi.org/10.2165/00003088-198409030-00004>
- Ayala, A., Muñoz, M. F., & Argüelles, S. (2014). Lipid peroxidation: production, metabolism, and signaling mechanisms of malondialdehyde and 4-hydroxy-2-nonenal. *Oxidative Medicine and Cellular Longevity*, *2014*, 360438, 1-31. <https://doi.org/10.1155/2014/360438>
- Bakhtin, S., Shved, E., Bupal'ko, Y., & Stepanova, Y. (2018). Behaviour modelling of organic bases in the oxyalkylation reaction of proton-containing nucleophiles. *Progress in Reaction Kinetics and Mechanism*, *43*(2), 121-135. <https://doi.org/10.3184/146867818x15161889114501>
- Bandopadhyay, S., Manchanda, S., Chandra, A., Ali, J., & Deb, P. K. (2020). Chapter 5 - Overview of different carrier systems for advanced drug delivery. In R. K. Tekade (Ed.), *Drug Delivery Systems* (pp. 179-233). Academic Press. <https://doi.org/10.1016/B978-0-12-814487-9.00005-3>
- Barve, A., Khan, R., Marsano, L., Ravindra, K., & McClain, C. (2008). Treatment of alcoholic liver disease. *Annals of Hepatology*, *71*, 5-15. [https://doi.org/10.1016/S1665-2681\(19\)31883-6](https://doi.org/10.1016/S1665-2681(19)31883-6)
- Baumber, J., & Ball, B. A. (2005). Determination of glutathione peroxidase and superoxide dismutase-like activities in equine spermatozoa, seminal plasma, and reproductive tissues. *American Journal of Veterinary Research*, *66*(8), 1415-19. <https://doi.org/10.2460/ajvr.2005.66.1415>
- Bhaskar Rao, A., Prasad, E., Deepthi, S. S., & Ansari, I. A. (2014). Synthesis and biological evaluation of glucosyl curcuminoids. *Archiv der Pharmazie*, *347*(11), 834-839. <https://doi.org/10.1002/ardp.201400195>

- Bhatia, N. K., Kishor, S., Katyal, N., Gogoi, P., Narang, P., & Deep, S. (2016). Effect of pH and temperature on conformational equilibria and aggregation behaviour of curcumin in aqueous binary mixtures of ethanol [10.1039/C6RA24256A]. *RSC Advances*, 6(105), 103275-88. <https://doi.org/10.1039/C6RA24256A>
- Boyd, B. J., Bergström, C. A. S., Vinarov, Z., Kuentz, M., Brouwers, J., Augustijns, P., Brandl, M., Bernkop-Schnürch, A., Shrestha, N., Préat, V., Müllertz, A., Bauer-Brandl, A., & Jannin, V. (2019). Successful oral delivery of poorly water-soluble drugs both depends on the intraluminal behavior of drugs and of appropriate advanced drug delivery systems. *European Journal of Pharmaceutical Sciences*, 137, 104967, 1-27. <https://doi.org/10.1016/j.ejps.2019.104967>
- Castell, J. V., Jover, R., Martínez-Jiménez, C. P., & Gmez-Lechn, M. J. (2006). Hepatocyte cell lines: their use, scope and limitations in drug metabolism studies. *Expert Opinion on Drug Metabolism & Toxicology*, 2(2), 183-212. <https://doi.org/10.1517/17425255.2.2.183>
- Cederbaum, A. I., Lu, Y., & Wu, D. (2009). Role of oxidative stress in alcohol-induced liver injury. *Archives of Toxicology*, 83(6), 519-548. <https://doi.org/10.1007/s00204-009-0432-0>
- Ceni, E., Mello, T., & Galli, A. (2014). Pathogenesis of alcoholic liver disease: role of oxidative metabolism. *World Journal of Gastroenterology*, 20(47), 17756-72. <https://doi.org/10.3748/wjg.v20.i47.17756>
- Chen, J.-W., Kong, Z.-L., Tsai, M.-L., Lo, C.-Y., Ho, C.-T., & Lai, C.-S. (2018). Tetrahydrocurcumin ameliorates free fatty acid-induced hepatic steatosis and improves insulin resistance in HepG2 cells. *Journal of Food and Drug Analysis*, 26(3), 1075-85. <https://doi.org/10.1016/j.jfda.2018.01.005>
- Chen, M.-F., Gong, F., Zhang, Y. Y., Li, C., Zhou, C., Hong, P., Sun, S., & Qian, Z.-J. (2019). Preventive effect of YGDEY from Tilapia fish skin gelatin hydrolysates against alcohol-induced damage in HepG2 cells through ROS-mediated signaling pathways. *Nutrients*, 11(2), 392, 1-16. <https://doi.org/10.3390/nu11020392>
- Chen, P., Hu, M., Liu, F., Yu, H., & Chen, C. (2019). S-allyl-L-cysteine (SAC) protects hepatocytes from alcohol-induced apoptosis. *FEBS Open Bio*, 9(7), 1327-36. <https://doi.org/10.1002/2211-5463.12684>

- Cichoż-Lach, H., & Michalak, A. (2014). Oxidative stress as a crucial factor in liver diseases. *World Journal of Gastroenterology*, 20(25), 8082-91. <https://doi.org/10.3748/wjg.v20.i25.8082>
- Constable, P. (2009). CHAPTER 111 - Clinical acid-base chemistry. In C. Ronco, R. Bellomo, & J. A. Kellum (Eds.), *Critical Care Nephrology (Second Edition)* (pp. 581-586). W.B. Saunders. <https://doi.org/10.1016/B978-1-4160-4252-5.50116-7>
- DALYs, G. B. D., & Collaborators, H. (2018). Global, regional, and national disability-adjusted life-years (DALYs) for 359 diseases and injuries and healthy life expectancy (HALE) for 195 countries and territories, 1990-2017: a systematic analysis for the Global Burden of Disease Study 2017. *Lancet (London, England)*, 392(10159), 1859-1922. [https://doi.org/10.1016/S0140-6736\(18\)32335-3](https://doi.org/10.1016/S0140-6736(18)32335-3)
- Damen, E. W. P., Wiegerinck, P. H. G., Braamer, L., Sperling, D., de Vos, D., & Scheeren, H. W. (2000). Paclitaxel esters of malic acid as prodrugs with improved water solubility. *Bioorganic & Medicinal Chemistry*, 8(2), 427-432. [https://doi.org/10.1016/S0968-0896\(99\)00301-6](https://doi.org/10.1016/S0968-0896(99)00301-6)
- Du, W., Hong, L., Yao, T., Yang, X., He, Q., Yang, B., & Hu, Y. (2007). Synthesis and evaluation of water-soluble docetaxel prodrugs-docetaxel esters of malic acid. *Bioorganic & Medicinal Chemistry*, 15(18), 6323-30. <https://doi.org/10.1016/j.bmc.2007.04.002>
- Elmore, S. (2007). Apoptosis: a review of programmed cell death. *Toxicologic Pathology*, 35(4), 495-516. <https://doi.org/10.1080/01926230701320337>
- Farshori, N. N., Al-Sheddi, E. S., Al-Oqail, M. M., Hassan, W. H. B., Al-Khedhairi, A. A., Musarrat, J., & Siddiqui, M. A. (2013). Hepatoprotective potential of *Lavandula coronopifolia* extracts against ethanol induced oxidative stress-mediated cytotoxicity in HepG2 cells. *Toxicology and Industrial Health*, 31(8), 727-737. <https://doi.org/10.1177/0748233713483188>
- Fragoza-Mar, L., Pérez-Caballero, G., Gutierrez, J. L. G., & Jiménez-Cruz, a. F. (2011). Modeling and theory in resonance assisted hydrogen bonding (RAHB) systems: β -diketones (OHO) and arylazophenols (NHO). In F. Jiménez-Cruz & J. L. García-Gutiérrez (Eds.). Transworld Research Network.
- Fredholt, K., Mørk, N., & Begtrup, M. (1995). Hemiesters of aliphatic dicarboxylic acids as

- cyclization-activated prodrug forms for protecting phenols against first-pass metabolism. *International Journal of Pharmaceutics*, 123(2), 209-216. [https://doi.org/10.1016/0378-5173\(95\)00062-N](https://doi.org/10.1016/0378-5173(95)00062-N)
- Furfine, E. S., Baker, C. T., Hale, M. R., Reynolds, D. J., Salisbury, J. A., Searle, A. D., Studenberg, S. D., Todd, D., Tung, R. D., & Spaltenstein, A. (2004). Preclinical pharmacology and pharmacokinetics of GW433908, a water-soluble prodrug of the human immunodeficiency virus protease inhibitor amprenavir. *Antimicrobial Agents and Chemotherapy*, 48(3), 791-798. <https://doi.org/10.1128/AAC.48.3.791-798.2004>
- García-Suástegui, W. A., Ramos-Chávez, L. A., Rubio-Osornio, M., Calvillo-Velasco, M., Atzin-Méndez, J. A., Guevara, J., & Silva-Adaya, D. (2017). The role of CYP2E1 in the drug metabolism or bioactivation in the brain. *Oxidative Medicine and Cellular Longevity*, 2017, 4680732, 1-15. <https://doi.org/10.1155/2017/4680732>
- Gerets, H. H. J., Tilmant, K., Gerin, B., Chanteux, H., Depelchin, B. O., Dhalluin, S., & Atienzar, F. A. (2012). Characterization of primary human hepatocytes, HepG2 cells, and HepaRG cells at the mRNA level and CYP activity in response to inducers and their predictivity for the detection of human hepatotoxins. *Cell Biology and Toxicology*, 28(2), 69-87. <https://doi.org/10.1007/s10565-011-9208-4>
- Gómez-Lechón, M., Tolosa, L., & Donato, M. T. (2014). Cell-based models to predict human hepatotoxicity of drugs. *Revista de Toxicologia*, 31(2), 149-156
- Greeshma, N., Prasanth, K. G., & Balaji, B. (2015). Tetrahydrocurcumin exerts protective effect on vincristine induced neuropathy: Behavioral, biochemical, neurophysiological and histological evidence. *Chemico-Biological Interactions*, 238, 118-128. <https://doi.org/10.1016/j.cbi.2015.06.025>
- Hamed, R., Awadallah, A., Sunoqrot, S., Tarawneh, O., Nazzal, S., AlBaraghthi, T., Al Sayyad, J., & Abbas, A. (2016). pH-dependent solubility and dissolution behavior of carvedilol—case example of a weakly basic BCS class II drug. *AAPS PharmSciTech*, 17(2), 418-426. <https://doi.org/10.1208/s12249-015-0365-2>
- Hauck, A. K., & Bernlohr, D. A. (2016). Oxidative stress and lipotoxicity. *Journal of Lipid Research*, 57(11), 1976-86. <https://doi.org/10.1194/jlr.R066597>
- Henzel, K., Thorborg, C., Hofmann, M., Zimmer, G., & Leuschner, U. (2004). Toxicity of

- ethanol and acetaldehyde in hepatocytes treated with ursodeoxycholic or tauroursodeoxycholic acid. *Biochimica et Biophysica Acta (BBA) - Molecular Cell Research*, 1644(1), 37-45. <https://doi.org/10.1016/j.bbamcr.2003.10.017>
- Hoek, J. B., Cahill, A., & Pastorino, J. G. (2002). Alcohol and mitochondria: a dysfunctional relationship. *Gastroenterology*, 122(7), 2049-63. <https://doi.org/10.1053/gast.2002.33613>
- Holder, G. M., Plummer, J. L., & Ryan, A. J. (1978). The metabolism and excretion of curcumin (1,7-Bis-(4-hydroxy-3-methoxyphenyl)-1,6-heptadiene-3,5-dione) in the rat. *Xenobiotica*, 8(12), 761-768. <https://doi.org/10.3109/00498257809069589>
- Huttunen, K. M., Raunio, H., & Rautio, J. (2011). Prodrugs--from serendipity to rational design. *Pharmacological Reviews*, 63(3), 750-771. <https://doi.org/10.1124/pr.110.003459>
- Ighodaro, O. M., & Akinloye, O. A. (2018). First line defence antioxidants-superoxide dismutase (SOD), catalase (CAT) and glutathione peroxidase (GPX): Their fundamental role in the entire antioxidant defence grid. *Alexandria Journal of Medicine*, 54(4), 287-293. <https://doi.org/10.1016/j.ajme.2017.09.001>
- Iranshahy, M., Iranshahi, M., Abtahi, S. R., & Karimi, G. (2018). The role of nuclear factor erythroid 2-related factor 2 in hepatoprotective activity of natural products: A review. *Food and Chemical Toxicology*, 120, 261-276. <https://doi.org/10.1016/j.fct.2018.07.024>
- Jankun, J., Wyganowska-Świątkowska, M., Dettlaff, K., Jelińska, A., Surdacka, A., Wątróbska-Świetlikowska, D., & Skrzypczak-Jankun, E. (2016). Determining whether curcumin degradation/condensation is actually bioactivation (Review). *International Journal of Molecular Medicine*, 37(5), 1151-8. <https://doi.org/10.3892/ijmm.2016.2524>
- Jimenez-Lopez, J. M., & Cederbaum, A. I. (2005). CYP2E1-dependent oxidative stress and toxicity: role in ethanol-induced liver injury. *Expert Opinion on Drug Metabolism & Toxicology*, 1(4), 671-685. <https://doi.org/10.1517/17425255.1.4.671>
- Johansson, L. H., & Håkan Borg, L. A. (1988). A spectrophotometric method for determination of catalase activity in small tissue samples. *Analytical Biochemistry*, 174(1), 331-336. [https://doi.org/10.1016/0003-2697\(88\)90554-4](https://doi.org/10.1016/0003-2697(88)90554-4)

- Kalliokoski, A., & Niemi, M. (2009). Impact of OATP transporters on pharmacokinetics. *British Journal of Pharmacology*, 158(3), 693-705. <https://doi.org/10.1111/j.1476-5381.2009.00430.x>
- Keleku-Lukwete, N., Suzuki, M., & Yamamoto, M. (2017). An overview of the advantages of KEAP1-NRF2 system activation during inflammatory disease treatment. *Antioxidants & Redox Signaling*, 29(17), 1746-55. <https://doi.org/10.1089/ars.2017.7358>
- Kessova, I. G., Ho, Y.-S., Thung, S., & Cederbaum, A. I. (2003). Alcohol-induced liver injury in mice lacking Cu, Zn-superoxide dismutase. *Hepatology*, 38(5), 1136-45. <https://doi.org/10.1053/jhep.2003.50450>
- Kim, S. J., Lee, J. W., Jung, Y. S., Kwon, D. Y., Park, H. K., Ryu, C. S., Kim, S. K., Oh, G. T., & Kim, Y. C. (2009). Ethanol-induced liver injury and changes in sulfur amino acid metabolomics in glutathione peroxidase and catalase double knockout mice. *Journal of Hepatology*, 50(6), 1184-91. <https://doi.org/10.1016/j.jhep.2009.01.030>
- Lee, S.-L., Huang, W.-J., Lin, W. W., Lee, S.-S., & Chen, C.-H. (2005). Preparation and anti-inflammatory activities of diarylheptanoid and diarylheptylamine analogs. *Bioorganic & Medicinal Chemistry*, 13(22), 6175-81. <https://doi.org/10.1016/j.bmc.2005.06.058>
- Lee, S., Lee, J., Lee, H., & Sung, J. (2019). Relative protective activities of quercetin, quercetin-3-glucoside, and rutin in alcohol-induced liver injury. *Journal of Food Biochemistry*, 43(11), e13002, 1-9. <https://doi.org/10.1111/jfbc.13002>
- Lee, Y.-J., Beak, S.-Y., Choi, I., & Sung, J.-S. (2017). Quercetin and its metabolites protect hepatocytes against ethanol-induced oxidative stress by activation of Nrf2 and AP-1. *Food Science and Biotechnology*, 27(3), 809-817. <https://doi.org/10.1007/s10068-017-0287-8>
- Leggio, L., & Lee, M. R. (2017). Treatment of alcohol use disorder in patients with alcoholic liver disease. *The American Journal of Medicine*, 130(2), 124-134. <https://doi.org/10.1016/j.amjmed.2016.10.004>
- Leung, T.-M., & Nieto, N. (2013). CYP2E1 and oxidant stress in alcoholic and non-alcoholic fatty liver disease. *Journal of Hepatology*, 58(2), 395-398. <https://doi.org/10.1016/j.jhep.2012.08.018>

- Li, J., Shi, J., Medina, J. E., Zhou, J., Du, X., Wang, H., Yang, C., Liu, J., Yang, Z., Dinulescu, D. M., & Xu, B. (2017). Selectively inducing cancer cell death by intracellular Enzyme-Instructed Self-Assembly (EISA) of dipeptide derivatives. *Advanced Healthcare Materials*, 6(15), 1601400, 1-9. <https://doi.org/10.1002/adhm.201601400>
- Li, K., Zhai, M., Jiang, L., Song, F., Zhang, B., Li, J., Li, H., Li, B., Xia, L., Xu, L., Cao, Y., He, M., Zhu, H., Zhang, L., Liang, H., Jin, Z., Duan, W., & Wang, S. (2019). Tetrahydrocurcumin ameliorates diabetic cardiomyopathy by attenuating high glucose-induced oxidative stress and fibrosis via activating the SIRT1 pathway. *Oxidative Medicine and Cellular Longevity*, 2019, 6746907, 1-16. <https://doi.org/10.1155/2019/6746907>
- Liang, H.-W., Yang, T.-Y., Teng, C.-S., Lee, Y.-J., Yu, M.-H., Lee, H.-J., Hsu, L.-S., & Wang, C.-J. (2021). Mulberry leaves extract ameliorates alcohol-induced liver damages through reduction of acetaldehyde toxicity and inhibition of apoptosis caused by oxidative stress signals. *International Journal of Medical Sciences*, 18(1), 53-64. <https://doi.org/10.7150/ijms.50174>
- Linhart, K., Bartsch, H., & Seitz, H. K. (2014). The role of reactive oxygen species (ROS) and cytochrome P-450 2E1 in the generation of carcinogenic etheno-DNA adducts. *Redox Biology*, 3, 56-62. <https://doi.org/10.1016/j.redox.2014.08.009>
- Lopez, J., & Tait, S. W. G. (2015). Mitochondrial apoptosis: killing cancer using the enemy within. *British Journal of Cancer*, 112(6), 957-962. <https://doi.org/10.1038/bjc.2015.85>
- Lowe, F. (2014). Biomarkers of oxidative stress. In I. Laher (Ed.), *Systems biology of free radicals and antioxidants* (pp. 65-87). Springer Berlin Heidelberg. https://doi.org/10.1007/978-3-642-30018-9_4
- Lu, C., Zhang, F., Xu, W., Wu, X., Lian, N., Jin, H., Chen, Q., Chen, L., Shao, J., Wu, L., Lu, Y., & Zheng, S. (2015). Curcumin attenuates ethanol-induced hepatic steatosis through modulating Nrf2/FXR signaling in hepatocytes. *IUBMB Life*, 67(8), 645-658. <https://doi.org/10.1002/iub.1409>
- Lu, Y., & Cederbaum, A. I. (2008). CYP2E1 and oxidative liver injury by alcohol. *Free Radical Biology & Medicine*, 44(5), 723-738.

<https://doi.org/10.1016/j.freeradbiomed.2007.11.004>

- Luo, D.-D., Chen, J.-F., Liu, J.-J., Xie, J.-H., Zhang, Z.-B., Gu, J.-Y., Zhuo, J.-Y., Huang, S., Su, Z.-R., & Sun, Z.-H. (2019). Tetrahydrocurcumin and octahydrocurcumin, the primary and final hydrogenated metabolites of curcumin, possess superior hepatic-protective effect against acetaminophen-induced liver injury: Role of CYP2E1 and Keap1-Nrf2 pathway. *Food and Chemical Toxicology*, *123*, 349-362. <https://doi.org/10.1016/j.fct.2018.11.012>
- Ma, Q. (2013). Role of nrf2 in oxidative stress and toxicity. *Annual Review of Pharmacology and Toxicology*, *53*, 401-426. <https://doi.org/10.1146/annurev-pharmtox-011112-140320>
- Madushani Herath, K. H. I. N., Bing, S. J., Cho, J., Kim, A., Kim, G., Kim, J.-S., Kim, J.-B., Doh, Y. H., & Jee, Y. (2018). Sasa quelpaertensis leaves ameliorate alcohol-induced liver injury by attenuating oxidative stress in HepG2 cells and mice. *Acta Histochemica*, *120*(5), 477-489. <https://doi.org/10.1016/j.acthis.2018.05.011>
- Majeed, M., Natarajan, S., Pandey, A., Bani, S., & Mundkur, L. (2019). Subchronic and reproductive/developmental toxicity studies of tetrahydrocurcumin in rats. *Toxicological Research*, *35*(1), 65-74. <https://doi.org/10.5487/TR.2019.35.1.065>
- Malik, P., & Mukherjee, T. K. (2014). Structure-function elucidation of antioxidative and prooxidative activities of the polyphenolic compound curcumin. *Chinese Journal of Biology*, *2014*, 396708, 1-9. <https://doi.org/10.1155/2014/396708>
- Manthey, J., Shield, K. D., Rylett, M., Hasan, O. S. M., Probst, C., & Rehm, J. (2019). Global alcohol exposure between 1990 and 2017 and forecasts until 2030: a modelling study. *The Lancet*, *393*(10190), 2493-2502. [https://doi.org/10.1016/S0140-6736\(18\)32744-2](https://doi.org/10.1016/S0140-6736(18)32744-2)
- Matés, J. M., Segura, J. A., Alonso, F. J., & Márquez, J. (2012). Oxidative stress in apoptosis and cancer: an update. *Archives of Toxicology*, *86*(11), 1649-65. <https://doi.org/10.1007/s00204-012-0906-3>
- Morio, Y., Tsuji, M., Inagaki, M., Nakagawa, M., Asaka, Y., Oyamada, H., Furuya, K., & Oguchi, K. (2013). Ethanol-induced apoptosis in human liver adenocarcinoma cells (SK-Hep1): Fas- and mitochondria-mediated pathways and interaction with MAPK signaling system. *Toxicology in Vitro*, *27*(6), 1820-29.

<https://doi.org/10.1016/j.tiv.2013.05.009>

- Mosoni, C., Dionisi, T., Vassallo, G. A., Mirijello, A., Tarli, C., Antonelli, M., Sestito, L., Rando, M. M., Tosoni, A., De Cosmo, S., Gasbarrini, A., & Addolorato, G. (2018). Baclofen for the treatment of alcohol use disorder in patients with liver cirrhosis: 10 years after the first evidence. *Frontiers in Psychiatry*, *9*, 474. <https://doi.org/10.3389/fpsyt.2018.00474>
- Muangnoi, C., Jithavech, P., Ratnatilaka Na Bhuket, P., Supasena, W., Wichitnithad, W., Towiwat, P., Niwattisaiwong, N., Haworth, I. S., & Rojsitthisak, P. (2018). A curcumin-diglutaric acid conjugated prodrug with improved water solubility and antinociceptive properties compared to curcumin. *Bioscience, Biotechnology, and Biochemistry*, *82*(8), 1301-08. <https://doi.org/10.1080/09168451.2018.1462694>
- Muangnoi, C., Phumsuay, R., Jongjitphisut, N., Waikasikorn, P., Sangsawat, M., Rashatasakhon, P., Paraoan, L., & Rojsitthisak, P. (2021). Protective effects of a lutein ester prodrug, lutein diglutaric acid, against H₂O₂-Induced oxidative stress in human retinal pigment epithelial cells. *International Journal of Molecular Sciences*, *22*(9), 4722, 1-16. <https://doi.org/10.3390/ijms22094722>
- Muangnoi, C., Ratnatilaka Na Bhuket, P., Jithavech, P., Supasena, W., Paraoan, L., Patumraj, S., & Rojsitthisak, P. (2019). Curcumin diethyl disuccinate, a prodrug of curcumin, enhances anti-proliferative effect of curcumin against HepG2 cells via apoptosis induction. *Scientific Reports*, *9*(1), 11718, 1-9. <https://doi.org/10.1038/s41598-019-48124-1>
- Mullard, A. (2021). 2020 FDA drug approvals. *20*, 85-90. <https://www.nature.com/articles/d41573-021-00002-0>
- Muncie, H. L., Jr., Yasinian, Y., & Oge, L. (2013). Outpatient management of alcohol withdrawal syndrome. *Am Fam Physician*, *88*(9), 589-595.
- Murugan, P., & Pari, L. (2006). Antioxidant effect of tetrahydrocurcumin in streptozotocin–nicotinamide induced diabetic rats. *Life Sciences*, *79*(18), 1720-28. <https://doi.org/10.1016/j.lfs.2006.06.001>
- Muthumani, M., & Miltonprabu, S. (2015). Ameliorative efficacy of tetrahydrocurcumin against arsenic induced oxidative damage, dyslipidemia and hepatic

- mitochondrial toxicity in rats. *Chemico-Biological Interactions*, 235, 95-105. <https://doi.org/10.1016/j.cbi.2015.04.006>
- Nagappan, A., Jung, D. Y., Kim, J.-H., Lee, H., & Jung, M. H. (2018). Gomisin N alleviates ethanol-induced liver injury through ameliorating lipid metabolism and oxidative stress. *International Journal of Molecular Sciences*, 19(9), 2601, 1-17. <https://doi.org/10.3390/ijms19092601>
- Nakmareong, S., Kukongviriyapan, U., Pakdeechote, P., Kukongviriyapan, V., Kongyingyoes, B., Donpunha, W., Prachaney, P., & Phisalaphong, C. (2012). Tetrahydrocurcumin alleviates hypertension, aortic stiffening and oxidative stress in rats with nitric oxide deficiency. *Hypertension Research*, 35(4), 418-425. <https://doi.org/10.1038/hr.2011.180>
- Neff, G. W., Duncan, C. W., & Schiff, E. R. (2011). The current economic burden of cirrhosis. *Gastroenterology & Hepatology*, 7(10), 661-671.
- Novaes, J. T., Lillico, R., Sayre, C. L., Nagabushnam, K., Majeed, M., Chen, Y., Ho, E. A., Oliveira, A. L. d. P., Martinez, S. E., Alrushaid, S., Davies, N. M., & Lakowski, T. M. (2017). Disposition, metabolism and histone deacetylase and acetyltransferase inhibition activity of tetrahydrocurcumin and other curcuminoids. *Pharmaceutics*, 9(4), 45, 1-17. <https://doi.org/10.3390/pharmaceutics9040045>
- Okada, K., Wangpoengtrakul, C., Tanaka, T., Toyokuni, S., Uchida, K., & Osawa, T. (2001). Curcumin and especially tetrahydrocurcumin ameliorate oxidative stress-induced renal injury in mice. *The Journal of Nutrition*, 131(8), 2090-95. <https://doi.org/10.1093/jn/131.8.2090>
- Organization, W. H. (2018). Global status report on alcohol and health 2018. *World Health Organization*.
- Osawa, T., Sugiyama, Y., Inayoshi, M., & Kawakishi, S. (1995). Antioxidative activity of tetrahydrocurcuminoids. *Bioscience, Biotechnology, and Biochemistry*, 59(9), 1609-12. <https://doi.org/10.1271/bbb.59.1609>
- Osna, N. A., Donohue, T. M., Jr., & Kharbanda, K. K. (2017). Alcoholic liver disease: pathogenesis and current management. *Alcohol Research : Current Reviews*, 38(2), 147-161.

- Pan, M.-H., Huang, T.-M., & Lin, J.-K. (1999). Biotransformation of curcumin through reduction and glucuronidation in mice. *Drug Metabolism and Disposition*, 27(4), 486, 1-9.
- Pari, L., & Amali, D. (2005). Protective role of tetrahydrocurcumin (THC) an active principle of turmeric on chloroquine induced hepatotoxicity in rats. *Journal of Pharmacy & Pharmaceutical Sciences : a Publication of the Canadian Society for Pharmaceutical Sciences, Société Canadienne Des Sciences Pharmaceutiques*, 8, 115-123.
- Pari, L., & Murugan, P. (2004). Protective role of tetrahydrocurcumin against erythromycin estolate-induced hepatotoxicity. *Pharmacological Research*, 49(5), 481-486. <https://doi.org/10.1016/j.phrs.2003.11.005>
- Pari, L., & Murugan, P. (2006). Tetrahydrocurcumin: Effect on chloroquine-mediated oxidative damage in rat kidney. *Basic & Clinical Pharmacology & Toxicology*, 99(5), 329-334. https://doi.org/10.1111/j.1742-7843.2006.pto_503.x
- Park, C.-H., Song, J. H., Kim, S.-N., Lee, J. H., Lee, H.-J., Kang, K. S., & Lim, H.-H. (2019). Neuroprotective effects of tetrahydrocurcumin against glutamate-induced oxidative stress in hippocampal HT22 cells. *Molecules (Basel, Switzerland)*, 25(1), 144, 1-10. <https://doi.org/10.3390/molecules25010144>
- Peiyuan, H., Zhiping, H., Chengjun, S., Chungqing, W., Bingqing, L., & Imam, M. U. (2017). Resveratrol ameliorates experimental alcoholic liver disease by modulating oxidative stress. *Evidence-Based Complementary and Alternative Medicine : eCAM*, 2017, 4287890, 1-11. <https://doi.org/10.1155/2017/4287890>
- Perrin, C. L. (2017). Linear or nonlinear least-squares analysis of kinetic data? *Journal of Chemical Education*, 94(6), 669-672. <https://doi.org/10.1021/acs.jchemed.6b00629>
- Poovorawan, K., Treeprasertsuk, S., Thepsuthammarat, K., Wilairatana, P., Kitsahawong, B., & Phaosawasdi, K. (2015). The burden of cirrhosis and impact of universal coverage public health care system in Thailand: Nationwide study. *Annals of Hepatology*, 14(6), 862-868. <https://doi.org/10.5604/16652681.1171773>
- Rabelo, A. C. S., de Pádua Lúcio, K., Araújo, C. M., de Araújo, G. R., de Amorim Miranda, P. H., Carneiro, A. C. A., de Castro Ribeiro, É. M., de Melo Silva, B., de Lima, W. G.,

- & Costa, D. C. (2018). Baccharis trimera protects against ethanol induced hepatotoxicity in vitro and in vivo. *Journal of Ethnopharmacology*, 215, 1-13. <https://doi.org/10.1016/j.jep.2017.12.043>
- Rahman, I., Kode, A., & Biswas, S. K. (2006). Assay for quantitative determination of glutathione and glutathione disulfide levels using enzymatic recycling method. *Nature Protocols*, 1(6), 3159-65. <https://doi.org/10.1038/nprot.2006.378>
- Rattanamongkolgul, S., Wongjitrat, C., & Puapankitcharoen, P. (2010). Prevalence of cirrhosis registered in Nakhon Nayok, Thailand. *Journal of the Medical Association of Thailand = Chotmaihet Thangphaet*, 93 Suppl 2, S87-91.
- Rautio, J., Kumpulainen, H., Heimbach, T., Oliyai, R., Oh, D., Järvinen, T., & Savolainen, J. (2008). Prodrugs: design and clinical applications. *Nature Reviews Drug Discovery*, 7(3), 255-270. <https://doi.org/10.1038/nrd2468>
- Redza-Dutordoir, M., & Averill-Bates, D. A. (2016). Activation of apoptosis signalling pathways by reactive oxygen species. *Biochimica et Biophysica Acta (BBA) - Molecular Cell Research*, 1863(12), 2977-92. <https://doi.org/10.1016/j.bbamcr.2016.09.012>
- Rehm, J., Gmel, G. E., Sr., Gmel, G., Hasan, O. S. M., Imtiaz, S., Popova, S., Probst, C., Roerecke, M., Room, R., Samokhvalov, A. V., Shield, K. D., & Shuper, P. A. (2017). The relationship between different dimensions of alcohol use and the burden of disease-an update. *Addiction (Abingdon, England)*, 112(6), 968-1001. <https://doi.org/10.1111/add.13757>
- Rehm, J., & Imtiaz, S. (2016). A narrative review of alcohol consumption as a risk factor for global burden of disease. *Substance Abuse Treatment, Prevention, and Policy*, 11(1), 37, 1-12. <https://doi.org/10.1186/s13011-016-0081-2>
- Rehm, J., Samokhvalov, A. V., & Shield, K. D. (2013). Global burden of alcoholic liver diseases. *Journal of Hepatology*, 59(1), 160-168. <https://doi.org/10.1016/j.jhep.2013.03.007>
- Rehm, J., & Shield, K. D. (2019). Global burden of alcohol use disorders and alcohol liver disease. *Biomedicines*, 7(4), 99, 1-10. <https://doi.org/10.3390/biomedicines7040099>
- Rehm, J., Taylor, B., Mohapatra, S., Irving, H., Baliunas, D., Patra, J., & Roerecke, M.

- (2010). Alcohol as a risk factor for liver cirrhosis: A systematic review and meta-analysis. *Drug and Alcohol Review*, 29(4), 437-445. <https://doi.org/10.1111/j.1465-3362.2009.00153.x>
- Reis, N. F. A., de Assis, J. C., Fialho, S. L., Pianetti, G. A., & Fernandes, C. (2016). Stability-indicating UHPLC method for determination of nevirapine in its bulk form and tablets: identification of impurities and degradation kinetic study. *Journal of Pharmaceutical and Biomedical Analysis*, 126, 103-108. <https://doi.org/10.1016/j.jpba.2016.05.005>
- Ren, B., Gan, L., Zhang, L., Yan, N., & Dong, H. (2018). Diisopropylethylamine-triggered, highly efficient, self-catalyzed regioselective acylation of carbohydrates and diols. *Organic & Biomolecular Chemistry*, 16(31), 5591-97. <https://doi.org/10.1039/C8OB01464G>
- Sabitha, R., Nishi, K., Gunasekaran, V. P., Agilan, B., David, E., Annamalai, G., Vinothkumar, R., Perumal, M., Subbiah, L., & Ganeshan, M. (2020). p-Coumaric acid attenuates alcohol exposed hepatic injury through MAPKs, apoptosis and Nrf2 signaling in experimental models. *Chemico-Biological Interactions*, 321, 109044, 1-10. <https://doi.org/10.1016/j.cbi.2020.109044>
- Samira Goldar, M. S. K., Sima Mansoori Derakhshan, Behzad Baradaran. (2015). Molecular mechanisms of apoptosis and roles in cancer development and treatment. *Asian Pacific Journal of Cancer Prevention*, 16(6), 2129-44. <https://doi.org/10.7314/APJCP.2015.16.6.2129>
- Sanches, B. M. A., & Ferreira, E. I. (2019). Is prodrug design an approach to increase water solubility? *International Journal of Pharmaceutics*, 568, 118498, 1-12. <https://doi.org/10.1016/j.ijpharm.2019.118498>
- Sangartit, W., Kukongviriyapan, U., Donpunha, W., Pakdeechote, P., Kukongviriyapan, V., Surawattanawan, P., & Greenwald, S. E. (2014). Tetrahydrocurcumin protects against cadmium-induced hypertension, raised arterial stiffness and vascular remodeling in mice. *PloS One*, 9(12), e114908, 1-21. <https://doi.org/10.1371/journal.pone.0114908>
- Sangartit, W., Pakdeechote, P., Kukongviriyapan, V., Donpunha, W., Shibahara, S., & Kukongviriyapan, U. (2016). Tetrahydrocurcumin in combination with deferiprone

- attenuates hypertension, vascular dysfunction, baroreflex dysfunction, and oxidative stress in iron-overloaded mice. *Vascular Pharmacology*, 87, 199-208. <https://doi.org/10.1016/j.vph.2016.10.001>
- Savla, R., Browne, J., Plassat, V., Wasan, K. M., & Wasan, E. K. (2017). Review and analysis of FDA approved drugs using lipid-based formulations. *Drug Development and Industrial Pharmacy*, 43(11), 1743-58. <https://doi.org/10.1080/03639045.2017.1342654>
- Schafer, Z. T., & Kornbluth, S. (2006). The apoptosome: physiological, developmental, and pathological modes of regulation. *Developmental Cell*, 10(5), 549-561. <https://doi.org/10.1016/j.devcel.2006.04.008>
- Seitz, H. K., Bataller, R., Cortez-Pinto, H., Gao, B., Gual, A., Lackner, C., Mathurin, P., Mueller, S., Szabo, G., & Tsukamoto, H. (2018). Alcoholic liver disease. *Nature Reviews Disease Primers*, 4(1), 16, 1-22. <https://doi.org/10.1038/s41572-018-0014-7>
- Senthil Kumar, K. J., Liao, J.-W., Xiao, J.-H., Gokila Vani, M., & Wang, S.-Y. (2012). Hepatoprotective effect of lucidone against alcohol-induced oxidative stress in human hepatic HepG2 cells through the up-regulation of HO-1/Nrf-2 antioxidant genes. *Toxicology in Vitro*, 26(5), 700-708. <https://doi.org/10.1016/j.tiv.2012.03.012>
- Setshedi, M., Wands, J. R., & Monte, S. M. d. l. (2010). Acetaldehyde adducts in alcoholic liver disease. *Oxidative Medicine and Cellular Longevity*, 3(3), 178-185. <https://doi.org/10.4161/oxim.3.3.12288>
- Setthacheewakul, S., Kedjinda, W., Maneenuan, D., & Wiwattanapatapee, R. (2011). Controlled release of oral tetrahydrocurcumin from a novel self-emulsifying floating drug delivery system (SEFDDS). *AAPS PharmSciTech*, 12(1), 152-164. <https://doi.org/10.1208/s12249-010-9568-8>
- Shield, K., Manthey, J., Rylett, M., Probst, C., Wettlaufer, A., Parry, C. D. H., & Rehm, J. (2020). National, regional, and global burdens of disease from 2000 to 2016 attributable to alcohol use: a comparative risk assessment study. *The Lancet Public Health*, 5(1), e51-e61. [https://doi.org/10.1016/S2468-2667\(19\)30231-2](https://doi.org/10.1016/S2468-2667(19)30231-2)
- Singal, A. K., Bataller, R., Ahn, J., Kamath, P. S., & Shah, V. H. (2018). ACG clinical

- guideline: alcoholic liver disease. *The American Journal of Gastroenterology*, 113(2), 175-194. <https://doi.org/10.1038/ajg.2017.469>
- Singh, N., & Bose, K. (2015). Apoptosis: pathways, molecules and beyond. In K. Bose (Ed.), *Proteases in Apoptosis: Pathways, Protocols and Translational Advances* (pp. 1-30). Springer International Publishing. https://doi.org/10.1007/978-3-319-19497-4_1
- Song, K. I., Park, J. Y., Lee, S., Lee, D., Jang, H.-J., Kim, S.-N., Ko, H., Kim, H. Y., Lee, J. W., Hwang, G. S., Kang, K. S., & Yamabe, N. (2015). Protective effect of tetrahydrocurcumin against cisplatin-induced renal damage: in vitro and in vivo studies. *Planta Med*, 81(04), 286-291. <https://doi.org/10.1055/s-0035-1545696>
- Song, Z., Deaciuc, I., Song, M., Lee, D. Y. W., Liu, Y., Ji, X., & McClain, C. (2006). Silymarin protects against acute ethanol-induced hepatotoxicity in mice. *Alcoholism, Clinical and Experimental Research*, 30(3), 407-413. <https://doi.org/10.1111/j.1530-0277.2006.00063.x>
- Stegemann, S., Leveiller, F., Franchi, D., de Jong, H., & Lindén, H. (2007). When poor solubility becomes an issue: from early stage to proof of concept. *European Journal of Pharmaceutical Sciences : Official Journal of the European Federation for Pharmaceutical Sciences*, 31(5), 249-261. <https://doi.org/10.1016/j.ejps.2007.05.110>
- Stella, V., Borchardt, R., Hageman, M., Oliyai, R., Maag, H., & Tilley, J. (2007). *Prodrugs: Challenges and Rewards Part 1*. <https://doi.org/10.1007/978-0-387-49785-3>
- Sugiyama, K., Kawada, T., Sato, H., & Hirano, T. (2001). Comparison of suppressive potency between prednisolone and prednisolone sodium succinate against mitogen-induced blastogenesis of human peripheral blood mononuclear cells in-vitro. *Journal of Pharmacy and Pharmacology*, 53(5), 727-733. <https://doi.org/10.1211/0022357011775857>
- Sugiyama, Y., Kawakishi, S., & Osawa, T. (1996). Involvement of the β -diketone moiety in the antioxidative mechanism of tetrahydrocurcumin. *Biochemical Pharmacology*, 52(4), 519-525. [https://doi.org/10.1016/0006-2952\(96\)00302-4](https://doi.org/10.1016/0006-2952(96)00302-4)
- Sun, X., Wang, P., Yao, L.-P., Wang, W., Gao, Y.-M., Zhang, J., & Fu, Y.-J. (2018). Paeonol alleviated acute alcohol-induced liver injury via SIRT1/Nrf2/NF- κ B signaling

- pathway. *Environmental Toxicology and Pharmacology*, 60, 110-117. <https://doi.org/10.1016/j.etap.2018.04.016>
- Taguchi, K., Motohashi, H., & Yamamoto, M. (2011). Molecular mechanisms of the Keap1–Nrf2 pathway in stress response and cancer evolution. *Genes to Cells*, 16(2), 123-140. <https://doi.org/10.1111/j.1365-2443.2010.01473.x>
- Thavorncharoensap, M., Teerawattananon, Y., Yothasamut, J., Lertpitakpong, C., Thitiboonsuwan, K., Neramitpitagkul, P., & Chaikledkaew, U. (2010). The economic costs of alcohol consumption in Thailand, 2006. *BMC Public Health*, 10(1), 323, 1-12. <https://doi.org/10.1186/1471-2458-10-323>
- Trabelsi, I., Essid, K., & Frikha, M. H. (2017). Synthesis of mixed anhydrides of fatty acids: stability and reactivity. *Industrial Crops and Products*, 97, 552-557. <https://doi.org/10.1016/j.indcrop.2017.01.003>
- Vacek, J. C., Behera, J., George, A. K., Kamat, P. K., Kalani, A., & Tyagi, N. (2018). Tetrahydrocurcumin ameliorates homocysteine-mediated mitochondrial remodeling in brain endothelial cells. *Journal of Cellular Physiology*, 233(4), 3080-92. <https://doi.org/10.1002/jcp.26145>
- Vig, B. S., Huttunen, K. M., Laine, K., & Rautio, J. (2013). Amino acids as promoieties in prodrug design and development. *Advanced Drug Delivery Reviews*, 65(10), 1370-85. <https://doi.org/10.1016/j.addr.2012.10.001>
- Vijaya Saradhi, U. V. R., Ling, Y., Wang, J., Chiu, M., Schwartz, E. B., Fuchs, J. R., Chan, K. K., & Liu, Z. (2010). A liquid chromatography-tandem mass spectrometric method for quantification of curcuminoids in cell medium and mouse plasma. *Journal of Chromatography. B, Analytical Technologies in the Biomedical and Life Sciences*, 878(30), 3045-51. <https://doi.org/10.1016/j.jchromb.2010.08.039>
- Wagner, C. E., Marshall, P. A., Cahill, T. M., & Mohamed, Z. (2013). Visually following the hydrogenation of curcumin to Tetrahydrocurcumin in a natural product experiment that enhances student understanding of NMR spectroscopy. *Journal of Chemical Education*, 90(7), 930-933. <https://doi.org/10.1021/ed3002489>
- Wakabayashi, M., McKetin, R., Banwell, C., Yiengprugsawan, V., Kelly, M., Seubsman, S.-a., Iso, H., Sleight, A., & Thai Cohort Study, T. (2015). Alcohol consumption patterns in Thailand and their relationship with non-communicable disease.

- BMC Public Health*, 15(1), 1297, 1-9. <https://doi.org/10.1186/s12889-015-2662-9>
- Wang, G., Fu, Y., Li, J., Li, Y., Zhao, Q., Hu, A., Xu, C., Shao, D., & Chen, W. (2021). Aqueous extract of *Polygonatum sibiricum* ameliorates ethanol-induced mice liver injury via regulation of the Nrf2/ARE pathway. *Journal of Food Biochemistry*, 45(1), e13537, 1-11. <https://doi.org/10.1111/jfbc.13537>
- Wang, S., Pacher, P., De Lisle, R. C., Huang, H., & Ding, W.-X. (2016). A mechanistic review of cell death in alcohol-induced liver injury. *Alcoholism, Clinical and Experimental Research*, 40(6), 1215-23. <https://doi.org/10.1111/acer.13078>
- Wei, G., Chen, B., Lin, Q., Li, Y., Luo, L., He, H., & Fu, H. (2017). Tetrahydrocurcumin provides neuroprotection in experimental traumatic brain injury and the Nrf2 signaling pathway as a potential mechanism. *Neuroimmunomodulation*, 24(6), 348-355. <https://doi.org/10.1159/000487998>
- Welsh, M., Mangravite, L., Medina, M. W., Tantisira, K., Zhang, W., Huang, R. S., McLeod, H., & Dolan, M. E. (2009). Pharmacogenomic discovery using cell-based models. *Pharmacological Reviews*, 61(4), 413-429. <https://doi.org/10.1124/pr.109.001461>
- Westerink, W. M. A., & Schoonen, W. G. E. J. (2007). Cytochrome P450 enzyme levels in HepG2 cells and cryopreserved primary human hepatocytes and their induction in HepG2 cells. *Toxicology in Vitro*, 21(8), 1581-91. <https://doi.org/10.1016/j.tiv.2007.05.014>
- WHO. (2021). *Alcohol, recorded per capita (15+) consumption (in litres of pure alcohol), three-year average with 95%CI*. Retrieved 07Jun2021 from [https://www.who.int/data/gho/data/indicators/indicator-details/GHO/alcohol-total-per-capita-\(15-\)-consumption-\(in-litres-of-pure-alcohol\)-with-95-ci](https://www.who.int/data/gho/data/indicators/indicator-details/GHO/alcohol-total-per-capita-(15-)-consumption-(in-litres-of-pure-alcohol)-with-95-ci)
- Williams, F. M. (1985). Clinical significance of esterases in man. *Clinical Pharmacokinetics*, 10(5), 392-403. <https://doi.org/10.2165/00003088-198510050-00002>
- Williams, S. H. (2005). Medications for treating alcohol dependence. *Am Fam Physician*, 72(9), 1775-80.
- Yan, S.-l., Wang, Z.-h., Yen, H.-f., Lee, Y.-j., & Yin, M.-c. (2016). Reversal of ethanol-induced hepatotoxicity by cinnamic and syringic acids in mice. *Food and Chemical Toxicology*, 98, 119-126. <https://doi.org/10.1016/j.fct.2016.10.025>

- Yang, S., Chen, M.-F., Ryu, B., Chen, J., Xiao, Z., Hong, P., Sun, S., Wang, D., Qian, Z.-J., & Zhou, C. (2020). The protective effect of the polysaccharide precursor, D-Isofloridoside, from *laurencia undulata* on alcohol-induced hepatotoxicity in HepG2 cells. *Molecules (Basel, Switzerland)*, *25*(5), 1024, 1-15. <https://doi.org/10.3390/molecules25051024>
- Yuan, R., Tao, X., Liang, S., Pan, Y., He, L., Sun, J., Wenbo, J., Li, X., Chen, J., & Wang, C. (2018). Protective effect of acidic polysaccharide from *Schisandra chinensis* on acute ethanol-induced liver injury through reducing CYP2E1-dependent oxidative stress. *Biomedicine & Pharmacotherapy*, *99*, 537-542. <https://doi.org/10.1016/j.biopha.2018.01.079>
- Zaman, S., Wang, R., & Gandhi, V. (2014). Targeting the apoptosis pathway in hematologic malignancies. *Leukemia & Lymphoma*, *55*(9), 1980-92. <https://doi.org/10.3109/10428194.2013.855307>
- Zhang, Y., Wang, C., Yu, B., Jiang, J.-D., & Kong, W.-J. (2018). Gastrodin protects against ethanol-induced liver injury and apoptosis in HepG2 cells and animal models of alcoholic liver disease. *Biological and Pharmaceutical Bulletin*, *41*(5), 670-679. <https://doi.org/10.1248/bpb.b17-00825>
- Zhao, R.-Z., Jiang, S., Zhang, L., & Yu, Z.-B. (2019). Mitochondrial electron transport chain, ROS generation and uncoupling (Review). *International Journal of Molecular Medicine*, *44*(1), 3-15. <https://doi.org/10.3892/ijmm.2019.4188>
- Zimmermann, K. C., & Green, D. R. (2001). How cells die: apoptosis pathways. *Journal of Allergy and Clinical Immunology*, *108*(4), S99-S103. <https://doi.org/10.1067/mai.2001.117819>



จุฬาลงกรณ์มหาวิทยาลัย
CHULALONGKORN UNIVERSITY

VITA

NAME นันทพงศ์ จงจิตพิศุทธิ์
DATE OF BIRTH 30 ธันวาคม 2534
PLACE OF BIRTH กรุงเทพมหานคร
INSTITUTIONS ATTENDED ปริญญาตรี เกษศาสตร์ จุฬาลงกรณ์มหาวิทยาลัย
HOME ADDRESS 53/79 หมู่ที่ 10 ต.บางครุ อ.พระประแดง จังหวัดสมุทรปราการ
 10130

